# BIOLOGICAL EFFECTS OF LOW-INTENSITY ULTRASOUND ON DENTAL STEM CELLS

By

QIANHUA GAO, DDS, MS

A thesis submitted to the University of Birmingham for the degree of

DOCTOR OF PHILOSOPHY


UNIVERSITY OF BIRMINGHAM

Department of Oral Biology

The School of Dentistry

College of Medical and Dental Sciences

University of Birmingham

JUNE 2016

## Abstract

**Introduction**: The value of low-intensity pulsed ultrasound (LIPUS) in regeneration of the dental tissue has not been fully investigated. The aim of this investigation is to research the potential of LIPUS on specific dental stem cells with the following objectives (1) to observe the biological effects of LIPUS under different ultrasound parameters, and (2) specify the role of signalling pathways in regulating stem cell responses.

**Materials and Methods:** Dental pulp stem cells (DPSCs), periodontal ligament stem cells (PDLSCs), and bone marrow stem cells (BMSCs) were isolated and cultured from Wistar rats. LIPUS was applied to the cells at the following intensities: 250mW/cm$^2$ and 750mW/cm$^2$.

**Results**: LIPUS significantly increased cell growth and proliferation of DPSCs, PDLSCs and BMSCs. LIPUS at 750mW/cm$^2$ exerted the greatest effects on DPSCs. The maximum effects of PDLSCs was seen at 250mW/cm$^2$. BMSCs showed equal responses to both LIPUS intensities.

LIPUS influenced the underlying signalling mechanism and MAPKs activation. In DPSC, ERK1/2 was activated immediately, whereas ERK1/2 inhibition modulated the proliferation effects. In BMSC, JNK MAPK was activated, and the post-LIPUS proliferation was decreased by JNK inhibition. In PDLSC, JNK MAPK was activated immediately post-treatment, and p38 MAPK was activated until 1 hour. Subsequently, specific JNK and p38 inhibition decreased proliferation effects after LIPUS.

Piezo1/2 were up-regulated post-treatment in DPSC, but not statistically significant in PDLSC. Ruthenium Red (RR), an inhibitor of Piezo1/2, only inhibited ERK1/2 activation, but not JNK or p38 MAPK. Furthermore, when Piezo1/2 were inhibited before LIPUS exposure, it modulated the increase of proliferation in DPSC, not in PDLSC.

**Conclusion**: 1) LIPUS does promote proliferation of dental stem cells, and intensity is most important not duration; 2) the proliferation of dental stem cells is dependent on MAPK signalling, and there was variation in different MSC lineages; 3) LIPUS may also have an effect on ion channels such as Piezo1/2. Such mechanically activated mechanisms have implications for future stem cell-based dental tissue regeneration.

## ACKNOWLEDGEMENTS

Firstly, I have to thank my supervisors, Dr Ben Scheven, Prof. Paul Cooper and Prof. Damien Walmsley. Each of them was irreplaceable and helpful in my journey of PhD. They provided guidance and constructive criticism in different aspects of my study. The help and advice they offered was priceless and I feel like I have developed so much over time.

I would also like to thank my colleagues and friends in Birmingham. I would especially like to thank Gay Smith, Michelle Holder and Sue Finney during the course of my studies. I like to thank who shared the 7th floor postgraduate office, I could not expect nicer and more helpful people than you. Also, I would thank my dear friends Jing Wu, Hongyan Zhao and Sunan Deng. Indeed, PhD is a life course full of stress and challenges. Thank you so much for accompany and mental support.

I also thank Han Han, for making me stay positive no matter what happens, and for his utmost patience and devotion.

Final thanks go to my family. My mother, father and elder sister have always been there for me. I am extremely blessed to have such supportive family in all aspects of my life.

## TABLE OF CONTENTS

## LIST OF FIGURES

LIST OF TABLES

## LIST OF ABBREVIATIONS

| | |
|---|---|
| α -MEM | Alpha-Modified Essential Medium |
| ANOVA | Analysis of variance |
| AP-1 | Activator protein-1 |
| ASC | Adult Stem Cell |
| ARS | Alizarin red S |
| BMP7 | Bone Morphogenetic Protein 7 |
| BMSC | Bone Marrow Stem Cell |
| BNR | Beam Non-uniformity Ratio |
| BrdU | 5-Bromo-2'-deoxy-uridine |
| BSP | Bone Sialoprotein |
| COL1 | Collagen Type-I |
| DFC | Dental Follicle Progenitor Cells |
| DMEM | Dulbecco's Modified Eagle Medium |
| DMP1 | Dentine Matrix Protein 1 |
| DMSO | Dimethyl Sulfoxide |
| DNA | Deoxyribonucleic Acid |
| DPSC | Dental Pulp Stem Cell |
| DSP | Dentine Sialoprotein |
| DSPP | Dentine Sialophosphoprotein |
| ECM | Extracellular Matrix |
| EDTA | Ethylenediaminetetraacetic Acid |
| ELISA | Enzyme-linked Immunosorbent Assay |
| ESC | Embryonic Stem Cell |
| ESWL | Extracorporeal Shock Wave Lithotripsy |
| FBS | Fetal Bovine Serum |
| FGF | Fibroblast Growth Factor |

| | |
|---|---|
| GAPDH | Glyceraldehydes-3-phosphate-dehyd |
| G-mounting | Glycerol Gelatin Mounting Medium |
| HIFU | High-intensity Focused Ultrasound |
| Hz | Hertz |
| IL | Interleukin |
| IMS | Industrial Methylated Spirit |
| kHz | Kilohertz |
| LIPUS | Low Intensity Pulsed Ultrasound |
| MA | Mechanically activated |
| MAPK | Mitogen-activated Protein Kinase |
| MHz | Megahertz |
| MSC | Mesenchymal Stem Cell |
| MTT | 3-(4,5-Dimethylthiazol-2-yl)-2,5-Diphenyltetrazolium Bromide |
| mW | Milliwatt |
| mW/cm2 | Milliwatt per Centimetre Squared |
| OCN | Osteonectin |
| OD | Optical Density |
| OPN | Osteopontin |
| ORO | Oil Red O |
| Pa | Pascal |
| PBS | Phosphate Buffered Saline |
| PCR | Polymerase Chain Reaction |
| PCNA | Proliferating Cell Nuclear Antigen |
| PDGF | Platelet Derived Growth Factor |
| PDL | Periodontal Ligament |
| PDLSC | Periodontal Ligament Stem Cell |
| RCT | Root Canal Therapy |

| | |
|---|---|
| RNA | Ribonucleic Acid |
| ROCK | Rho-associated Protein Kinase |
| RR | Ruthenium Red |
| RT | Reverse Transcriptase |
| SCAP | Stem Cells from Apical Papilla |
| SHED | Stem Cells from Exfoliated Deciduous Teeth |
| TLR | Toll-Like Receptor |
| TRP | Transient Receptor Potential |
| US | Ultrasound |
| W | Watt |
| VEGF | Vascular Endothelial Growth Factor |

# Chapter 1

# Introduction

# Chapter 1 Introduction

Despite the relatively high prevalence of the diseases of tooth and periodontal tissues , pulpitis and periodontitis are currently mainly treated by root canal therapy or debridement which removes bacteria as well as the infected dental tissue. The loss of dental tissue is challenging as root canal therapy (RCT) removes pulp tissue from the root canal and replaces it with an inert root filling material. Debridement approaches remove plaque and calculus on teeth to maintain oral hygiene and control caries and periodontitis progression.

Cell homing can be utilised in tissue regeneration given the chemotaxis environment to recruit endogenous cells, including stem/progenitor cells, into anatomic tissue compartments. Chemotaxis environment is supplemented by multiple cytokines to induce active recruitment of regenerative stem/progenitor cells. The delivery of fibroblast growth factor (FGF), vascular endothelial growth factor (VEGF), platelet derived growth factor (PDGF), alone or in combination with nerve growth factor and bone morphogenetic protein 7 (BMP7) induce cell homing, angiogenesis, and mineralized tissue formation. Chemotaxis-induced cell homing can lead to regeneration of the dentin-pulp complex (Kim et al., 2010). However, the removal of existing pulp stem cells by RCT, hampers the regeneration potential of the tooth. Within healthy tissues, the progenitor/stem cell niches are usually maintained in a quiescent state. During

the process of reparative dentinogenesis, significant dental tissue injury leads to the death of the odontoblasts within the dentine-pulp complex matrix which lie beneath the injurious lesion. Subsequently a cascade of complex and as yet not fully clarified events, are signalled by the released of dentine matrix components if the injurious process is arrested (Cooper et al., 2010). These signals then cause the progenitor/stem cell population to proliferate and be recruited to the site of injury where they differentiate into odontoblast-like cells (Tecles et al., 2005).

The regenerative feature of dentine-pulp complex is the basis for dental tissue engineering, and this study is aimed at enhancing the proliferative process of dental pulp stem cells in vitro using optimized low intensity pulsed ultrasound (LIPUS).

### *1.1 Ultrasound and Medicine*

Ultrasound (US) encompasses sound waves greater than 20kHz which are beyond the human hearing range. Since its first introduction to medicine in the 1920s (Miller et al., 2012), the use of US has grown substantially ranging from applications in clinical diagnosis and surgery to novel therapeutic approaches to repair hard and soft tissues throughout the body.

Therapeutic ultrasound utilises the ability of US to break chemical bonds or form active radicals using a process generally known as sonolysis (Pflieger et al., 2014). Sound waves can be destructive and rely on the process of cavitation whereby small bubbles are formed that rapidly implode and release an intense shock wave that produces relatively large amounts of heat energy and a variety of highly active radicals, which can completely destroy or activate adjacent material (O'Brien, 2007). Indeed, the heat energy released by cavitation breaks down bonds between large molecules. In medical procedures, cavitation can be used to destroy blood clots, kidney stones, dental plaque and calculus (Shaw and Hodnett, 2008). The application of US to dentistry began in 1955 (Zinner, 1955) and US periodontal scaling is now widely applied in tooth cleaning (Walmsley et al., 1992).

Ultrasound devices are non-invasive and easy-to-use hand-instruments thus are popular in dentistry. Dental US devices generally operate with frequencies from 20kHz up to several megahertz depending on the particular application. Megahertz frequency US, between 1-20 MHz, is referred to as being high-frequency and has been applied as a diagnostic tool for early carious enamel lesions and periodontal disease (Ghorayeb et al., 2008). Kilohertz-frequency US is in the 20 - 200 kHz range, and is termed “low frequency”. It is currently more

broadly used in daily dental practice for periodontal scaling and root canal cleaning (Ahmadi et al., 2012).

Whilst kHz US is widely used in dentistry, there is another form of ultrasound and termed LIPUS, which might bring out biological effects on cells (Marvel et al., 2010). LIPUS is a relatively novel therapy generally using 1.5 MHz frequency, pulsed and repeated at 1 kHz, and intensity around 30mW/cm$^2$, for 20 minutes/day. The physical and biological effects of LIPUS are dependent on the US conditions which can be optimized by adjusting parameters related to the energy profile of ultrasound, including frequency, intensity, power, wavelength and ultrasonic pressure (see Table 1). Various physical parameters related to US contribute to its biological effects including: intensity, frequency and duration of treatment sessions, wavelength, amplitude, beam non-uniformity ratio (BNR), continuous/pulsed therapy, tissue composition, coupling medium (transmissive medium of acoustic sound waves), effective radiating area of transducer head, movement and angle of transducer (Patel et al., 2015).

**Table 1.** Factors affecting the energy profile of the ultrasound beam

| Parameters | Definition | Unit |
|---|---|---|
| **Frequency** | Number of cycles per second | Hertz (Hz) |
| **Intensity** | Acoustic energy transmitted across unit area per second | Watt per centimeter squared ($W/cm^2$) |
| **Power** | Acoustic energy produced per second | Watt (W) |
| **Ultrasonic pressure** | Deviation of the pressure from its original value | Pascal ($Pa=N/m^2$) |
| **Wavelength** | | Meter (m) |
| **Time** | | Second (s) |

Frequency, intensity and treatment time are understood to be the three most critical parameters for application (Harle et al., 2001). The difference of LIPUS and medical US is the frequency and intensity. In therapeutic US, frequency is especially important which determine its effective depth/size for tissue treatment. Intensity determines the energy of transmitting ultrasound and therefore the local temperature and thermal effect. The optimization of US treatment parameters in various clinical fields has been widely studied. Notably, clinical conditions for therapeutic US (20kHz to 20MHz) applications have been improved to enhance its efficacy and specificity in a range of clinical areas including: cosmetics (20–500kHz) (Esenaliev, 2006), dentistry (25–42 kHz), lithotripsy (100–200 kHz) (Mitragotri, 2005), drug delivery (20KHz-2MHz), high intensity focused ultrasound (0.6-7MHz) is used in fracture healing (0.5-7.5MHz), and physiotherapy (1-3MHz) (Table 2).

**Table 2.** US conditions and medical applications **(Ahmadi et al., 2012)**

| Intensity range | Application | Description | Low-frequency range | Temporal-average intensity[a] |
|---|---|---|---|---|
| **Low intensity** | Sonophoresis; Glucose extraction; Drug delivery to the brain | •Sonophoresis: Transdermal drug delivery<br>•Glucose extraction: Extraction of glucose or other material from the skin in an opposite direction compared to sonophoresis | 20–100 kHz<br>Drug delivery to the brain: 80–180 kHz | 0.05–3.5 W/cm$^2$ |
| | Cosmetic applications | •Skin scrubbing,<br>•Microderm-abrasion – a method for facial rejuvenation | 20–500 kHz | Various |
| **High intensity** | Dentistry | Two main applications are:<br>•Dental descaling (tooth cleaning and calculus removal)<br>•Root canal therapy | 25–42 kHz | 0.58 W/cm$^2$ |
| | Lithotripsy | Extracorporeal shock wave lithotripsy (ESWL) -the non-invasive breaking of kidney stones using acoustic pulses | 100–200 kHz | In the range of 10 MPa |
| | Sonothrombol-ysis | Sonothrombolysis – the break down (lysis) of blood clots using acoustic waves | 20–25 kHz | 0.5–50 W/cm$^2$ |
| | Surgical | Tissue dissection and fragmentation | 20–60 kHz | 10–850 W/cm$^2$ |
| | Lipoplasty | Ultrasonic lipoplasty – the use of ultrasound waves to loosen fat beneath the skin's surface before its removal by means of suction | 20–50 kHz | 10–300 W/cm$^2$ |
| | Phacoemulsifi-cation | Phacoemulsification cataract surgery - break up and removal of a cloudy lens, or cataract, from the eye to improve vision | 25–62 kHz | Up to 1000 W/cm$^2$ continuous wave |

[a] Temporal-average intensity is mostly the average intensity over time, or over one repetition period for pulsed US.

## *1.2 High-intensity Focused Ultrasound (HIFU) and Low Intensity Pulsed Ultrasound (LIPUS)*

Intensity is the acoustic energy transmitted by US, therefore this determines the thermal effect of US on localised areas. Intensity of US is commonly categorized into two areas: high-intensity and low-intensity. High-intensity ultrasound (HIFU) directs focused acoustic energy ranging from ~5W/cm$^2$ to several thousand W/cm$^2$. High-intensity focused ultrasound is used in cancer therapy as the heat generated by the absorbed wave energy of HIFU causes local temperature rise to such a level as to destroy cancer tissue. Indeed, when local temperature rises excessively, irreversible tissue damage is caused (Al-Bataineh et al., 2012).

Low-intensity devices generally deliver an intensity range of between 0.025-3W/cm$^2$. Continuous wave US results in significant increases in temperature, thereby to reduce US-induced temperature rise of exposed tissues, US can be delivered by pulsed mode, whereas the acoustic wave is emitted intermittently rather than continuously. Pulsing the ultrasound beam reduces the temperature rise proportionately to the pulsing ratio. LIPUS has been shown to induce fracture healing (Dyson and Brookes, 1983), orthodontic root resorption (Liu et al., 2012), whole teeth regeneration (Rego et al., 2012), muscle laceration injury healing (Chan et al., 2010) and soft tissue healing within cartilage (Khanna et al., 2009) (Table 2). In addition, therapeutic low-intensity US, especially LIPUS,

has shown significant promise for hard tissue engineering and regenerative medicine. Notably, LIPUS could be applied clinically to stimulate dental tissue repair (Scheven et al., 2009b). Studies have already suggested that exposure of dental tissue to US may trigger dentinogenesis in the dentine-pulp complex as well as accelerating periodontal tissue healing (Al-Daghreer et al., 2012).

## *1.3 Biophysics of LIPUS*

As a propagating pressure wave, US is capable of exerting thermal and mechanical effects which influences the physiology of mammalian tissues. Thermal, cavitation and micro-streaming effects are the main recognized and well documented mechanisms responsible for eliciting the biological effects of ultrasound.

### 1.3.1 Thermal and Non-Thermal Effects

When US waves propagate through a tissue, US energy transforms into heat after being absorbed and attenuated. Intensity describes the transmitted energy of US and is therefore related to the thermal effect of US and the significance of thermal effects rises with increasing intensity. However, because of the low-intensity and pulsed nature of LIPUS, there is minimal increase monitored in local temperature (≤1°C) (Malizos et al., 2006). The thermal aspect can therefore commonly be excluded from the mechanism of action of LIPUS. Instead, the most likely mechanism of its clinical benefit in fracture and soft tissue healing is considered to be largely dependent on its non-thermal biomechanical effects (Dyson, 1982).

When thermal effects are insignificant or strictly controlled, the assumption is that the biological responses of the targeted cell or tissue are most likely derived from a non-thermal, mechanical effect by US (Baker et al., 2001). Non-thermal effects include cavitation, acoustic micro-streaming and radiation.

#### 1.3.2.1 Cavitation

Acoustic cavitation is the term used to describe the influence of an ultrasonic wave on the formation, growth, oscillation and collapse of gaseous bubbles in liquid (Fig. 1). A propagating wave through liquid consists of expansion (negative pressure) and compression (positive pressure) half cycles. When the sound wave pressure is high, in the expansion half cycles, the distance between liquid molecules can increase to an extent which creates unstable gas bubbles. The energy generated following collapse of these bubbles may result in hydrodynamic shearing and micro-streaming fields which possibly are sufficient to disrupt chemical bonds and bioactive molecules and tissues. Under lower sound wave pressure, stable cavitation maintains pre-existing bubbles without formation and increase in bubbles (Stride and Coussios, 2010).

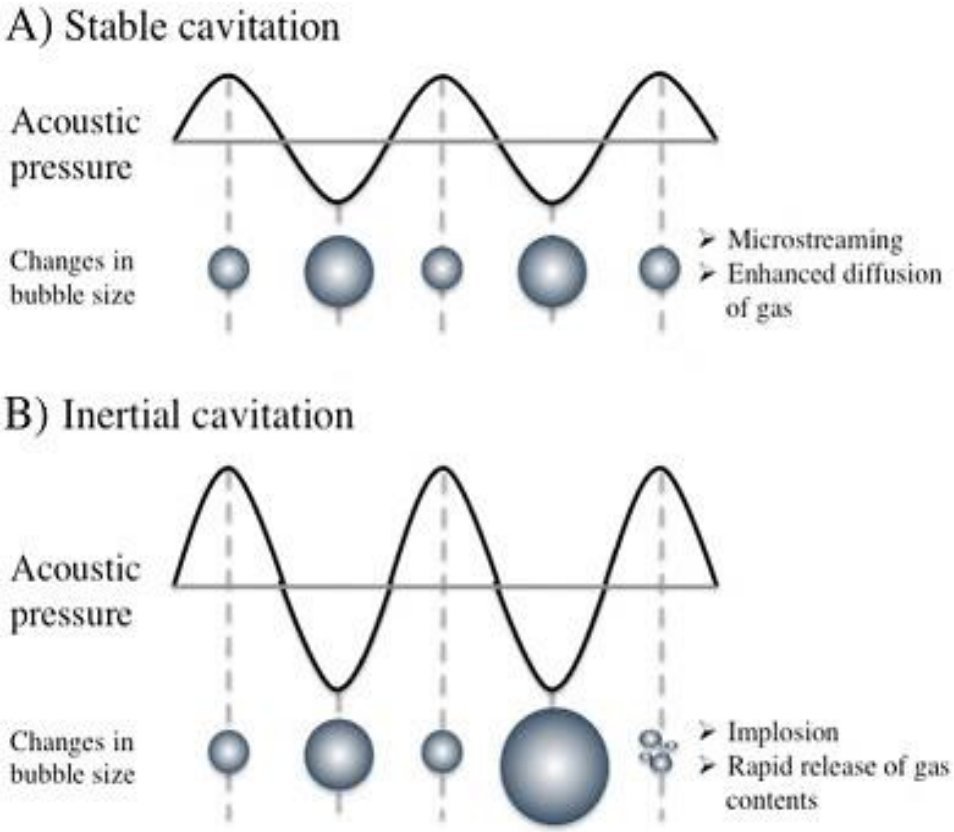


**Figure 1.** Cavitation and microstreaming effects in response to acoustic pressure of ultrasound. A) Stable cavitation —low-intensity ultrasound is related to periodic oscillating bubbles which generate fluid forces around them. B) Inertial cavitation —bubbles rapidly grow and violently collapse when subjected to high-intensity ultrasound. Diagram taken from the following reference (Fix et al., 2015).

### 1.3.2.2 Acoustic Micro-streaming

Acoustic micro-streaming is the fluid shear forces generated by the formation of a steady state streaming pattern within the liquid close to the surface of an oscillatory object (normally, but not exclusively associated with gaseous bubbles). The occurrence of acoustic micro-streaming rises with the intensity of US. Acoustic micro-streaming can be disruptive to cells when spontaneous cavitation occurs with high-intensity US. In contrast, at lower frequencies, mechanical stress produced by oscillation micro-streaming can be beneficial by allowing cell membranes to be more penetrable to foreign particles or impacting the cell cytoskeletal structure and resulting in intracellular signal transduction. Acoustic micro-streaming is considered as an important mechanism of biological action for low-intensity US (Rego et al., 2012, Tran et al., 2008, Khan and Laurencin, 2008, Romano et al., 2009).

### 1.2.3.3 Radiation Force

Acoustic radiation is an US-induced force on the medium to elicit a biophysical motion when particles are pushed by the acoustic wave in the propagating direction (O'Brien, 2007). The magnitude of the radiation force mainly depends upon the intensity of US, thus the effect of radiation in low-intensity US might be relatively weak (Ahmadi et al., 2012). However notably, in biophysical studies, radiation force has been implicated to associate with US-induced

biological responses such as tactile response (Dyson and Brookes, 1983), bone repair (Dyson and Brookes, 1983), and auditory response (Foster and Wiederhold, 1978).

## *1.4 Biological Effects of LIPUS*

### 1.4.1 Biomechanical Mechanisms Associated with LIPUS

The earliest research regarding therapeutic US was published in 1920, and indicated that US could stimulate cellular biological reactions (Wood, 1927). Subsequently, therapeutic US has been extensively studied with the aim of translating it for clinical applications, by better understanding the parameters for delivery and the underlying mechanism(s) of action (Baker et al., 2001, ter Haar, 2007, Mason, 2011, Miller et al., 2012).

LIPUS is reported to stimulate cellular processes mainly by micro-streaming. The mechanical aspects of micro-streaming led to the supposition that mechanotransduction is the underlying signalling mechanism of LIPUS. Subsequently LIPUS is associated with stimulating various cellular biological processes such as calcium oscillation (spontaneously oscillated cytosolic $Ca^{2+}$ concentration or upon receptor ligand binding), production of growth factors, extra cellular matrix production, proliferation, migration, and osteogenic

differentiation. Concurrently, mechanical forces stimulate similar changes in cellular biological reactions which indicates LIPUS might share similar signalling mechanisms to influence cellular behaviour (Mahoney et al., 2009).

### 1.4.2 Low-intensity Ultrasound and Tissue Regeneration

#### *1.4.2.1 Bone Regeneration*

The therapeutic application of US for tissue repair is mostly evidenced for bone repair (Pounder and Harrison, 2008, Khan and Laurencin, 2008). Indeed, LIPUS has shown to be effective in accelerating fracture repair in non-union, delayed or impaired fracture healing and treatment of distraction osteogenesis. LIPUS therapy of 20 min/day is generally applied *in vivo* and *in vitro* research although the evidence for the need for such a treatment time period is limited (Khan and Laurencin, 2008). Despite the apparently positive experimental and clinical data supporting LIPUS as a treatment for bone repair, the cellular processes and underlying molecular mechanism and relating signalling pathways remain largely unknown. A wide range of *in vivo* and *in vitro* experiments have demonstrated that LIPUS is able to stimulate various cellular activities including extracellular matrix synthesis, cell migration, cell proliferation, cell differentiation, bioactive molecule synthesis, gene expression, and cytosolic

$Ca^{2+}$ and integrin expression (Bandow et al., 2007, Borsje et al., 2010, Feng et al., 2010, Li et al., 2012, Man et al., 2012a).

### *1.4.2.2 LIPUS and Stem-cell Based Tissue Repair*

The biological effects of US on soft tissue are controversial. However, an in vitro study with LIPUS showed increased extracellular matrix production in 3D-cultured fibroblasts (Bohari et al., 2012) while no effect was detected on cell proliferation. Furthermore, studies have indicated that LIPUS positively affects human adipose derived adult stem cells (hASCs) and bone marrow derived mesenchymal stem cells (hMSCs) (Marvel et al., 2010, Jiang et al., 2012). A number of studies have demonstrated the mechanical responsiveness of stem cells (Titushkin et al., 2010), yet the clinical translation of this mechanical stress is not well known. US provides a feasible non-invasive clinical application, thus it is foreseeable that low-intensity US may be easily applied as adjuvant therapy in future stem cell research and tissue engineering approaches.

## *1.5 LIPUS and Dental Tissue Regeneration*

In the dental clinic, low-frequency kHz US is used in dental surface cleaning, periodontal scaling and endodontic instrumentation (Walmsley et al., 1988b, Lumley et al., 1988, Walmsley et al., 1992, Walmsley et al., 1988a). The evidence for the application of LIPUS in fracture repair supports further exploration into its potential for dental tissue repair (Scheven et al., 2009b). Notably a variety of in vitro studies have been performed in dental tissue related cells such as odontoblast-like cells (Scheven et al., 2007, Scheven et al., 2009a), periodontal ligament cells (Ren et al., 2012), gingival fibroblasts (Mostafa et al., 2009), and cementoblasts (Dalla-Bona et al., 2008).

LIPUS has been demonstrated to accelerate periodontal tissue wound healing after mucoperiosteal flap surgery demonstrating the US-responsiveness of periodontally-related cells, e.g. periodontal ligament cells, cementoblasts, mandibular osteoblasts (Ikai et al., 2008). Orthodontic force application to in vitro dentoalveolar structures has shown increased cementum and predentine thickness, and subodontoblast and periodontal ligament cell counts in the US treated groups (El-Bialy et al., 2011). Enhanced gingival fibroblast growth factor secretion and differentiation were also observed in the absence of effects on fibroblast proliferation (Mostafa et al., 2009).

The human dentine-pulp complex is responsible for dentine repair and regeneration. Proliferation and differentiation of odontoblast-like cells were up-regulated along with increased vascular endothelial growth factor (VEGF) expression under low frequency, low-intensity US (Scheven et al., 2009a), which may be regulated by Wnt canonical signalling (Man et al., 2012b). Higher odontoblast cell counts were also observed in the dentine–pulp complex after US exposure (Al-Daghreer et al., 2012). As recruitment of dental pulp stem cells/progenitor cells and odontoblast-like cell differentiation are key steps in reparative dentinogenesis, these observations support the hypothesis regarding the potential positive effects of US on DPSC-related pulp repair (Scheven et al., 2009b).

### *1.6 Mesenchymal Stem Cells Related to Dental Tissue Regeneration*

Many conventional therapies used to repair tissue defects currently rely on the use of replacement materials such as exogenous tissue, artificial and natural biomaterials and implants however it would be therapeutically advantageous if the existing tissue could be stimulated to repair itself using multilineage stem cells. In current research, stem cell related regenerative therapy involving transplantation of cells to enhance tissue regeneration and endogenous cell homing by recruiting host cells residing in nearby tissues is being explored extensively (Lin et al., 2009, Chen et al., 2011, Chen et al., 2012). Furthermore, the clinical potential of stem cell-based tissue regeneration to treat dental tissue damage is now recognised (Seo et al., 2004, Shi et al., 2005, Lin et al., 2009, Yoshida et al., 2012) and a number of different mesenchymal stem cells (MSCs) of dental origin have now been identified including: Dental pulp stem cells (DPSCs) (Gronthos et al., 2000), stem cells from exfoliated deciduous teeth (SHED) (Miura et al., 2003), periodontal ligament stem cells (PDLSCs) (Seo et al., 2004), stem cells from apical papilla (SCAP) (Sonoyama et al., 2008), dental follicle progenitor cells (DFCs) (Handa et al., 2002) and MSCs from gingival tissues (Mitrano et al., 2010) (Fig. 2). Dental tissue regeneration and engineering has been explored extensively in vitro and in vivo with multi-source dental stem cells. Unlike bone marrow derived stem cells,

dental stem cells exhibit higher proliferation capacity and are generally more easily accessed from extracted teeth (Gronthos et al., 2000).

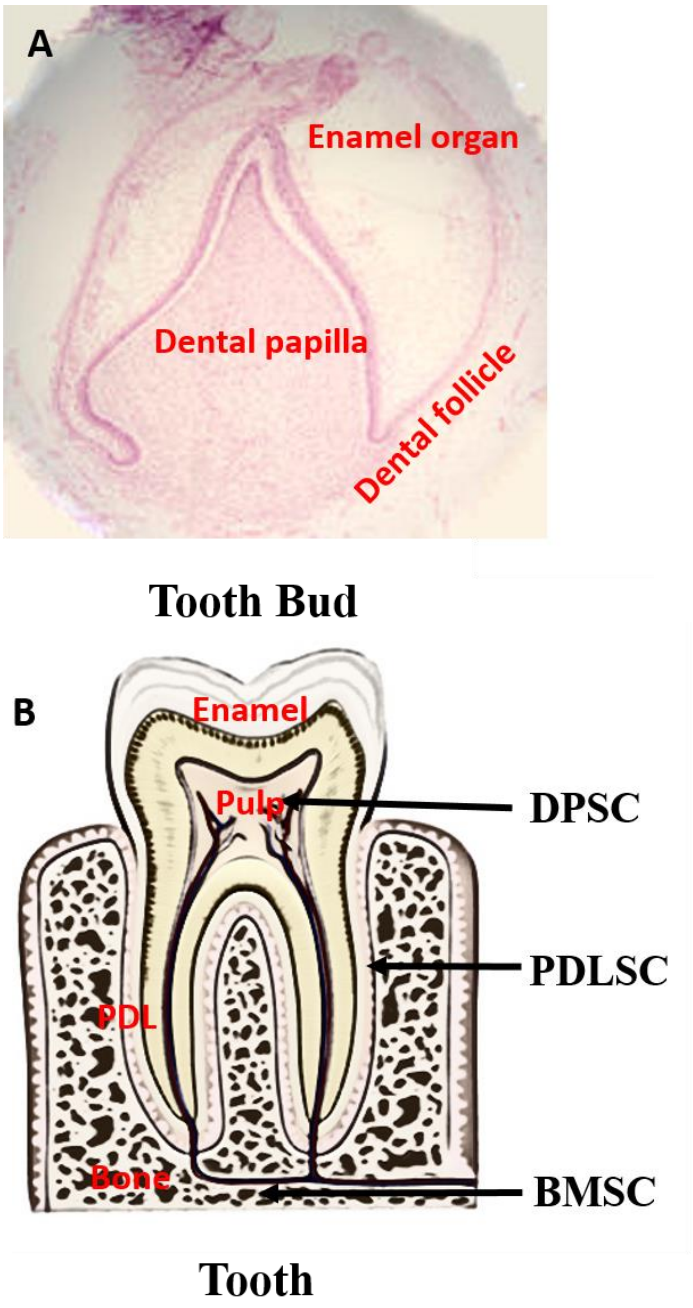


**Figure 2.** Scheme of mesenchymal stem cells originating from teeth and supporting tissues. A) Late bell stage of tooth development. Making up the tooth bud, Enamel organ gives rise to enamel, dental papilla gives rise to dental pulp, whilst dental follicle gives rise to PDL and supporting bones. In this study, DPSC is isolated from dental pulp tissue which derived from dental papilla at the stage of tooth development, PDLSC is isolated from periodontal ligament (PDL) which derived from dental follicle, whereas BMSC resides in supporting bone around tooth. Modified from Wikipedia.

### 1.6.1 Dental Pulp Stem Cells (DPSCs)

The dentine-pulp complex develops from cranial neural crest-derived cells during tooth development. Within the tooth the interior structure comprises a loose pulpal connective tissue containing cells, extracellular matrix, blood vessels, and nerves, encased by the rigid dentine, which provides a role as a barrier against bacterial, chemical, and physical insults. Pulp tissue also contains a variety of cell types, including fibroblasts, odontoblasts, blood cells, neuronal cells, inflammatory cells, along with DPSCs.

The first human dental stem cells were isolated from dental pulp tissue of extracted third-molar teeth (Gronthos et al., 2000, Gronthos et al., 2002). These DPSCs are understood to reside predominately in a stem cell niche in the perivascular regions of the dental pulp, from where they migrate to the site of injury in reparative dentinogenesis. Cell surface marker expression for DPSCs is similar to that of BMSCs and includes: CD13, CD29 (integrin-1), CD44, CD90 (Thy-1), CD105 (endoglin), CD106 (vascular cell adhesion molecule -1), CD146, CD166 (activated leukocyte cell adhesion molecule), STRO-1 and STRO-3 (Shi et al., 2005, Bakopoulou et al., 2011).

DPSCs are capable of regenerating dentine- and bone-like hard tissue and pulp-like soft tissue in in vivo studies (Laino et al., 2006, Graziano et al., 2008). In addition,

DPSCs have the potential to differentiate into chondrocytes, adipocytes, osteoblasts, as well as into neuronal cells (Arthur et al., 2008, Sugiyama et al., 2011). Interestingly, DPSCs showed a higher osteogenic potential compared with bone marrow MSCs (Ito et al., 2011). Thus, DPSCs have been recognized as a highly-proliferative and easily accessible source of stem cells and have been widely studied for various tissue engineering applications, such as tooth engineering, periodontal ligament regeneration and bone regeneration (Peng et al., 2009, Huang et al., 2009, Kim et al., 2011).

### 1.6.2 Periodontal Ligament Stem Cells (PDLSCs)

The PDL is located between the cementum and the alveolar bone / tooth socket as the central part of the tooth-supporting apparatus that surrounds and holds the tooth in position (Luan et al., 2006). As the most common threat to the integrity of the dentition, periodontitis is a bacterially driven chronic inflammatory disease of the periodontium (the periodontal ligament, alveolar bone and root cementum) which can result in tooth loss. Clinically available non-surgical/surgical treatments (i.e., periodontal ultrasonic scaling, bone graft placement and guided tissue/bone regeneration) have shown limited success in terms of complete regeneration of the complex triple layered structure of the tooth and its supporting tissues. In recent

years, stem cell-based regeneration (including cell transplantation and endogenous cell homing) has shown improved efficiency and reliability in reconstruction of tooth-supporting tissue regeneration (Lin et al., 2009, Chen et al., 2012, Yoshida et al., 2012, El-Bialy et al., 2012). The ex vivo expansion and delivery of stem cells into human patients has already commenced in clinical trials (Chen et al., 2011, Chen et al., 2012, Yoshida et al., 2012).

Human PDLSCs were first described in 2004 (Seo et al., 2004). PDLSCs represent a relatively small population of MSC-like cells which reside in the PDL connective tissue. They demonstrate self-renewing capacity and multilineage differentiation potential to give a variety of cell types including osteoblasts, fibroblasts and tooth cementoblasts, as well as adipocytes, chondrocytes and neurocytes in in vitro induction experiments (Kaneda et al., 2006, Techawattanawisal et al., 2007, Kim et al., 2009).

Like DPSCs, PDLSCs have no single recognised specific marker identified and they share common cell surface markers with bone marrow MSCs and DPSCs, which include CD13, CD29, CD44, CD90, CD105, STRO-1 (Seo et al., 2004, Laino et al., 2006, Schumann et al., 2006). An advantage of PDLSC is their relatively easy access and availability such as following 3rd molar tooth extraction (Wang et al., 2011). Using PDLSCs as the stem cell source, cementum /PDL-like

tissue regeneration with collagen fibres connecting cementum and PDL have been generated in in vivo studies (Seo et al., 2004).

### *1.7 Mechanotransduction Pathways of LIPUS*

The mechanical induction component of LIPUS is most likely responsible for its various associated biological responses. As ultrasound passes through the tissues, the particles will oscillate and it is this small movement that will influence the activity of the cell (See 1.3.2.1). Cellular mechanotransduction is the mechanism by which cells convert mechanical signals into biochemical responses. This cellular biological response to mechanical stimuli is complex, and specific signalling pathways are activated, followed by changes in extracellular matrix gene expression and protein synthesis (Schriefer et al., 2005). Mechanosensitive components are considered to be cell surface receptors, ion channels, integrins, focal adhesion molecules and the actin cytoskeleton (Katsumi et al., 2004, Mobasheri et al., 2005, Schwartz and DeSimone, 2008).

In adherent cells, integrins reportedly serve as major signalling receptors involved in mechanotransduction (Katsumi et al., 2004). Integrins connect the extracellular matrix proteins to the cytoskeleton and focal adhesion complexes, which can act as mechanosensors (Titushkin et al., 2010). In addition to the critical and universal

role in mechanotransduction in various cell types, integrins are also linked to signalling pathways which affect cell proliferation, differentiation, migration, and apoptosis (Schriefer et al., 2005).

Focal adhesion complexes are usually associated with the actin stress fibres and are sensitive to mechanical forces either by conformational changes of individual focal adhesion molecules (e.g. FAK, src, vinculin, paxillin) or their relative positions (Bershadsky et al., 2006, Wozniak et al., 2004). Mechanical stimuli trigger integrin dependent activation of intracellular signal transduction molecules such as mitogen-activated protein kinase (MAPK) (Kook and Lee, 2012) which regulate adhesion-dependent gene expression, and cell proliferation and differentiation (Chen et al., 2001). Notably MAPK signalling (including ERK, JNK, p38 MAPK etc.) has previously been demonstrated to play a role in mechanotransduction in various cell types, such as osteoclasts (Liedert et al., 2006), periodontal ligament cells (Kook and Lee, 2012) and muscle cells (Li and Xu, 2007).

The influx of $Ca^{2+}$ through mechanically-activated ion channels provides a further possible cellular means of detection of mechanical stimuli due to US. Calcium is a universal second messenger that regulates various cellular processes such as ion channels, and its activation leads to intracellular signalling proteins which regulate alterations in gene expression, proliferation, differentiation, and cytoskeletal

reorganization. Notably MSCs demonstrate relatively highly active calcium oscillations (Kawano et al., 2006). In addition, $Ca^{2+}$ transportation is regarded to be closely involved in mechanotransduction mechanisms in mature osteoclasts (Guo et al., 2006). Furthermore, the intracellular flow of $Ca^{2+}$ appears to be regulated by specific voltage-gated calcium channels (Kawano et al., 2006).

Piezo proteins (Piezo1 and Piezo2) provide a further class of transmembrane pore-forming ion channels which have recently been highlighted as mechanically responsive ion channels present on mammalian cells (Coste et al., 2012). Interestingly, Piezoelectric effect of bone has been well-known as the translation of a mechanical stimulus into a biological signal controlling growth or resorptive processes of bone. Piezo1/2 have been shown to induce mechanically activated (MA) cationic currents in various cell types, connecting mechanical forces to biological signals (Bagriantsev et al., 2014). The role of Piezo1/2 in cellular migration, proliferation, and elongation has been implicated to be involved with integrin activation (Volkers et al., 2015). Piezo1 and Piezo2 proteins were recently identified to be encoded by the FAM38A and FAM38B genes respectively (Lee et al., 2014). Notably Piezo2 is highly expressed in dorsal root ganglia suggesting involvement in neural system responses. In addition, both proteins have been shown to transduce mechanical forces to biological signals by inducing cationic

currents in several eukaryotic cell types (Ranade et al., 2014, Schrenk-Siemens et al., 2015).

## 1.8 Hypothesis, Aims and Objectives

This PhD study was designed to investigate the effects and mechanisms of LIPUS on dental stem cells isolated from different sources to corroborate the hypothesis that LIPUS can increase the proliferation of dental stem cells which is related to mechanically responsive cell signalling processes.

The aims of this study were:

1) LIPUS will increase proliferation of dental stem cells.
2) Proliferation of dental stem cells is regulated by specific MAPKs.
3) Piezo proteins are involved in the transduction of the initial LIPUS-associated biomechanical signals to activate MAPKs as an important cell membrane-located mechanotransduction component on stem cells.

Subsequently this study had the following research objectives:

1) Establishment and comparison of DPSC and PDLSC cultures, whilst BMSC were used as the gold standard MSC-type.

2) Analyse of effects of LIPUS conditions on proliferation of DPSC, PDLSC and BMSC.
3) Determination of LIPUS effects on MAPKs activation in relation to cell proliferation.
4) Study of the presence and role of Piezo1/2 in LIPUS stimulation of DPSC and PDLSC, and their involvement in MAPK signalling.

# Chapter 2

# Materials and Methods

## *2.1 Cell Isolation and Culture of rat Mesenchymal Stem Cell Populations*

Isolation of mesenchymal stem cells from various tissues has been highly developed since this term first introduced two decades ago (Augello et al., 2010, Caplan, 1991). Previous work has already proved that the lab protocol related to the isolation of DPSCs and BMSCs are reproducible and reliable (Davies et al., 2015). In each independent experiment, DPSCs, BMSCs and PDLSCs were isolated from three independent rats (three biological repeats). Cells derived from each rat were assayed three times (technical repeats) and combined to calculate a mean.

### 2.1.1 Isolation of DPSC

Incisors were extracted by removing the surrounding tissues (jaw bone and periapical tissues) with scissors and scalpel. Pulp tissue was dissected from incisors carefully mechanically extracted from Wistar male rats (120–140g) ( , UK). Dental pulp was minced using scalpels and digested in a solution of Trypsin/Ethylenediaminetetraacetic Acid (EDTA) (2.5 g/L trypsin in 0.38 g/L EDTA) (Invitrogen, UK) for 50 min, at 37℃ with vigorous agitation (Gale et al., 2011).

Enzymatically released cells were passed through a 70µm cell sieve (BD Falcon) to remove tissue residues and the filtrate was collected in a 50mL falcon tube (Nunc, UK). The filtered solutions were then centrifuged at 900g for 5 min (Eppendorf 5804R, Eppendorf, UK) and washed with 5mL phosphate-buffered saline (PBS). Cell pellets were seeded in 75cm$^2$ tissue culture flasks (Nunc, UK) and cultured in 10mL complete culture medium (α-MEM supplemented with 20% FBS, 100U/mL penicillin, and 100µg/mL streptomycin) in a 37°C incubator (Galaxy S+, RS Biotech Ltd, UK) in a humidified atmosphere of 5% $CO_2$. DPSCs were subcultured when they reached 70% confluence (usually after ~ 7 – 10 days). Medium was discarded and cells were gently rinsed with PBS three times prior to addition of 3mL preheated Trypsin/EDTA for 3 - 5 min, followed by addition of 3 - 5mL of complete α-MEM medium to terminate enzyme activity. The cell suspension was transferred to a 15mL falcon tube (Nunc, UK) and centrifuged at 500g for 5 min (Eppendorf 5804R, Eppendorf, UK). DPSCs were resuspended in complete α-MEM medium supplemented with 20% fetal bovine serum (FBS), 100U/mL penicillin, 100µg/mL streptomycin and seeded into two 75cm$^2$ tissue culture flasks (Nunc, UK). Primary cell cultures from passage 2 - 4 were used in all downstream experimental work.

### 2.1.2 Isolation of PDLSC

Gingival tissue was carefully removed from molars extracted from Wistar male rats (120–140g) ( , UK). Molars with attached PDL tissue were rinsed once in PBS supplemented containing 100U/mL penicillin and 100µg/mL streptomycin. The enzymatic digestion procedure used on the PDL was adapted from previous reports (Kaneda et al., 2006, Techawattanawisal et al., 2007). Molars were placed into a 15mL falcon tube (Nunc, UK) containing 5mL α-MEM with 2mg/mL collagenase (Sigma-Aldrich, UK) and Trypsin/EDTA (2.5 g/L trypsin in 0.38 g/L EDTA), and incubated at 37℃ for 45 minutes, with gentle agitation. The resulting cell suspension was passed through a 70µm cell sieve and the filtrate was collected in a 50mL falcon tube (Nunc, UK). The cell suspension was then centrifuged at 900g for 5 min and washed with 3 mL of PBS. Cells were seeded in 25cm$^2$ tissue culture flasks and cultured in α-MEM supplemented with 20% FBS, 100U/mL penicillin, and 100µg/mL streptomycin at 37℃ in a humidified atmosphere of 5% $CO_2$.

When 70% culture confluence was reached (~ 7 -14 days), the PDL-derived cells were subcultured as described above for DPSCs. PDL cells were resuspended in complete medium and subcultured to two 25cm$^2$ culture flasks. Primary cell cultures from passage 2 were used in all downstream experimental work.

### 2.1.3 Isolation of BMSC

The femurs and tibia were removed from Wistar male rats (120–140g) ( , UK) and immersed in α-MEM, 100U/mL penicillin, 100µg/mL streptomycin. Joints at both ends of the diaphysis were removed using sterile scissors. A 20 mL syringe (BD Bioscience, UK) containing α-MEM was attached to a 22 gauge needle (Appleton Woods, UK), which was inserted into the bone marrow cavity and used for flushing the tissue using α-MEM medium. Cells were collected in a falcon tube (Nunc, UK) and centrifuged at 900g for 5 min. Cell pellets were resuspended in complete medium and transferred to a $75cm^2$ culture flask for incubation at 37℃ in a 5% $CO_2$ supplemented incubator. Half of the culture medium was removed after 24 h of culture and fresh medium was added. Medium was changed every 2 to 3 days until 70% confluence was achieved (usually at ~ 7 to 10 days) (Davies et al., 2015). Primary cell cultures from passage 2 - 4 were used in all downstream experimental work.

## *2.2 Storage of Cell Isolates*

Passage 0 and passage 1 of DPSC, PDLSC and BMSC cells were cryopreserved under liquid nitrogen (BOC Gases) for use in future experiments. Trypsin/EDTA (Gibco, UK) was used to detach monolayers prior to storage. Cells were

centrifuged for 5 min at 900g, the cell pellet was aspirated and resuspended in 1mL 90% (v/v) FBS (Gibco, UK) containing 10% (v/v) dimethyl sulfoxide (DMSO) (Sigma-Aldrich, UK). The cell suspension was then transferred to cryogenic vials (Corning, UK). The cryogenic vials were incubated at 4℃ for 1 h, -20℃ for 2 h, followed by -80℃ overnight freezing and finally transferred to liquid nitrogen for storage in the vapour phase.

Vials of cells were recovered from storage by thawing in 37℃ water bath for ~2 min. Residual DMSO was removed by pelleting cells using centrifugation at 900g for 5 min prior to resuspension in α-MEM culture medium, the supernatant was aspirated, and the cell pellet was carefully resuspended and transferred to a 15mL falcon tube (Nunc, UK) prior to seeding in a 75cm$^2$ culture flask (Nunc, UK) with complete medium.

## 2.3 *Multilineage Differentiation Induction*

For differentiation experiments, 50,000 DPSCs, PDLSCs or BMSCs were seeded in each well of 6-well plate (Corning, UK) and maintained in α-MEM / 10% FBS for 24 h prior to adding the freshly prepared differentiation induction medium (Table 3).

**Table 3.** Medium supplementation for lineage-specific differentiation

| Lineage Induction | Medium | Supplementation |
|---|---|---|
| Osteogenic | α-MEM with 10% FBS | 2-Phospho-L-ascorbic acid 5mM<br>β-glycerophosphate 10mM<br>Penicillin 100U/mL<br>Streptomycin 100μg/mL |
| Adipogenic | α-MEM with 10% FBS | Dexamethasone 1μM<br>Indomethacin 200μM<br>Isobutyl-methylxanthine (IBMX) 0.5mM<br>Penicillin 100U/mL<br>Streptomycin 100μg/mL |
| Control | α-MEM with 10% FBS | Penicillin 100U/mL<br>Streptomycin 100μg/mL |

### 2.3.1 Osteogenic Differentiation and Alizarin Red Staining

70% confluent cultures were incubated in osteogenic medium (Table 3) for up to 3-weeks. Medium was changed every 2–3 days. Cultures were fixed using 10% neutral buffered formaldehyde (Leica Biosystems, UK) at room temperature for 15 min, and the calcification of the extracellular matrix was visualized using alizarin red S (ARS) staining. The stain solution used comprised of 2 mg/mL 40 mM ARS in 0.5 M acetic acid (BDH Laboratory Supplies, UK) and its pH adjusted to 4.2 using 1 % (v/v) ammonium hydroxide (BDH Laboratory Supplies, UK). Cultures were washed with PBS in duplicate, and ARS stain solution was added to the cultures which were then incubated for a further 20 min at room temperature. Cultures were washed with distilled water for four consecutive washes. Stained cells were kept at 4℃ before examination under a phase-contrast microscope (Axiovert 25, Zeiss, UK).

### 2.3.2 Adipogenic Differentiation and Oil Red O Staining

Subconfluent (~70%) cultures were incubated in adipogenic medium (Table 3) for up to 3- weeks. Medium was changed every 2–3 days. Cells were stained with oil red O (ORO) stain, which is a lysochromic dye used to visualize intracellular lipid droplets. An oil red O stock solution was prepared by dissolving 0.5g of oil red O

stain (VWR, UK) in 200mL isopropanol (VWR, UK). This mix was heated at 56℃ for 1 h and allowed to cool at room temperature for 2 h. A working solution was prepared by mixing 3 parts of stock solution with 2 parts distilled water. Immediately before staining, this solution was filtered to remove undissolved dye. Cultures were initially washed with PBS twice and then fixed with 4% formalin for 10 min in 4℃, and incubated with oil red O working solution for 40 min at room temperature with gentle agitation. Cultures were then washed once with 60% isopropanol (Sigma-Aldrich, UK), followed by 2 washes in PBS. Phase-contrast microscope (Axiovert 25, Zeiss, UK) was used to obtain images of stained culture plates.

### *2.4 Set-up of LIPUS Treatment for Use in vitro*

A DuoSon therapeutic ultrasound device (SRA Developments, UK) was used for ultrasound delivery (Fig. 4). The DuoSon device was calibrated annually by the suppliers using a radiation force balance (SRA Developments, UK). The calibrated device delivers ultrasound at low frequency (45kHz) and at high frequency (1MHz). Pulsed (a 63Hz repetition rate with a pulse duration of 3.2 milliseconds) high frequency ultrasound was applied in the studies reported below.

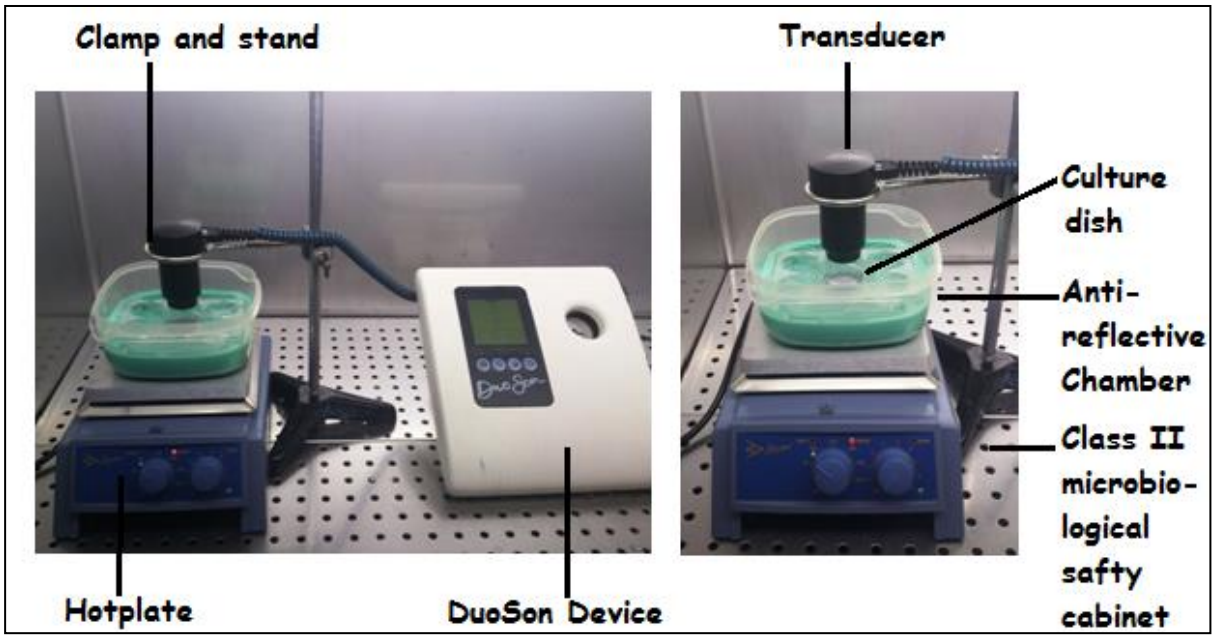


**Figure 4.** Set-up of DuoSon therapeutic ultrasound device to deliver ultrasound to *in vitro* cultured cells in the culture dish. The single culture dish was housed in the multiwall plate. The 37°C water bath in the anti-reflective chamber has direct contact to the bottom of the dish to control the environment temperature of cells under ultrasound irradiation.

### 2.4.1 Ultrasound Treatment Conditioning

A silicon anti-reflection chamber was custom built to house culture dishes of stem cells for ultrasound treatment (Man et al., 2012a, Balmaseda et al., 1986). This chamber was moulded to fit a 6-well plate (Corning, UK) with a water bath used to strictly maintain the temperature of media in culture plates at 37℃ during LIPUS treatment.

As described in previous studies (Patel et al., 2015, Man et al., 2012b), the DuoSon ultrasound transducer was placed in the culture medium resulting in the culture medium being used as the contact medium for ultrasound delivery. Prior to ultrasound delivery, for disinfection, the silicone chamber and the modified multi-well culture plate were immersed in 70% industrial methylated spirit (IMS) (VWR, UK) for at least 8 h and then left to air-dry under ultraviolet light exposure overnight in a Class II laminar flow hood (Fisher Scientific, UK).

Immediately prior to use, the chamber was filled with autoclaved dd$H_2O$ and placed into a 37℃ incubator with 95% humidified air with 5% $CO_2$. The hotplate (Bibby, UK) and DuoSon were swabbed with 70% IMS and allowed to air-dry in the culture hood. The transducer head was dis-assembled and washed with 100% ethanol, allowed to air-dry and rinsed with α-MEM prior to ultrasound delivery. The head unit of the ultrasound transducer was positioned inside the well of the 6-

well plate without disturbing the adherent cells seeded on the culture dish (Fig. 4). This enabled the transducer to be kept 2mm from cells adhered to the culture disk. Ultrasound delivery was then activated by selecting the mode and time on the DuoSon device control panel. The temperature of the water bath was monitored constantly using a standard thermometer.

### 2.4.2 **Delivery of LIPUS Treatment**

Two low-intensity levels and two single treatment durations were used: 250mW/cm$^2$ and 750mW/cm$^2$ was applied for 5 min and 20 min respectively to the cell cultures. Four experimental groups (5 min 250mW/cm$^2$; 20 min 250mW/cm$^2$; 5 min 750mW/cm$^2$; 20 min 750mW/cm$^2$) plus one control group designed identically to the 20 min experimental groups but with no ultrasound irradiation were used for all ultrasound experiments.

100,000 viable cells were seeded into each well of 6-well plate in α-MEM / 10% FBS for 24 h before ultrasound treatment. Cultures were washed with PBS and 7mL fresh supplemented culture medium were added to each culture dish immediately before ultrasound exposure. The transducer was carefully immersed into the medium and held within the well without touching the bottom of the culture dish during exposure (see Fig. 4) (Man et al., 2012b, Gao et al., 2016).

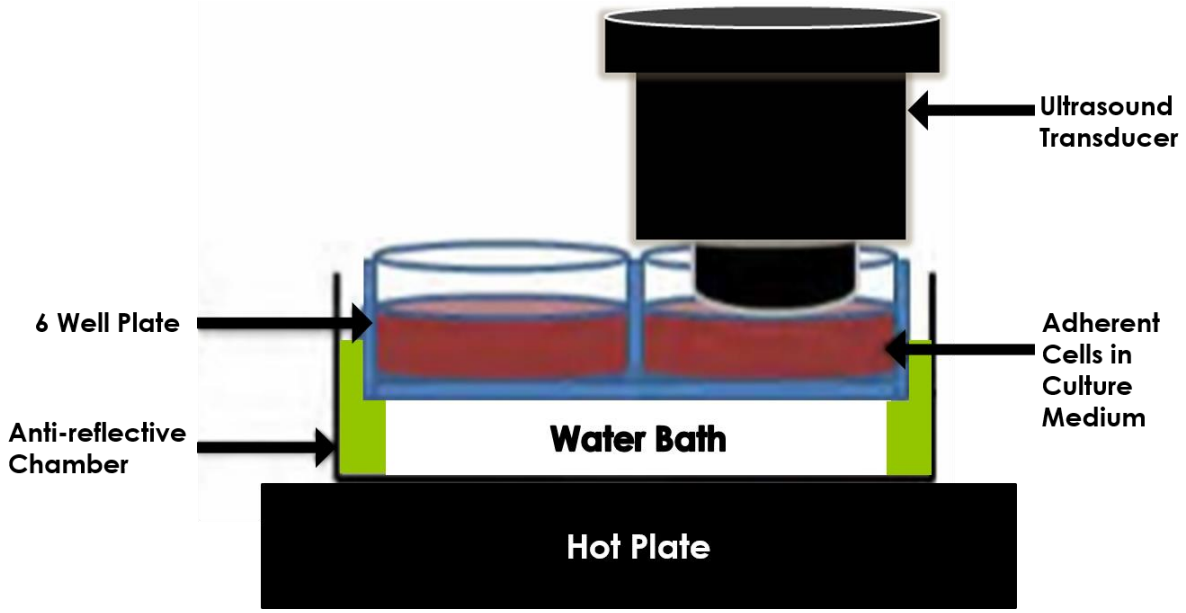


**Figure 4.** Schematic of the *in vitro* system used for LIPUS treatment of cells cultured in a 6-well plate. The water bath was used to maintain the temperature of the culture medium at 37°C. An silicon anti-reflective chamber was used to hold the 6-well plate in position and to limit the reflection of ultrasonic waves based on the previously reported set-up (Man et al., 2012b, Patel et al., 2015)

.

## *2.5 Cell Count and Trypan Blue Assay*

Following LIPUS treatment, cultures were trypsinised and cell numbers counted using a haemocytometer. The Trypan blue assay was undertaken using a cell counting procedure. 10μL of a cell suspension was mixed thoroughly with an equal volume of 0.4 % (w/v) Trypan blue cell stain (Sigma-Aldrich, UK). The suspension was then transferred to a haemocytometer (Hawksley, UK) and viable cells (trypan blue unstained cell) counted manually under a phase-contrast microscope (Axiovert 25, Zeiss, UK). All samples were counted five times.

Cell growth were calculated using the equation below.

**% Viable Cell = Viable cell number/Total cell number**

## *2.6 Cell Proliferation using BrdU Staining*

Methods to analyse cell proliferation are comprised of four main types: DNA synthesis, metabolic activity, cell proliferation antigens and ATP concentration. Here, Cell proliferation was analysed by the BrdU assay using 5-Bromo-2'-deoxy-uridine Labelling and Detection Kit II (Roche, Germany) because of its reliability and accuracy in detecting DNA synthesis. 5-Bromo-2'-deoxy-uridine (BrdU) binds to DNA in place of thymidine and therefore cells undergoing DNA synthesis can be easily visualized by the BrdU incorporated detected using antibodies under light microscopy.

### 2.6.1 Cell Seeding

Coverslips were washed with ddH2O followed by a 70% ethanol rinse followed by autoclaving for disinfection. 10,000 cells were seeded onto the coverslips (Fisher Scientific, UK) and placed in the wells of a 6-well plate (Corning, UK). Culture medium was added and cultures utilised when cells appeared to be 4h adherence to the coverslip. The plate assembly was then placed in an incubator at 37℃ for a minimum of 4h prior to the cells being washed with sterile 1x phosphate buffered saline (PBS, Sigma-Aldrich, UK).

### 2.6.2 BrdU Staining

Prior to the staining procedure, Glycerol Gelatin mounting medium (G-mounting) (Sigma-Aldrich, UK) was preheated in a 50℃ incubator for fixation and storage of stained coverslips. BrdU labelling medium was performed as per the manufacturer's protocol. 25µL BrdU labelling reagent was mixed with 25 mL culture medium and incubated with cell samples for 1 h at 37℃, 5% $CO_2$. After washing 3 times with PBS, the cells were fixed with ethanol fixative at -20℃ for at least 20 min. Cultures were washed 3 times with PBS to remove the fixative. Anti-BrdU working solution was prepared by mixing 100 µL Anti-BrdU with 900 µL incubation buffer. This was then incubated with the cells for 30 min at 37℃ and 5% $CO_2$. The cultures were washed three times with PBS prior to incubation with an anti-mouse-Ig-AP solution for 30 min at 37℃ in a humidified atmosphere of 5% $CO_2$ and then washed three times with PBS. The colour substrate solution was prepared in the dark room and included 5µL NBT, 4µL BCIP and 1mL substrate buffer. The coverslips were then incubated with colour substrate for 20 min at room temperature. 60µL of preheated G-mounting was pipetted onto the slides and covered with coverslips. When cooled to room temperature, the slides were stored at 4℃ prior to use.

### 2.6.3 Determination of the Proliferation Ratio

Stained coverslips were viewed by microscopy (Axiovert 25, Zeiss, UK) and images captured using a digital camera prior to analysis. Captured images were analysed with ImageJ software and using a Java program developed by Kurt De Vos (University of Sheffield, UK) obtained online (http://rsbweb.nih.gov/ij/plugins/cell-counter.html) (Young et al., 2013). Immunopositive and negative cells in images were marked manually by an observer, and only those cells with nuclei observable by light microscopy were counted (Fig. 5). The labelling index as a measure for cell proliferation was calculated using a cell counter as the percentage of immunopositive cells compared with the total cell number in a microscopic field. Cell counts were presented as averages from 5 different fields of view per time point and from three independent experiments.

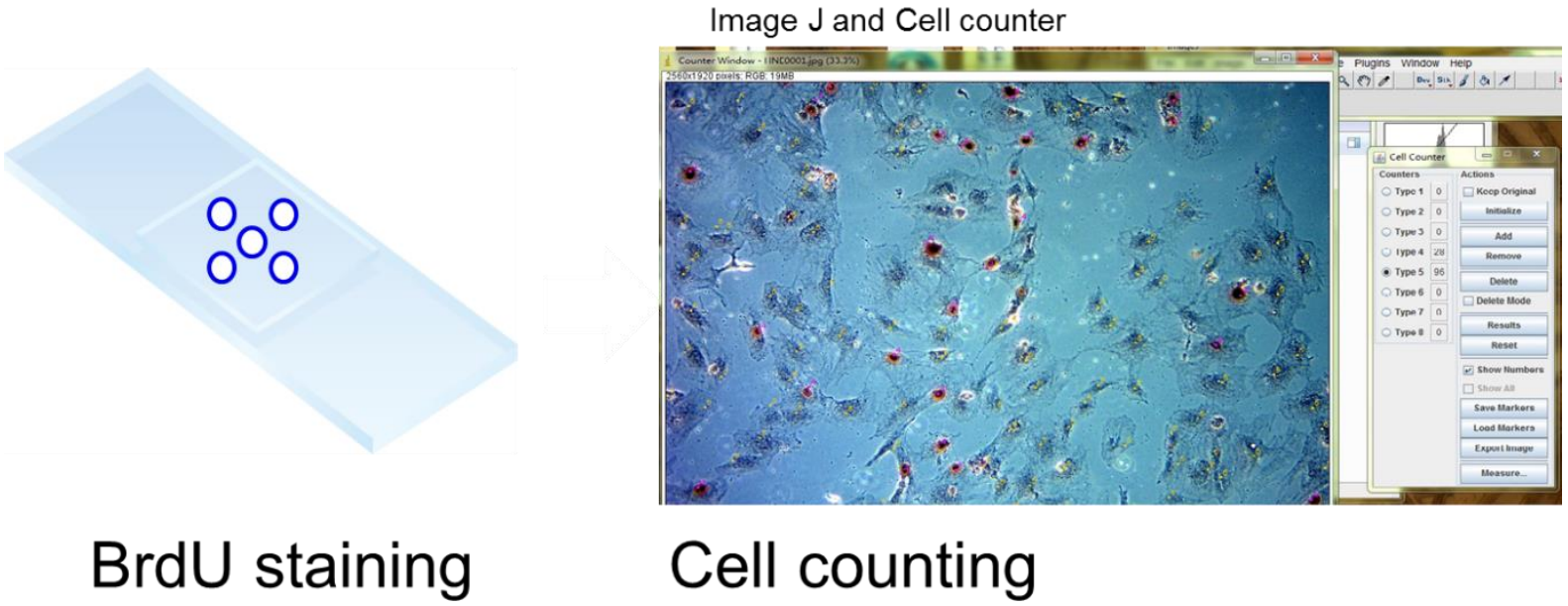


**Figure 5.** Procedure used for BrdU staining of cells cultured on microscope slides. Step 1, cells were cultured on slides until 50% confluent and were subjected to LIPUS treatment. Step 2, cells are stained with 5-Bromo-2'-deoxy-uridine Labelling and Detection Kit II following manufacturers' instruction (Roche, Germany). Images from five random fields of view were captured. Step 3, Captured images were processed using the ImageJ plugin 'Cell Counter' (Young et al., 2013).

### *2.7 Use of Pharmacological Inhibitors and MTT Assay*

For pathway inhibition experiments, cultures were treated with the pharmacological MAPK inhibitors PD98059 (ERK1/2), SB203580 (p38) and SP600125 (JNK) (TOCRIS, Bristol, UK) 2 h prior to ultrasound exposure (KOOK AND LEE, 2012). Cell metabolic analysis using the 3-(4,5-Dimethylthiazol-2-yl)-2,5-Diphenyltetrazolium Bromide (MTT) assay was performed for all cell types prior to pathway inhibition experiments using concentrations of 10µM, 20µM and 40µM of PD98059, SB203580 and SP600125, which had been previously utilised in comparative studies (Kojima et al., 2007, Wang et al., 2007).

MTT cytotoxicity analysis was also applied for Ruthenium Red (Sigma-Aldrich, UK) analysis in concentrations of 5µM, 10µM, 20µM, as this is pharmacological inhibitor of Piezo1 and Piezo2 activity. For the MTT assay cultures in 75cm$^2$ culture flasks were trypsinised and cells pelleted by centrifugation in a sterile 15mL falcon tube (Nunc, UK) at 900g for 5 min. The supernatant was removed and cells were resuspended in 1mL complete DMEM media. Cell number was counted and recorded as described above (Section 2.5). Complete media was used to dilute the cells to 75,000 cells per mL. 100µL of medium containing 7500 total cells was then added into each well of the 96-well plate (Nunc, UK) prior to incubation overnight. All the culture medium was removed carefully and the cells

were treated with different concentrations of inhibitors diluted by complete media separately and incubated for a further 24 h. 20μL of 5mg/mL MTT (Sigma-Aldrich, UK) was then added to each well of the 96-well plate aseptically. Control wells comprised MTT reagent alone. After incubation with MTT for 3.5 h at 37°C, media in the wells were carefully removed without disturbing the cells. 150μL MTT solvent was added to each well and then the 96-well plate was agitated using a plate shaker for 15 min in the dark. The absorbance was read in a ELx800 plate reader (Biotek, UK) at 590nm with a reference filter of 620nm for three times for each plate.

## *2.8 Enzyme-linked Immunosorbent Assay (ELISA)*

ELISA is a plate-based quick and sensitive method to quantitatively analyse the change of specific proteins. ERK 1/2 ELISA Kit (ab176660), p38 MAPK alpha ELISA Kit (ab176664) and JNK 1/2 ELISA Kit (ab176662) are purchased from Abcam and repeated 3 times each experiment.

### 2.8.1 Total Protein Isolation

Protein samples were collected and prepared using methods provided by the manufacturer (Abcam, UK) from experimental and control groups. The 6-well plate was gently washed with ice-cold PBS following ultrasound treatment. The cells in each well were lysed with 100µL of freshly prepared Lysis Mix per well (supplied in kit), with shaking (~300 rpm) at room temperature for 10 min. Then the supernatant was aliquoted to Eppendorf tubes on ice and stored at -80℃ prior to future use. The freeze/thaw cycles were minimized and the protein samples were used within 2 weeks.

### 2.8.2 Bradford Assay

The Bradford method (1976) was used to analyse the total protein content of samples. 5µL of a 0.1–1.4mg/mL protein sample was applied to wells in the 96 well plates.

The Bradford reagent (Sigma-Aldrich, UK) was gently mixed in the bottle and allowed to equilibrate at room temperature. Serial dilutions were then prepared in buffer at concentrations ranging from 0.1–1.4 mg/mL using BSA protein standard (Sigma-Aldrich, UK). 5µL of the protein standards were added to separate wells in the 96 well plate and 5µL of buffer were added to the blank wells to provide a control. To analyse the exact protein concentration, experimental protein samples were prepared within the concentration 0.1–1.4 mg/mL. To each well being used, 250µL of the Bradford Reagent were added and mixed by agitation for 30 s. The samples were then incubated at room temperature for 15 min and the plates were measured using a ELx800 plate reader (Biotek, UK) at a 595nm absorbance. The net absorbance vs. the protein concentration of each standard was then plotted. Finally, a standard curve was generated and the protein concentration of the unknown samples was determined by comparing the net A595 values against the standard curve.

### 2.8.3 ELISA

ELISAs were used to determine total and phosphorylated p38, ERK1/2, JNK p38 MAP kinase using the MAPK ELISA Kit (Abcam, UK). The protein samples were stored at -80℃ were brought to room temperature. The desired number of microplate strips per experiment were obtained from the ELISA kits. 50µL/well of protein lysate was added to each well of the microplate. Then 50µL/well of Lysis Mix was added as negative control wells and 50µL/well of Control Lysates were added for the positive control wells. 50µL/well of kit Antibody Mix were then added to experimental and control wells. The microplate was covered with adhesive seal and incubate for 1 h at room temperature and agitated on a microplate shaker (400 rpm). The wells were then washed gently with 350µL/well 1X kit Wash Buffer 3 times. After the final wash, the remaining wash solution was completely removed. 100µL/well of TMB was added and incubated at room temperature in the dark for 20 min on a plate shaker set to 400rpm. Finally, 100µL/well of Stop Solution was added to each well and mixed briefly (1 min) on a microplate shaker. The OD value was recorded at 450nm using a ELx800 plate reader (Biotek, UK). The phosphorylated ratio was calculated as phospho-MAPKs/total MAPKs.

## *2.9 Gene Expression Analysis*

### 2.9.1 RNA Isolation

Total RNA was extracted from rat MSC cultures using the RNeasy mini kit (Qiagen, UK) in accordance with manufacturer's instructions. First, cells were collected by incubating cultures in 350μL of buffer RT with 10μL beta-mercaptoethanol (Sigma-Aldrich, UK) for 5 min at room temperature under constant agitation. Then the lysate was transferred to an Eppendorf tube (Nunc, UK) and mixed by rapid pipetting. An equal volume of ice-cold 70% ethanol was then added to the mixture and the lysate mixture was transferred to a spin column assembly. Total RNA binds to the membrane of the column and the genomic DNA was removed by digestion by addition of DNase I (Qiagen, UK) to the spin column assembly. After incubating for 15 minutes, contaminants were removed by serial washes and centrifugation using wash water and ethanol kit buffer. Purified RNA was then eluted in 30 μL RNase-free water. The RNA concentration and purity was determined using a Biophotometer (Eppendorf, UK).

For RNA visualisation, a 1% non-denaturing agarose gel was prepared using 0.6g of agarose (Web Scientific, UK) dissolved in 60mL of 1x TAE buffer, a mixture of 2M Tris-acetate and 0.05M EDTA (Qiagen, UK), by heating the suspension in a microwave (Sanyo, UK). The mixture was generated by combining 1μL of the

isolated RNA, 3µL RNase-free water and 1µL 10X loading buffer (Promega, UK). After loading into wells in the agarose gel, electrophoresis was performed at 120 V for ~ 40 min. The SYBR gold nucleic acid stained gel was visualised and analysed using a gel documentation and analysis unit (G:Box, Syngene, UK) to show the presence and integrity of the isolated RNA.

### 2.9.2 Reverse Transcription - PCR

cDNA was produced by QIAGEN Omniscript RT kit from reverse transcribed RNA. Following the manufacturer's instructions (Qiagen, UK), 2µg of RNA was diluted in 12µL of RNase-free water. 2µL of 10µM oligo-dT primer (Ambion, UK) was added to the diluted solution and incubated for 10 min at 80ºC, followed by quenching for 5 min on ice. A PCR master-mix was synthesised by combining 2 µL reverse transcriptase buffer, 2 µL deoxynucleoside triphosphates (dNTP), 1 µL RNase inhibitor (Promega, UK) and 1µL omniscript reverse transcriptase. The master-mix was mixed with the diluted RNA solution and incubated at 37ºC for 1 h followed by heating to 95 ºC for 5 min to allow the synthesis reaction of cDNA.

Lyophilised primers (Table 4) were dissolved in sterile water to a final concentration of 100µM for use. These stocks were further diluted with RNase-free water to provide a 25µM working stock solution and stored at -20℃ prior to use.

**Table 4.** Primer sequences and conditions used in the sqRT-PCR analysis

| Gene | Sequences | Classification | Annealing temperature (℃) | Cycle no. | Accession no. |
|---|---|---|---|---|---|
| *GAPDH* | F-CCCATCACCATCTTCCAGGAGC | Housekeeping | 60.5 | 27 | NM_017008 |
| | R-CCAGTGAGCTTCCCGTTCAGC | | | | |
| *CD29* | F-AATGGAGTGAATGGGACAGG | MSC marker | 60.5 | 27 | NM_017022.2 |
| | R-TCTGTGAAGCCCAGAGGTTT | | | | |
| *CD90* | F-AGCTCTTTGATCTGCCGTGT | MSC marker | 60.5 | 26–33 | NM_012673 |
| | R-CTGCAGGCAATCCAATTTTT | | | | |
| *Vimentin* | F-AGATCGATGTGGACGTTTCC | MSC marker | 60.5 | 27 | NM_031140.1 |
| | R-GCAGGTCCTGGTATTCACG | | | | |
| *Nanog* | F-TATCGTTTTGAGGGGTGAGG | Pluripotent marker | 60.5 | 33 | NM_001100781 |
| | R-CAGCTGGCACTGGTTTATCA | | | | |
| *Klf4* | F-ATCATGGTCAAGTTCCCAGC | Pluripotent marker | 60.5 | 27 | NM_052713 |
| | R-ACCAAGCACCATCGTTTAGG | | | | |
| *DMP1* | F-CGGCTGGTGGTCTCTCTAAG | Mineralization marker | 60.5 | 31–33 | NM_203493.3 |
| | R-CATCACTGTGGTGGTCCTTG | | | | |
| *OCN* | F-TCCGCTAGCTCGTCACAATTGG | Mineralization marker | 60.5 | 33 | NM_013414.1 |
| | R-CCTGACTGCATTCTGCCTCTCT | | | | |
| *OPN* | F-AAGCCTGACCCATCTCAGAA | Mineralization marker | 60.5 | 33 | NM_012881.1 |
| | R-GCAACTGGGATGACCTTGAT | | | | |
| *BSP* | F-ATGGAGATGGCGATAGTTCG | Mineralization marker | 60.5 | 27 | NM_012587.2 |
| | R-TCCACTTCTGCTTCTTCGTTC | | | | |

REDTaq® ReadyMix (Sigma-Aldrich, UK) was used to make REDTaq mastermix, comprising 12.5µL of REDTaq ready mix (SigmaAldrich, UK), 12.5µL of RNase-free water, 1µL of 1µM forward primer (Invitrogen, UK) and 1µL of 1µM reverse primer (Invitrogen, UK). 50ng of cDNA was added to the master mix containing the target gene of interest. The samples were gently agitated and briefly centrifuged to collect residual liquid and subsequently transferred to a Mastercycler® Gradient Thermal Cycler (Eppendorf, UK) for amplification. Activation of REDTaq® was achieved by heating the samples to 95℃ for 5 min prior to thermal cycling. After the designated number of cycles, 6µL of the amplified product was then used for visualisation and quantification by gel electrophoresis as described below (Section 2.9.3).

### 2.9.3 Gel Electrophoresis Analysis

1.5% agarose gel was produced by dissolving 0.8g of agarose in 60mL of 1x TAE buffer as described above (Section 2.9.1). The agarose was cooled under flowing water to 50-55℃ before adding 10mg/mL ethidium bromide (Helena Biosciences, UK). The gel was then carefully mixed and cast in a tray. Well-forming combs were added before the agarose gel cooled to room temperature. Once solidified, the gel was immersed in 1x TAE buffer in an electrophoresis tank (Bio-rad, UK) and the combs were removed.

Following electrophoresis, the gel was transferred to the G-BOX (Syngene, UK). For image quantification, GeneSnap image acquisition software (Syngene, UK) was used for visualization and analysis. To obtain the volume density of amplified samples, the band intensity of specific genes was normalised against the band intensity of GAPDH. Normalised values were expressed as a percentage of the highest volume density value obtained.

## *2.10 Western Blot Analysis*

Western blot analysis was used to visualise and quantitatively analysis the concentration of proteins involved in cellular processes such as signalling transduction and cell cycle progression.

### 2.10.1 Protein Isolation

6-well plates were placed on ice and the cells in each well were washed with 2mL of ice-cold PBS. Then 1mL of ice-cold PBS was added to each well and the cells are scraped off the dish using a plastic cell scraper (Millipore, UK). The cell suspension was gently transferred into a pre-cooled 15mL falcon tube (Nunc, UK) and stored on ice. After centrifugation, the supernatant was aspirated, and 0.5mL of ice-cold RIPA lysis buffer (Sigma-Aldrich, UK) was added to each sample. Constant agitation was maintained for 30 min at 4℃. After centrifugation (20 min at 12,000rpm at 4℃), the tubes were gently removed from the centrifuge and placed on ice. Finally, the pellet was discarded, the supernatant was aspirated to a fresh tube and stored at -20℃ prior to further experimental analysis.

### 2.10.2 Sample Loading and Gel Analysis

The protein quantification assay (Bradford Assay) (as previously described) was performed using a small volume of lysate to determine the protein sample concentrations. The volume of each protein sample was mixed with an equal volume of 2x Laemmli sample buffer. To reduce and denature, each cell lysate was boiled in sample buffer at 100℃ for 5 min. Lysates were aliquoted and stored at -20℃ prior to future use.

20 µg of protein were loaded and run on pre-cast 4–12% Bis-Tris gels (Invitrogen, UK). Gels were run in an electrophoretic tank (BIO-RAD).

Subsequently the proteins were transferred from gels to a polyvinylidene fluoride (PVDF) membrane using the Trans-Blot Turbo Transfer System (BIO-RAD). This system reduces transfer duration to 8 min without sacrificing performance when compared with traditional tank transfer.

### 2.10.3 Antibody Staining

Membranes were incubated with 5% fat-free milk prior to incubation with rabbit polyclonal antibodies directed against GAPDH (1:10000 Abcam), FAM38A (1:500 Abcam), FAM38B (1:500 Abcam), and c-fos (1:1000 Cell Signalling

Technology), c-jun (1:1000 Cell Signalling Technology), Proliferating Cell Nuclear Antigen (PCNA, 1:1000, Cell Signalling Technology), ERK (1:1000 Cell Signalling Technology), phospho-ERK (1:1000 Cell Signalling Technology), p38 MAPK (1:1000 Cell Signalling Technology), phospho-p38 MAPK (1:1000 Cell Signalling Technology), JNK (1:1000 Cell Signalling Technology), phospho-JNK (1:1000 Cell Signalling Technology) overnight at 4℃. Then the goat anti-rabbit (680 RD) florescent antibody was applied for 90 minutes at room temperature (1:5000, LI-COR) prior to washing with PBS. Visualisation and quantification was undertaken with the LI-COR Odyssey® scanner and software (LI-COR Biosciences). Quantification was performed on ImageJ.

### *2.11 Statistical Analysis*

The individual experiments involved 3 replicates per group. The data were processed by SPSS, and calculated mean / standard deviation was used for presentation in graphs and tables. Statistical differences between the experimental groups were determined using the Analysis of variance (ANOVA) followed by Tukey post-hoc analysis. $p<0.05$ was considered as statistically significant.

# Chapter 3

# Results

# Isolation and Multipotency of rat Mesenchymal Stem Cells

## *3.1 Introduction*

DPSCs, PDLSCs and BMSCs are three of the main stem cell sources used for dental tissue regeneration with a significant amount of research reporting that mechanical loading, such as orthodontic forces (Dhopatkar et al., 2005b), tensile stretch (Han et al., 2008, Lee et al., 2008, Lee et al., 2010), hydrostatic pressure (Yu et al., 2009) can affect matrix protein secretion, adhesion, proliferation and differentiation of these cells.

Study of the responsiveness of DPSC, PDLSC and BMSC to LIPUS is of considerable interest to enable this approach to be used as an adjuvant stimulus for dental tissue regeneration. This chapter describes the findings relating to DPSC, BMSC and PDLSC isolation from rat tissues and their subsequent characterisation as MSC-like cells.

## *3.2 Isolation and Culture of rat MSCs*

Following protocols derived from previous studies (See 2.1), DPSC, BMSC and PDLSC were isolated and subcultured for *in vitro* LIPUS treatment. The heterogeneity in terms of cell morphology of passage 0 cells can be observed in all stem cell types (Fig. 6)

### 3.2.1 Dental Pulp Stem Cells (DPSCs)

Digestion of the dental pulp using the trypsin-based protocol yielded ~5,000,000 cells from 8 incisors (derived from two 6-week-old male rats). Over the first week of culture, the DPSCs expanded as distinct colonies which subsequently merged in culture and the cells appeared fibroblast-like and spindle-shaped in morphology (Fig. 5).

### 3.2.2 Bone Marrow Stem Cells (BMSCs)

After 24 h, a heterogeneous culture of BMSCs scattered evenly on the surface of the culture flask was observed. Their polygonal cell shape was indicative as BMSCs (Fig. 6). After 3-7 days of culture, 70% confluence was achieved and cells were subcultured and expanded for further analyses.

### 3.2.3 Periodontal Ligament Stem Cells (PDLSCs)

Digestion of the PDL with type I collagenase combined with trypsin yielded ~200,000 cells from ~20 molars obtained from two 6-week-old male rats. After 7-14 days culture, the dissociated PDLSCs expanded as colonies which subsequently merged (Fig. 6). The cell morphology also appeared spindle-shaped and fibroblast-like. Cells were subsequently subcultured and expanded for further analyses.

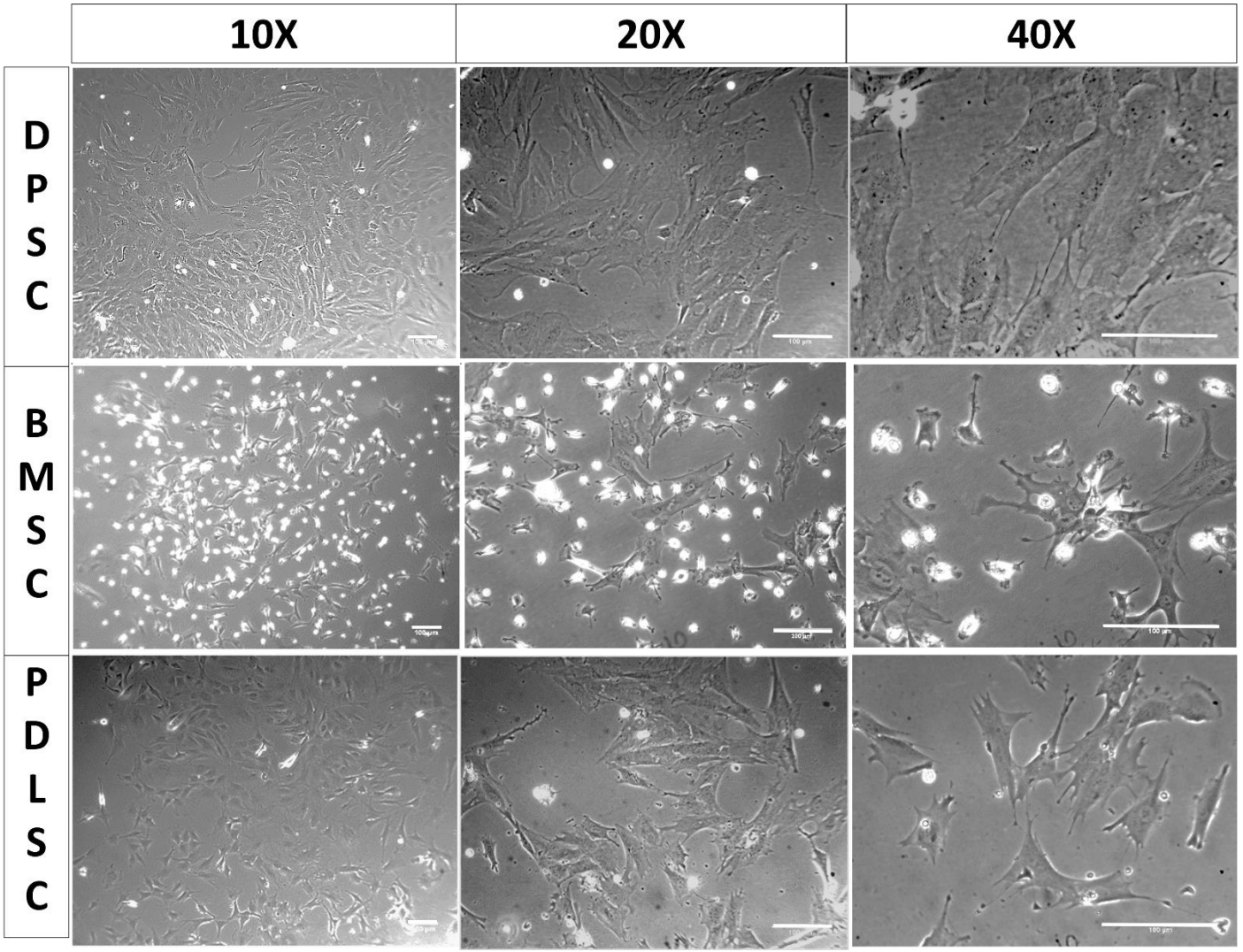


**Figure 6.** Representative phase-contrast images of primary cultures of DPSC, PDLSC and BMSC. Passage zero cultures (P0) at 10X, 20X, 40X magnification, respectively. Scale bars represent 100µm.

## *3.3 Multipotency of rat MSCs*

### 3.3.1 Dental Pulp Stem Cells (DPSCs)

DPSCs were cultured in osteogenic and adipogenic media to determine their differentiation potential. Following osteogenic induction, mineralized nodules were observed after culture for 3 weeks and mineralization was confirmed by ARS staining. No mineralization was observed in the control cultures which were not supplemented with lineage induction media (Fig. 7). DPSC demonstrated strong potential for osteogenic differentiation by producing a large amount of ARS positively stained, calcified nodules (Fig. 7).

In adipogenic induction, lipid-containing cells were observed after culture for 3 weeks. Oil red O staining highlighted the presence of lipid droplets within the cells. No lipid droplets were observed in the control culture (Fig. 7).

### 3.3.2 Bone Marrow Stem Cells (BMSCs)

Mineralization was confirmed in the BMSC cultures by ARS staining which was extensive following long-term culture in osteogenic-induction medium (Fig. 7). No ARS stained mineralization was observed in control cultures (Fig. 7). In BMSC, the mineralization was abundant and the calcified nodules formed a sheet-like

calcified layer.

In adipogenic induction media, lipid-filled cells were observed after culture following 3 weeks of induction (Fig. 7). No lipid droplets were observed in the control group.

### 3.3.3 Periodontal Ligament Stem Cells (PDLSCs)

In osteogenic media, PDLSC cultures formed limited and scattered mineralized nodules compared with DPSC and BMSC cultures. No mineralisation was observed in the control supplemented cultures (Fig. 7). Similarly, following adipogenic induction, no lipid droplets were present in the control group (Fig. 7) however lipid-filled cells were observed after culture for 3 weeks (Fig. 7).

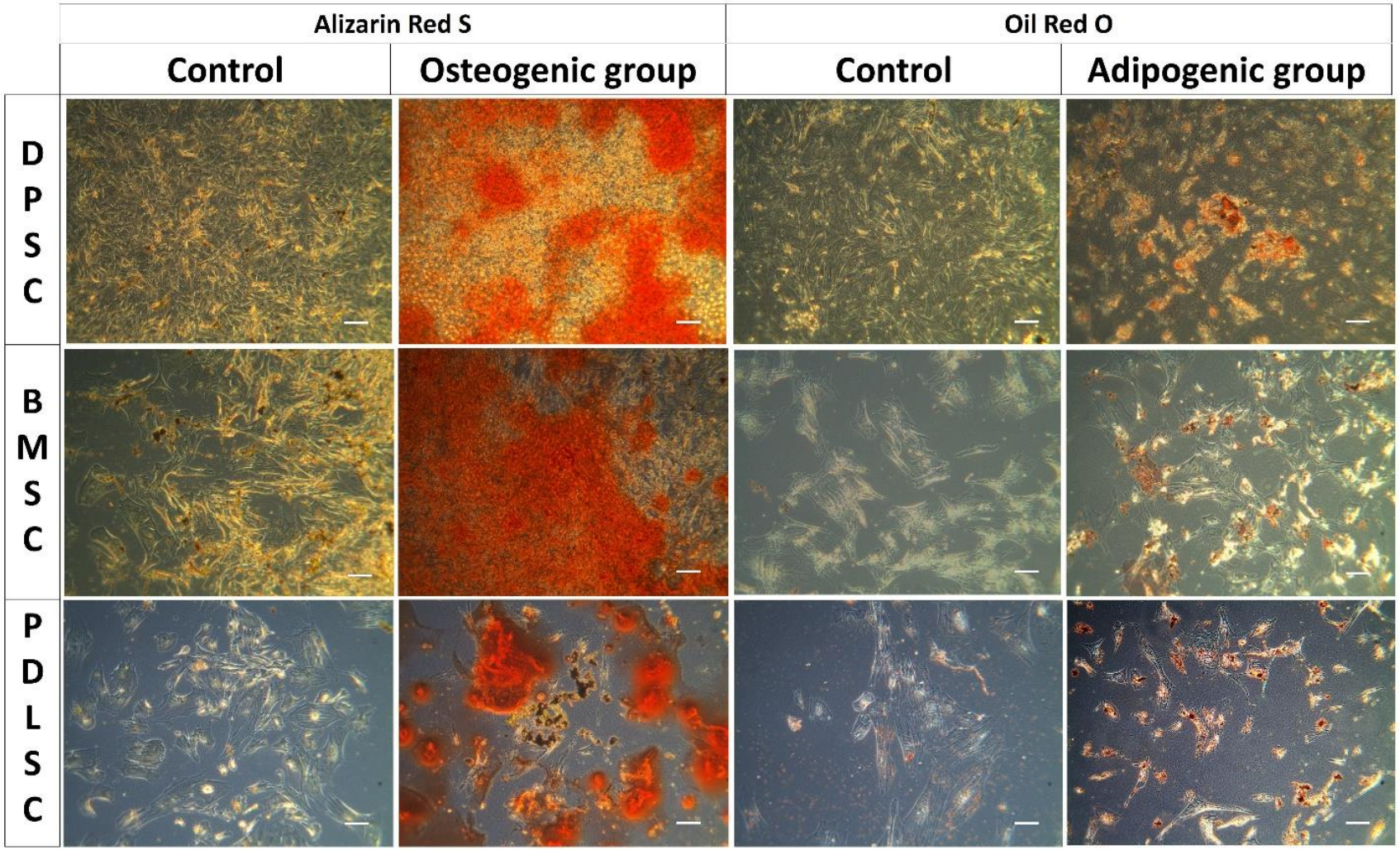


**Figure 7.** Differentiation induction analysis in DPSC, BMSC and PDLSC cultures. Osteogenic differentiation and mineralization was evident by ARS staining for mineralization. Oil red O staining was used to demonstrate lipid-filled cells to signify adipogenic differentiation. Representative images of three experiments were obtained using a phase-contrast microscope. Scale bars represent 100µm.

## *3.4 Gene Expression Characterisation of rat MSCs*

Semi quantitative RT- PCR (sqRT- PCR) analysis demonstrated the expression of CD29, CD90, vimentin, Nanog, Klf4, DMP1, OCN, OPN and BSP (Fig. 8). CD29, CD44, and vimentin are regarded as MSC markers; Nanog and Klf4 as pluripotent markers; DMP1, OCN, OPN and BSP as hard tissue, mineralization-related markers relevant to dental tissues. Relatively lower expressions of these genes, in particular the MSC marker CD90, were observed in cultures in passage 4 compared with passage 2. Thus, passage 2 cells were used in all downstream ultrasound studies.

### 3.4.1 Dental Pulp Stem Cells (DPSCs)

DPSCs in passage 2 and 4 showed differential expression of MSC and mineralization markers (Fig. 8). DPSCs in passage 2 generally showed higher relative gene expression levels of CD29, CD90, DMP1, OCN, OPN and BSP. DPSCs in passage 4 showed the limited expression of CD90. However, DPSCs in passage 4 demonstrated higher expression of the pluripotent marker Nanog. The expression of Klf4 showed no statistical difference between passage 2 and 4 cultures.

### 3.4.2 Bone Marrow Stem Cells (BMSCs)

For BMSC, cells in passage 2 and 4 showed differential expression of MSC and mineralization markers, except pluripotent markers Klf4 and Nanog (Fig. 8). BMSCs in passage 2 generally showed higher gene expression levels of CD29, CD90, Vimentin, DMP1, OCN, OPN and BSP. Expression of Klf4 and Nanog showed no statistical difference between cells in passage 2 and 4. Interestingly, both BMSCs and DPSCs in passage 4 showed weak expression of CD90.

### 3.4.3 Periodontal Ligament Stem Cells (PDLSCs)

PDLSCs in passage 2 showed higher gene expression of CD90, DMP1, OCN and OPN than passage 4 (Fig. 8). Expression of CD29, Vimentin, Nanog, Klf4 and BSP showed no statistical difference between cells in passage 2 and 4. Compared with DPSCs and BMSCs, PDLSCs showed limited differential expression levels of the marker genes studied.

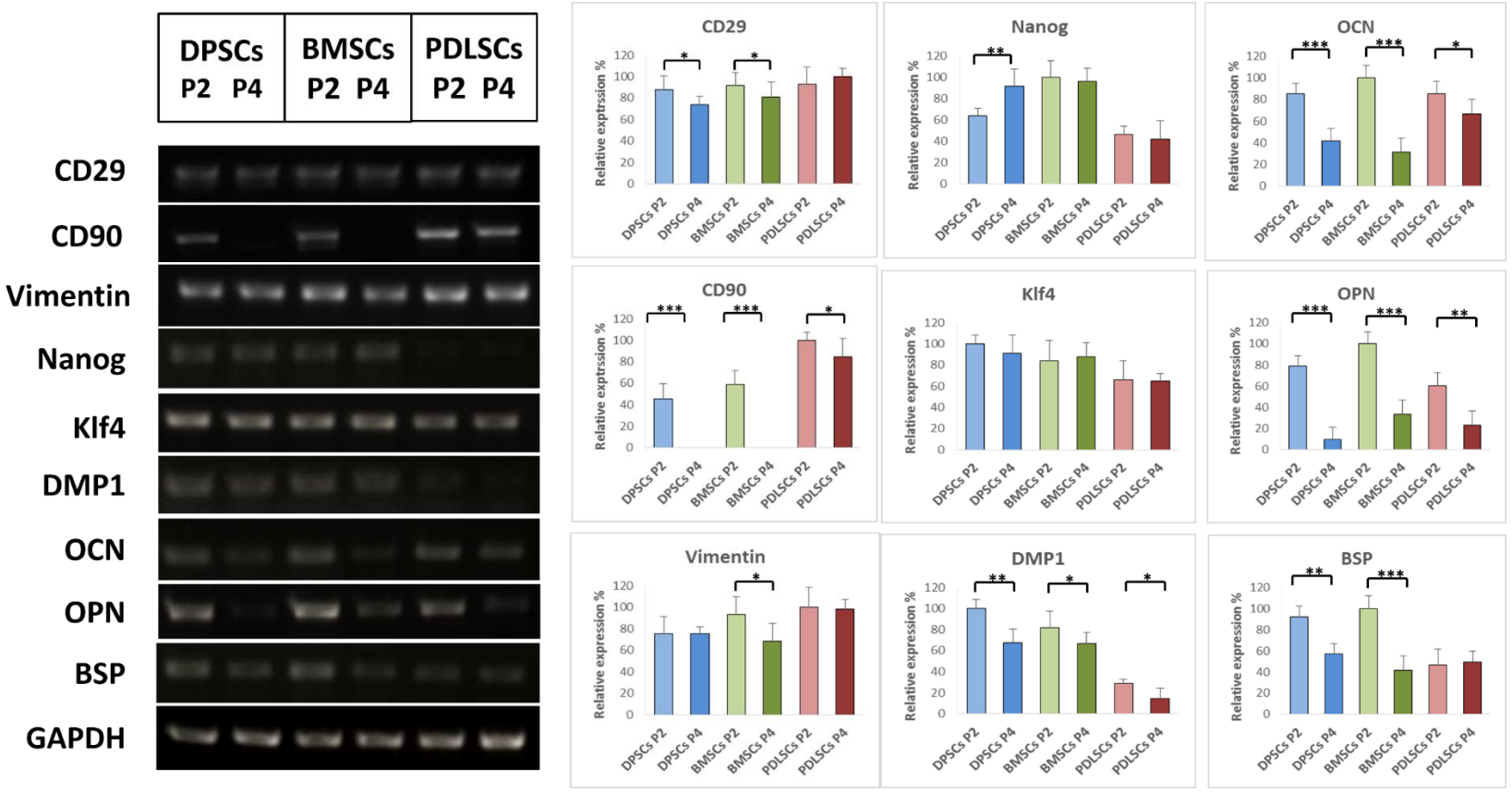


**Figure 8.** sqRT-PCR analysis for gene expression profiles demonstrating the influence of passage on the expression of genes related to the MSC and dental cell phenotypes. All three cell types expressed CD29, CD90, vimentin, Nanog, Klf4, DMP1, OCN, OPN, and BSP. The expression of marker genes in passage 2 and passage 4 are analysed and compared against each other. *$p$<0.05, **$p$<0.01 and ***$p$<0.001 versus experiments. Values represent the mean ± SD of three independent assays.

## *3.5 Conclusion*

The isolation and culture of DPSC, BMSC and PDLSC have been described together with their osteogenic and adipogenic differentiation potential. The gene expression of MSC markers, pluripotent markers and mineralization-related markers were highlighted using sqRT-PCR.

In conclusion, the isolated DPSC, BMSC and PDLSC showed typical characteristics of MSCs: 1) adherence to plastic surface, 2) multilineage differentiation potential, and 3) stable expression of MSC markers. Compared with passage 4 cells, passage 2 cultures displayed a higher expression of several markers genes, hence the latter cultures were used for the experiments described in the following results chapters.

# Chapter 4

# Results

# Effect of LIPUS on

# Proliferation of rat MSCs

## *4.1 Introduction*

The biological effect of LIPUS on cells are dependent on intensity and treatment duration but may also be cell type dependent (Hsu and Huang, 2004, Feng et al., 2010). Stem cell proliferation is an important response during the processes of tissue renewal, repair and regeneration (Cui et al., 2007, Sloan and Smith, 2007). This chapter aimed to compare the effects of LIPUS on cell growth and proliferation of DPSC, BMSC, and PDLSC and to identify the optimal parameters for each stem cell lineage to underpin further study.

## *4.2 Cell Growth*

Cells subjected to LIPUS were observed under phase-contrast microscopy. The morphology of the cells post-LIPUS appeared to remain unchanged. However, the post-treatment cells clustered in denser arrangements than the control group potentially indicating an increase of cell growth post-LIPUS treatment (Fig. 9).

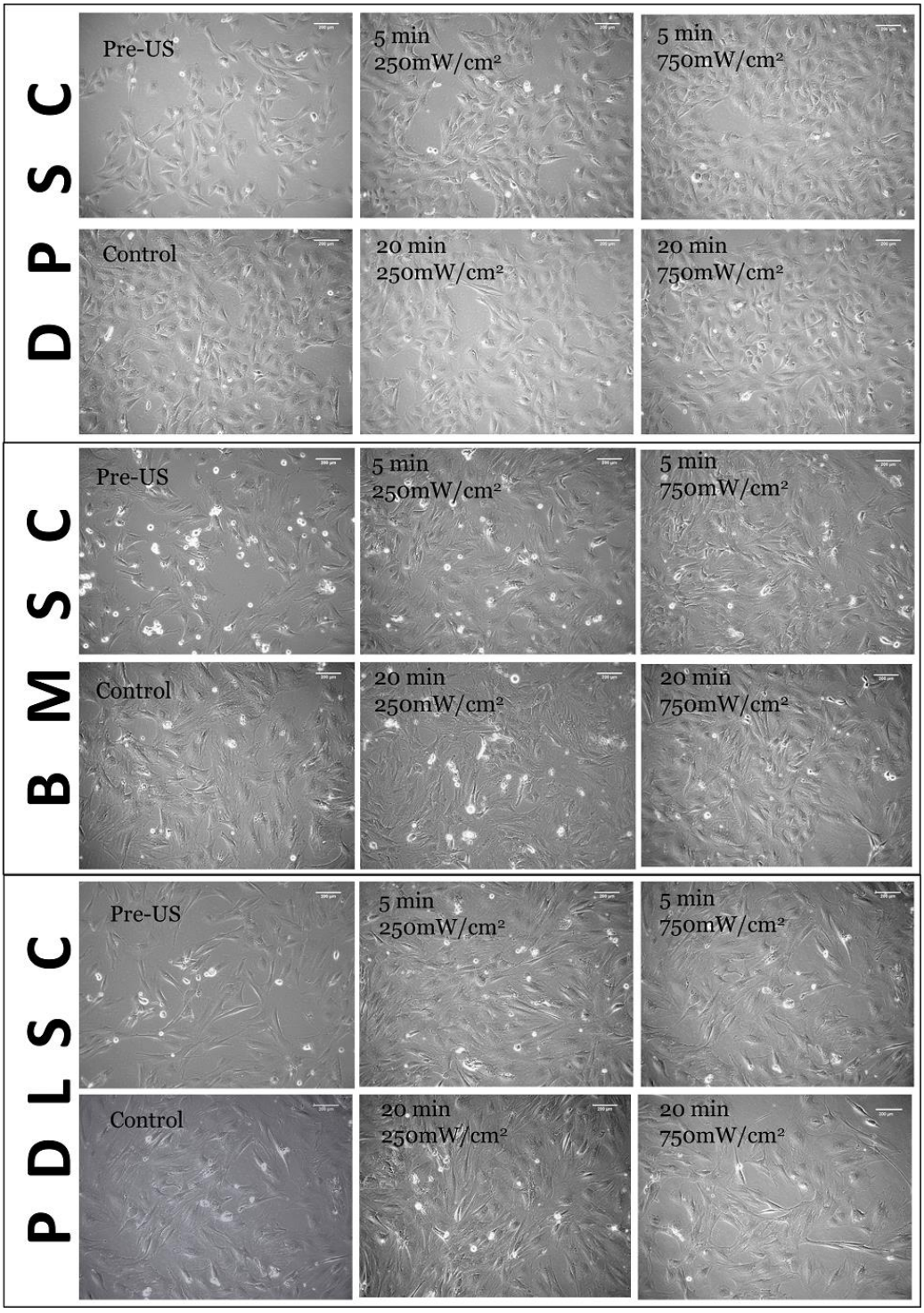


**Figure 9.** Representative phase contrast microscope images of control and LIPUS treated cells cultured for two days post-exposure. Images of cultures were captured 20X magnification. Scale bars represent 200µm.

Cell growth was increased by LIPUS after two day-culture in all experimental groups. However, the extent of the proliferative effects differed among cell types (Fig. 10). Increase in cell numbers in response to LIPUS in rat MSCs ranked as: DPSC < PDLSC < BMSC (Fig. 10). DPSC numbers increased by 14.1% ($p<0.05$) and 20.2% ($p<0.01$) compared with non-treated controls following 5 and 20 min 750mW/cm$^2$ ultrasound exposure, respectively; PDLSC cell number increased by 27.0% ($p<0.01$) and 20.3% ($p<0.05$) following 5 min and 20 min 250mW/cm$^2$ ultrasound exposure; BMSC numbers increased by 29.7% ($p<0.01$) and 50.2% ($p<0.01$) following 5 min and 20 minutes 750mW/cm$^2$ ultrasound exposure (Fig. 10).

The effect of LIPUS on DPSC numbers was only evident after 250mW/cm$^2$ of LIPUS or for PDLSCs after 750mW/cm$^2$ of LIPUS. In all groups, 5 min or 20 min exposure duration exerted no statistical differences in cell numbers for the same cell types and/or intensities ($p>0.05$). These findings indicated that low-intensity ultrasound promoted cell growth increases dependent on intensities, but not on the tested US exposure durations.

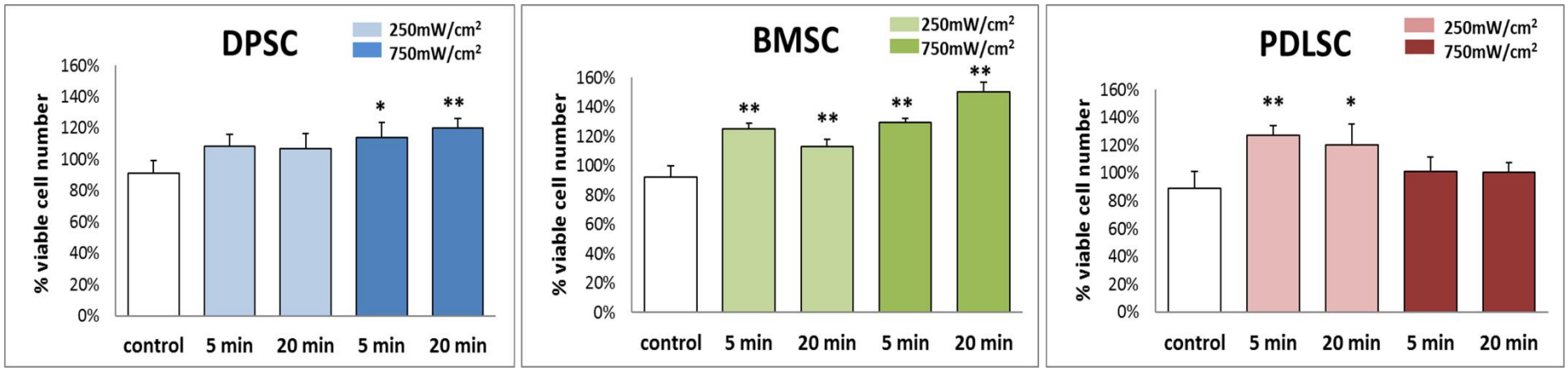


**Figure 10.** The effect of ultrasound on DPSC, BMSC and PDLSC cell numbers following exposure to 1MHz ultrasound at 250mW/cm$^2$ and 750mW/cm$^2$. Results are expressed as percentage of viable cell number after 48 h post-exposure. **P*<0.05, ***P*<0.01, compared with controls which were untreated with respect to LIPUS exposure.

### *4.3 Effect of LIPUS on Cell Proliferation Analysed by BrdU Labelling*

LIPUS increased cell proliferation of DPSC, BMSC and PDLSC, regardless of the LIPUS treatment duration as determined by BrdU labelling. Proliferation of DPSC was significantly increased in response to all ultrasound exposures with the highest proliferation ratio resulting from 750mW/cm$^2$ treatment (Fig. 11). In BMSCs, proliferation was equally increased in all ultrasound groups ($p$<0.05) while 750mW/cm$^2$ ultrasound induced a slightly higher increase in comparison with the lower intensity (Fig. 11). Interestingly, PDLSC proliferation was significantly increased following 5 min exposure to 250mW/cm$^2$ ultrasound ($p$<0.01) (Fig. 11). Notably, the 5 min treatment group showed the higher stimulation with regards to BrdU labelling as compared with the 20 min exposure group in PDLSC.

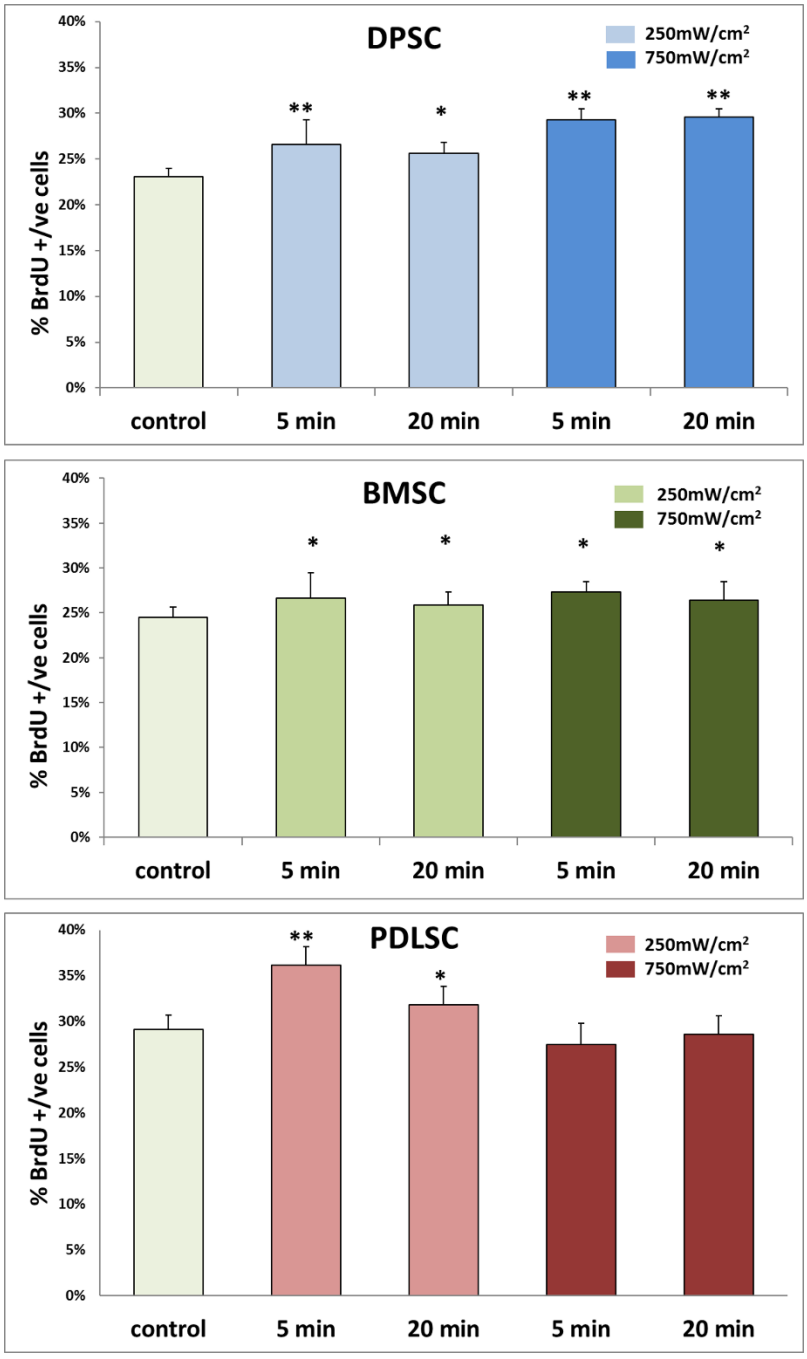


**Figure 11.** LIPUS effect on cell proliferation as determined by BrdU labelling 24 h after ultrasound treatment. Four ultrasound parameters were tested: 5 min 250mW/cm$^2$, 20 min 250mW/cm$^2$, 5 min 750mW/cm$^2$ and 20 min 750mW/cm$^2$. *$p<0.05$ and **$p<0.01$ versus the untreated controls. Values represent the mean percentage of BrdU positive cells ± SD of three independent experiments.

### *4.4 Selection of Ultrasound Parameters for Future Cell Analyses*

The above findings indicated that 1) LIPUS increased cell proliferation in a cell specific way. 2) The intensity of LIPUS influenced the level of increase. 3) The effect of extended treatment duration (20 min) did not produce a further significant difference in cell proliferation of the different cell types.

In the following experiments, the specific parameters which stimulated the highest level of increase in cell proliferation were selected. These were 5 min 750mW/cm$^2$ for DPSC and BMSC; 5 min 250mW/cm$^2$ for the PDLSC cultures.

### *4.5 Analysis of Levels of Proliferation-related Proteins Following US Exposure*

Western blotting was used to analyse levels of proliferation related proteins including PCNA, c-fos and c-jun in DPSC, BMSC and PDLSC post-LIPUS treatment. Level of proteins were normalized to that of GAPDH. The results demonstrated that LIPUS increased the expression of the proliferation related proteins analysed in DPSC, PDLSC and BMSC (Fig. 12). In DPSC and PDLSC, 4 h and 24 h after 5 min of ultrasound stimulation, the expression of PCNA, c-jun and c-fos were increased. Interestingly, the highest level of PCNA and c-jun were

observed 24 h after ultrasound while highest level of c-fos was observed 4 h after ultrasound (Fig. 12 A,B,E,F).

In BMSC, the protein levels of c-jun increased time-dependently. However, unlike DPSC and PDLSC, the highest level of PCNA and c-fos in BMSC were observed 4 h after ultrasound exposure (Fig. 12 C,D).

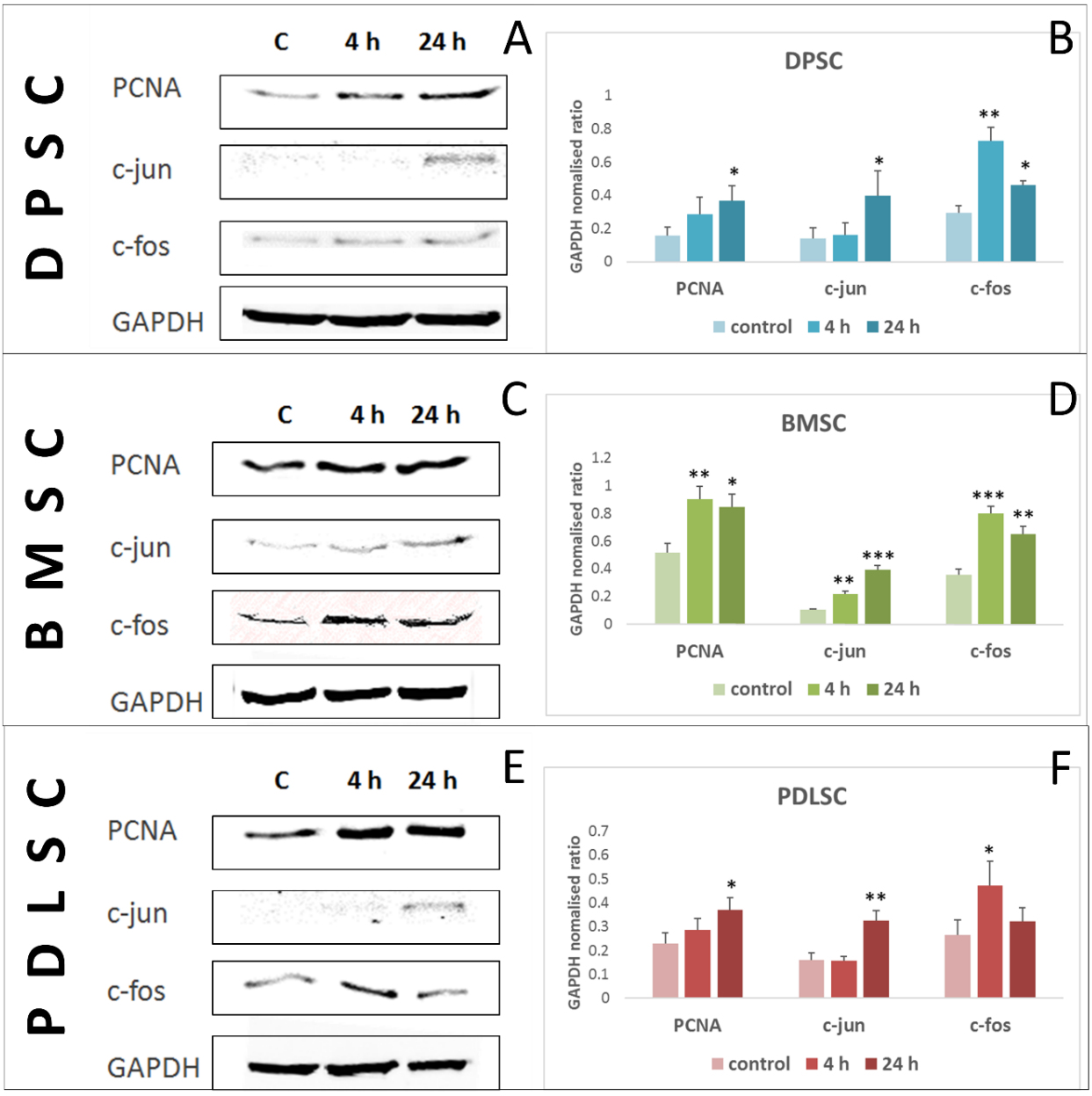


**Figure 12.** Western blot analysis of proliferation related proteins in DPSC, BMSC and PDLSC post-LIPUS treatment. Cell samples were treated by LIPUS and collected at 4 and 24 h post-exposure. GAPDH was used to normalise levels of protein in control and experimental groups. A, C, E): Representative Western-blotting image captured by LI-COR visualization. B, D, F): colorimetric analysis showing quantification of proliferation related proteins after LIPUS treatment. *$p$<0.05, **$p$<0.01 and ***$p$<0.001 compared with the untreated controls, n=3.

## *4.6 Conclusion*

Cell counts and BrdU staining analyses demonstrated LIPUS-induced changes in cell growth and proliferation, respectively. These data were supported by Western blot analyses showing the up-regulation of proliferation-related proteins (PCNA, c-fos and c-jun) in all dental stem cells analysed (i.e. DPSC, BMSC and PDLSC). The results indicated that the increase in proliferation is irrespective of LIPUS treatment duration, but dependent on the LIPUS intensity. Thus, in all following experiments, 5 min 750mW/cm$^2$ were applied to DPSC and BMSC and 5 min 250mW/cm$^2$ to PDLSC cultures.

# Chapter 5

# Results

# MAPK Signalling Following Ultrasound Stimulation

This chapter has partly been published in *Ultrasound Stimulation of Different Dental Stem Cell Populations: Role of Mitogen-activated Protein Kinase Signaling.* J Endod, 2016. *Q Gao，AD Walmsley，PR Cooper，BA Scheven.* **42**(3): p. 425-431

## *5.1 Introduction*

The mechanism by which LIPUS stimulates cells and tissues has generally been attributed to its biomechanical component. Through acoustic microstreaming and physical radiation, LIPUS may affect the cell membrane and the cytoskeleton to trigger downstream signalling processes (Padilla et al., 2014). MAPKs (ERK, JNK and p38 MAPK) have been demonstrated to play a role in mechanotransduction in various cell types, such as bone cells (Liedert et al., 2006), periodontal ligament cells (Kook and Lee, 2012), and muscle cells (Li and Xu, 2007). p38 and ERK pathways have also been reported to control cell proliferation following mechanical stimuli (Kook and Lee, 2012, Zhou et al., 2004).

This study analysed the cellular activation of ERK1/2, JNK and p38 MAPK after LIPUS treatment to gain further insight into the signalling mechanisms underpinning LIPUS-increased proliferation.

## *5.2 Activation of p38, ERK1/2, JNK MAPK after US Exposure*

Specific ultrasound treatment parameters which promoted the highest level of cell proliferation for each cell type (Section 4.3) were selected to analyse the activation of signalling pathways following ultrasound treatment.

### 5.2.1 Dental Pulp Stem Cells (DPSCs)

DPSCs were treated with 750mW/cm$^2$ LIPUS for 5 min (see Chapter 4). In DPSC, ERK1/2 was activated immediately post-treatment, followed by a decrease in the activation level until 1h after ultrasound exposure. Levels then increased again and remained relatively high up to 4 h post-treatment (Fig. 13).

### 5.2.2 Bone Marrow Stem Cells (BMSCs)

Ultrasound exposure of 5 min at 750mW/cm$^2$ was applied to BMSCs which led to an increase in phosphorylation of JNK MAPK (Fig. 13). Interestingly, JNK was also activated immediately post-treatment, followed by a decrease until 1h after ultrasound treatment, after which the JNK phosphorylation increased again and remained relatively high for up to 4 h post-treatment (Fig. 13). This activation

profile was similar to that detected in the US-induced ERK1/2 activation in DPSCs.

### 5.2.3 Periodontal Ligament Stem Cells (PDLSCs)

For PDLSCs, 5 min 250mW/cm$^2$ was applied based on results presented in Fig. 9 (see Chapter 4). After ultrasound treatment, JNK MAPK was activated immediately and remained relatively high from 1 h to 4 h post-treatment (Fig. 13). Activation of p-p38 MAPK was increased significantly only at 4 h after ultrasound exposure (Fig. 13).

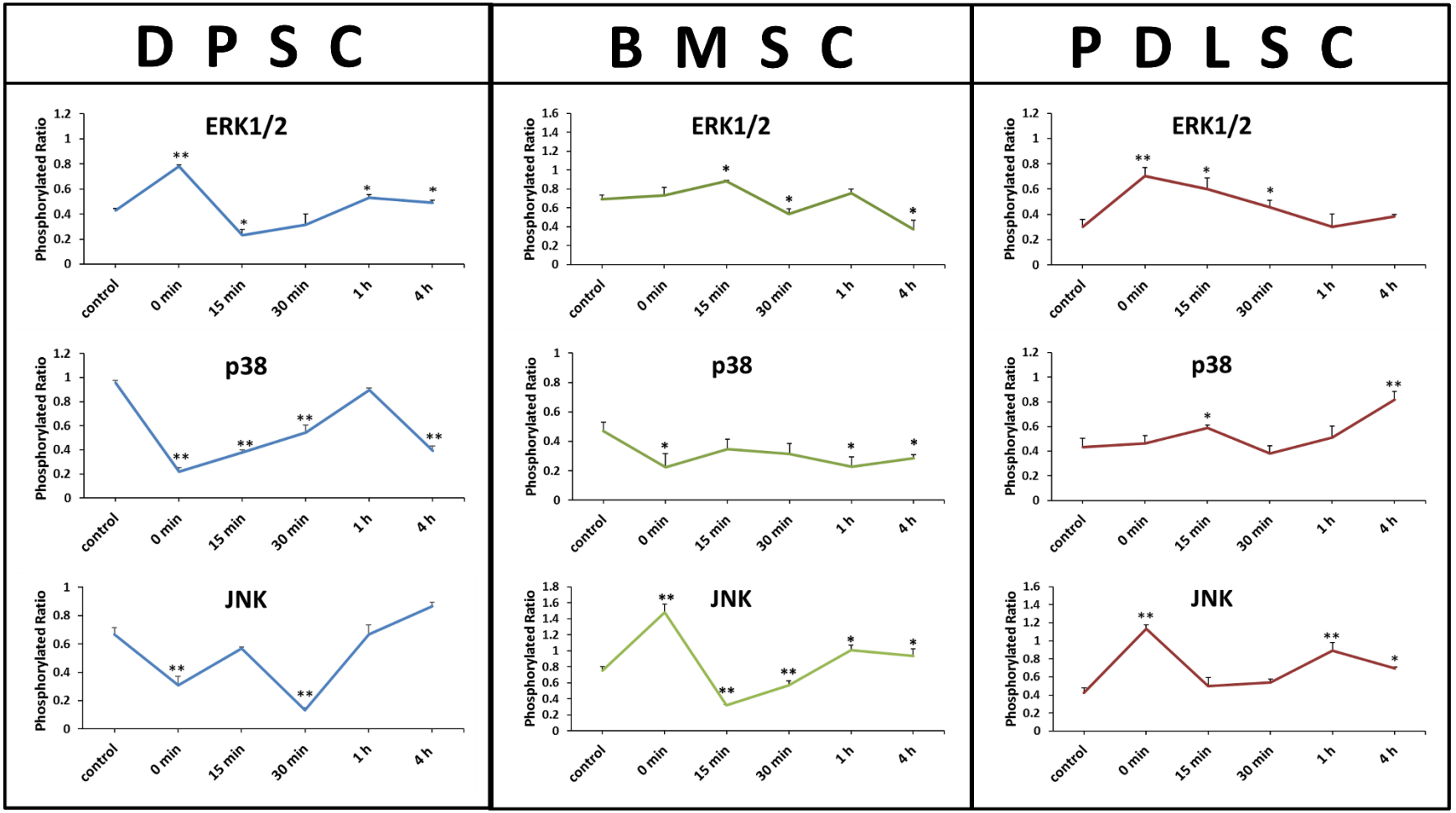


**Figure 13.** Activation of MAPKs is involved in ultrasound stimulated DPSC, BMSC and PDLSC proliferation. To indicate the role of MAPK in ultrasound induced proliferation, total and phosphorylated MAPK pathway protein (p-ERK1/2, p-JNK and p-p38) were determined by ELISA. The phosphorylation ratio was calculated up to 4 h after ultrasound application. *$p<0.05$ and **$p<0.01$ versus the untreated controls. Values represent the mean ± SD of three independent assays.

### *5.3 Long-term Activation of p38, ERK1/2, JNK MAPK after US Exposure*

Western blot analysis was performed in DPSC and PDLSC cultures to confirm activation of the MAPK signalling pathways post-LIPUS and to determine whether relatively long-term activation can be observed after the 5 min ultrasound treatment. BMSC was not analysed in this section because ELISA has been done prior to western blot.

ERK1/2, JNK and p38 MAPK (phosphorylated and total) were measured quantitatively 4 h and 24 h after LIPUS treatment (Fig. 14). The results demonstrated that MAPK phosphorylation increased in both DPSC and PDLSC cultures and persisted for up to 24 h after LIPUS treatment. In DPSC at 24 h post-LIPUS, the phosphorylation of ERK1/2 increased approximately 5-fold compared with untreated controls and was 2-fold increased compared with 4 h post-LIPUS treatment (Fig. 14B). In PDLSC, the highest level of JNK was observed 4 h after LIPUS treatment and JNK phosphorylation decreased at 24 h compare with levels at 4 h after treatment (Fig. 14G). Thus, long-term activation of MAPKs in both cell lineages post-LIPUS corresponded with previous short-term ELISA results presented in Chapter 4.

Meanwhile, phosphorylation of p38 increased time-dependently in PDLSC after LIPUS, and at 24 h after treatment the level of phospho-JNK was ~3-fold higher

than the untreated control (Fig. 14H). Interestingly, while the above signalling pathways were significantly activated, the phosphorylation of JNK MAPK in DPSC, p38 MAPK in DPSC and ERK1/2 in PDLSC signalling pathways decreased (Fig. 14 C,D,F).

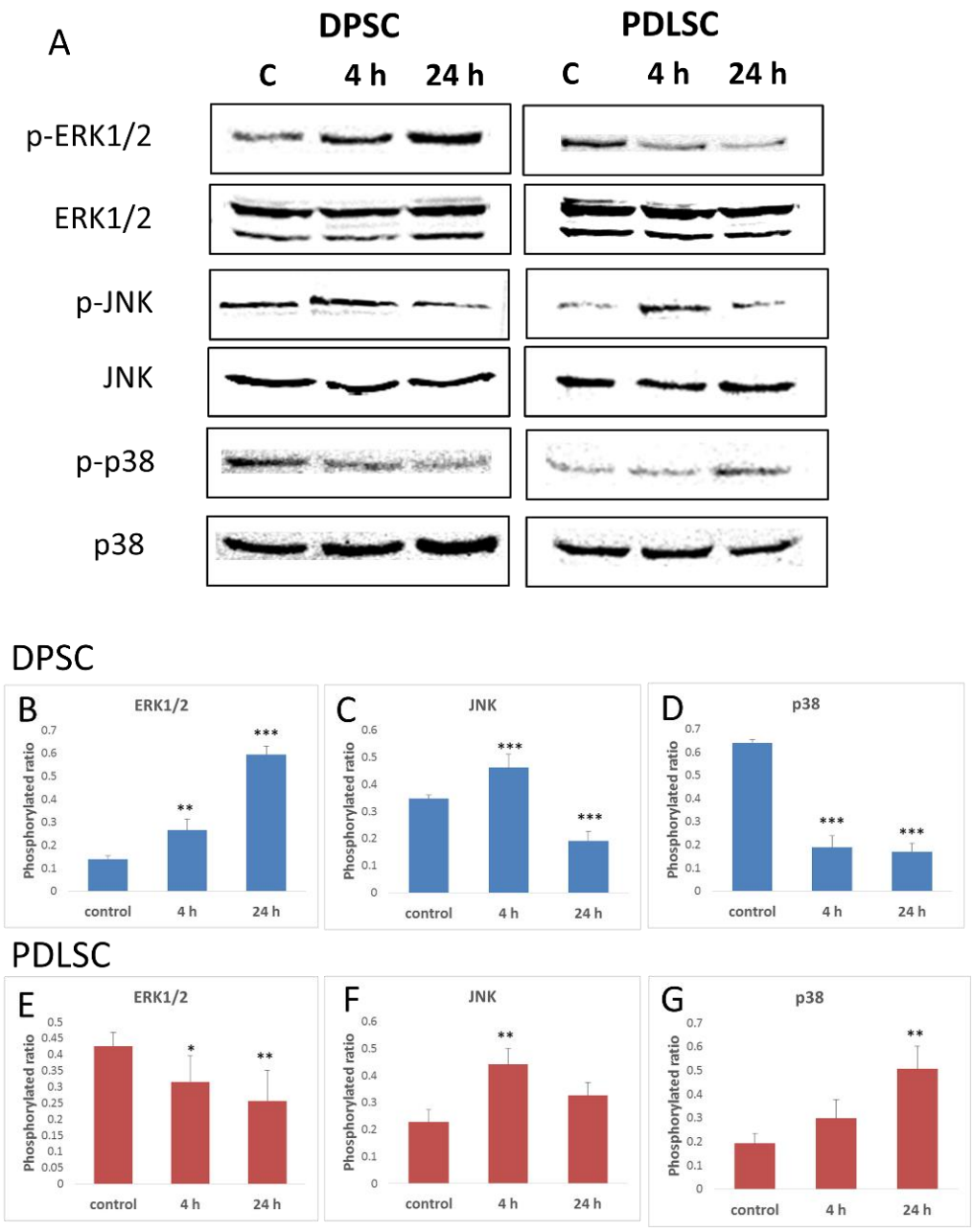


**Figure 14.** LIPUS effects on MAPK signalling in DPSC and PDLSC. A): Immunoblotting image of DPSC and PDLSC when subjected to LIPUS for 5 min and then processed for Western blot analysis 4 h and 24 h post-treatment. B) – F): Change of MAPKs activation in DPSC and PDLSC in long-term groups. The phosphorylated ratio MAPKs are presented as parameter of MAPK activation. Phosphorylated ratio = phospho-MAPKs / total MAPKs. *P<0.01, **P<0.01 and ***P<0.001 versus the untreated controls. Values represent the mean ± SD of three independent assays.

### *5.4 Analysis of the Cellular Effects of Specific Inhibitors of ERK1/2, p38, JNK MAPK Following LIPUS Exposure*

Three MAPK inhibitors were used: PD98059 is a selective inhibitor of ERK1/2; SB203580 is a selective inhibitor of p38 MAPK; and SP600125 is a selective JNK inhibitor (Kook and Lee, 2012). Application of 10μM of these inhibitors is the recommended culture media concentration as reported in the literature, as well as by the manufacturer (TOCRIS, Bristol, UK) (Kook and Lee, 2012). However, to avoid cell type-specific cytotoxicity, the MTT assay was performed to select the appropriate concentration for each cell type. Three concentrations were subsequently selected for analysis: 10μM, 20μM and 40μM. Cell samples are collected 24 h (Day 1) and 48 h (Day 2) after culture with inhibitor. With the increase of inhibitor concentration, cell number generally decreased, and this was especially apparent in the 40μM exposure group (Fig. 15). Conclusively, 10μM inhibitors was applied in the subsequent pathway inhibition experiments.

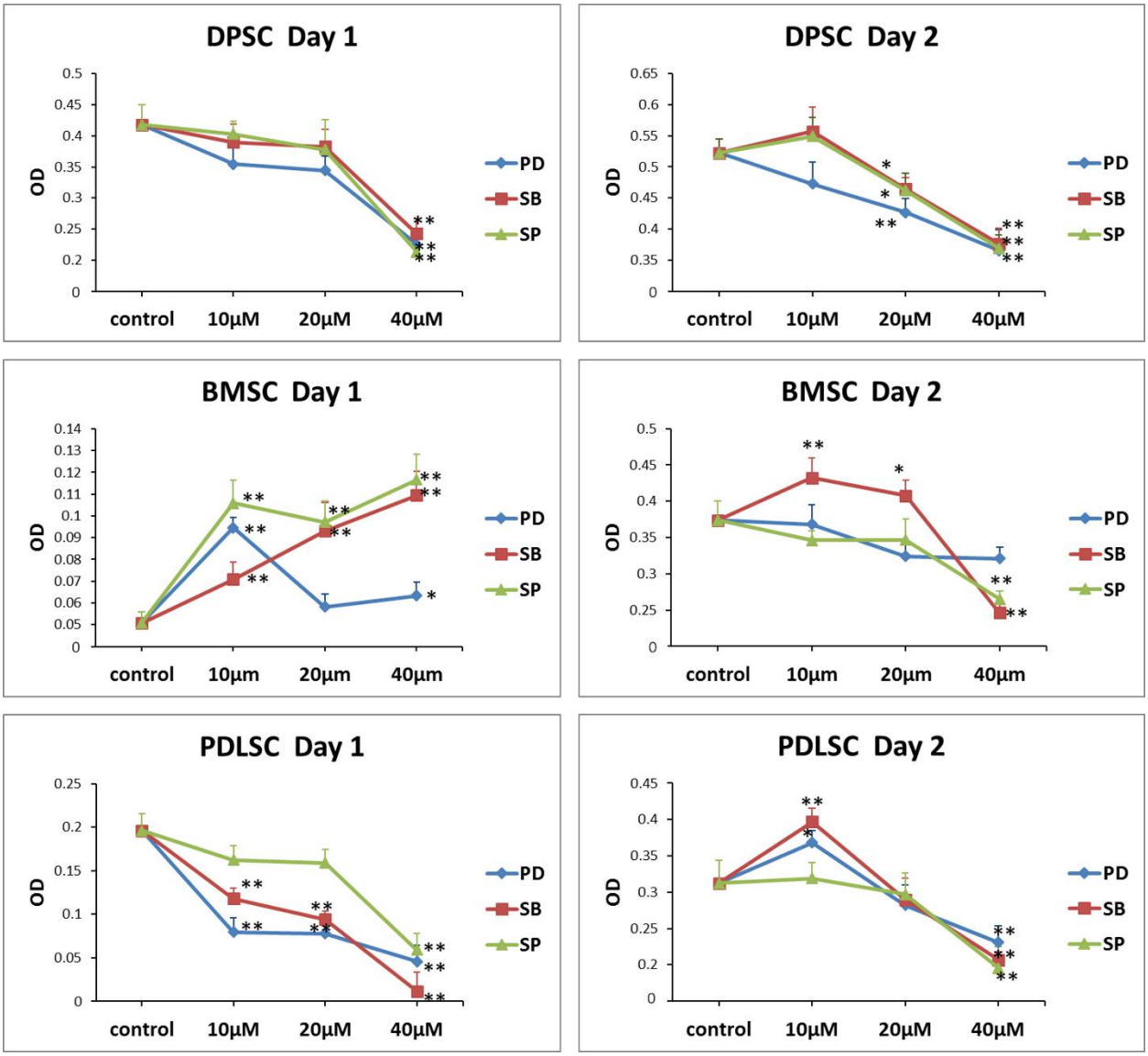


**Figure 15.** Analysis of cytotoxicity of specific MAPK inhibitors using the MTT assay. Three concentrations were tested: 10, 20 and 40µM. MTT assay was performed 24 h and 48 h after treatment with inhibitors. The absorbance values were obtained using an ELx800 plate reader (Biotek, UK) at 590nm. *$p$<0.01 and **$p$<0.01 comparison between experiment groups. Values represent the mean ± SD for three independent assays.

## *5.5 Specific Inhibition of MAPK Pathways Suppress Cell Proliferation Following US Exposure*

### 5.5.1 Dental Pulp Stem Cells (DPSCs)

By culture addition of PD98059, an ERK1/2 inhibitor, 2h prior to ultrasound exposure, US-stimulated proliferation of DPSCs was abrogated indicating a key role of ERK1/2 activation in regulating this process (Fig. 16). However, addition of the JNK and p38 inhibitors SP600125 and SB203580 exerted no inhibitory effects on LIPUS-induced proliferation.

### 5.5.2 Bone Marrow Stem Cells (BMSCs)

The LIPUS-induced proliferation was not observed in the JNK inhibition group (by adding SP600125) indicating a key role of JNK activation in BMSC cultures. BMSC proliferation was not inhibited by PD98059 and SB203580 culture supplementation, excluding the role of ERK1/2 and p38 in BMSC LIPUS activation (Fig. 16).

### 5.5.3 Periodontal Ligament Stem Cells (PDLSCs)

JNK inhibition by SP600125 and p38 inhibition by SB203580 in PDLSCs subjected to ultrasound treatment blocked proliferation post-treatment. These data

indicated involvement of both p38 and JNK MAPK signalling in PDLSC LIPUS activation (Fig. 16).

## *5.6 Conclusion*

LIPUS induced the activation of MAPKs up to 24 h in a cell type-specific manner, as shown by ELISA in combination with Western-blot analyses. In DPSC, ERK1/2 appears to be responsive to LIPUS, but not JNK and p38 MAPK signalling. In BMSCs, JNK signalling is sensitive to LIPUS treatment. However, JNK and p38 were both responsive to LIPUS in PDLSCs.

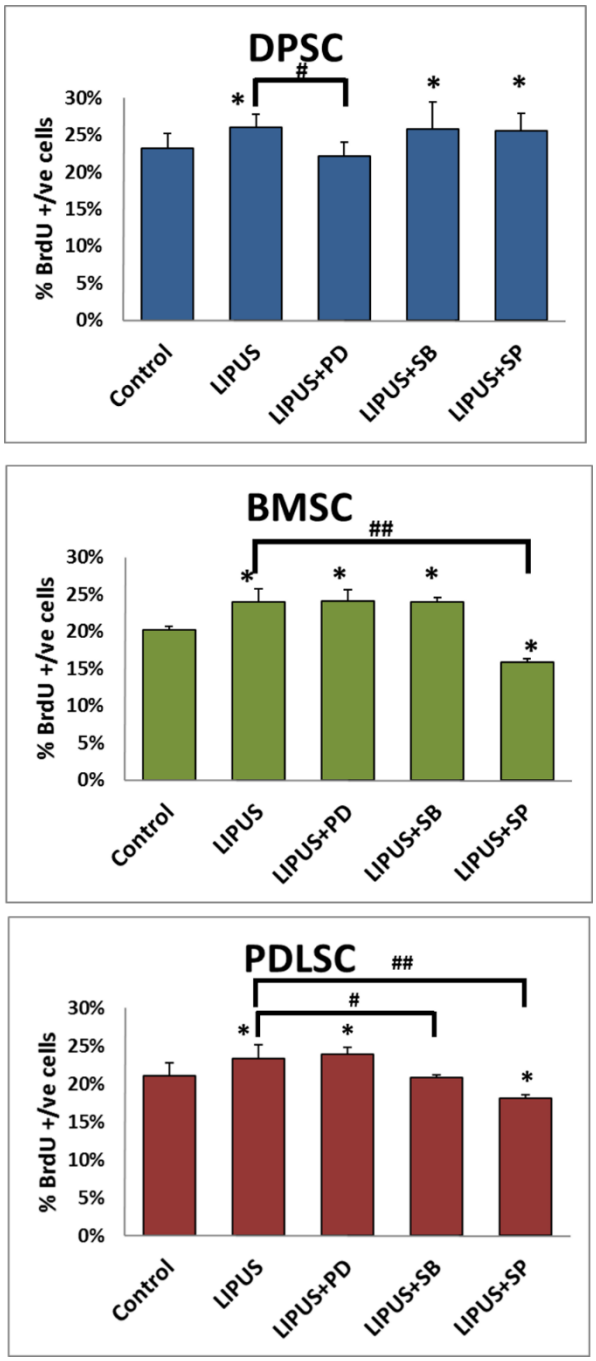


**Figure 16.** MAPKs inhibitors were used to identify the role of specific pathways in cellular LIPUS activation. For DPSCs, ultrasound-induced cell proliferation was inhibited by the ERK1/2 inhibitor. For BMSCs, proliferation was inhibited by the JNK inhibitor, whilst in PDLSCs inhibited by the JNK and p38 inhibitor. **P*<0.05 and ***P*<0.01 compared with the untreated controls. #*P*<0.05 and ##*P*<0.01 comparison between experiment groups. Values represent the mean ± SD of three independent assays.

# Chapter 6

# Results

# Role of Piezo-type Mechanosensitive Ion Channels in LIPUS-induced ERK1/2 MAPK Signalling

This chapter has in part, been submitted in a paper to a dental journal.

## *6.1 Introduction*

Piezo1 and Piezo2 have been implicated in transferring mechanical forces into biological signals by inducing cationic currents in various eukaryotic cell types, such as endothelial cells and neural crest cells (Ranade et al., 2014, Schrenk-Siemens et al., 2015). Interestingly, Piezo1 and Piezo2 channels might also be involved in integrin activation to affect cellular migration, proliferation and elongation (Volkers et al., 2015). The possible role of Piezo1 and Piezo2 as upstream effectors of integrin-mediated MAPKs activation is therefore studied in this chapter.

Currently only non-specific inhibitors are available for Piezo proteins (Bagriantsev et al., 2014). In this study, Ruthenium Red (RR) was used which reversibly blocks Piezo1 and Piezo2 channels from the extracellular environment. RR is also known as an efficient polycationic pore blocker of TRP channels, which blocks Piezo1 and Piezo2 induced mechanically activated (MA) currents (Bagriantsev et al., 2014).

This chapter focused on the signalling mechanism of ultrasound stimulated proliferation in dental stem cells (DPSC and PDLSC), thus BMSC was excluded in the following experiments.

### *6.2 Expression of Piezo1 and Piezo2 after US Exposure*

Piezo1 and Piezo2 protein expression levels were measured quantitatively by Western blotting in DPSC and PDLSC cultures. In DPSC, LIPUS increased expression of Piezo2 time-dependently. At 24 h post-treatment, Piezo1and Piezo2 were increased by ~3-fold. In PDLSCs, an increase of Piezo1 and decrease in Piezo2 levels were noted after LIPUS treatment; however, these changes were not found to be statistically significant (Fig. 17).

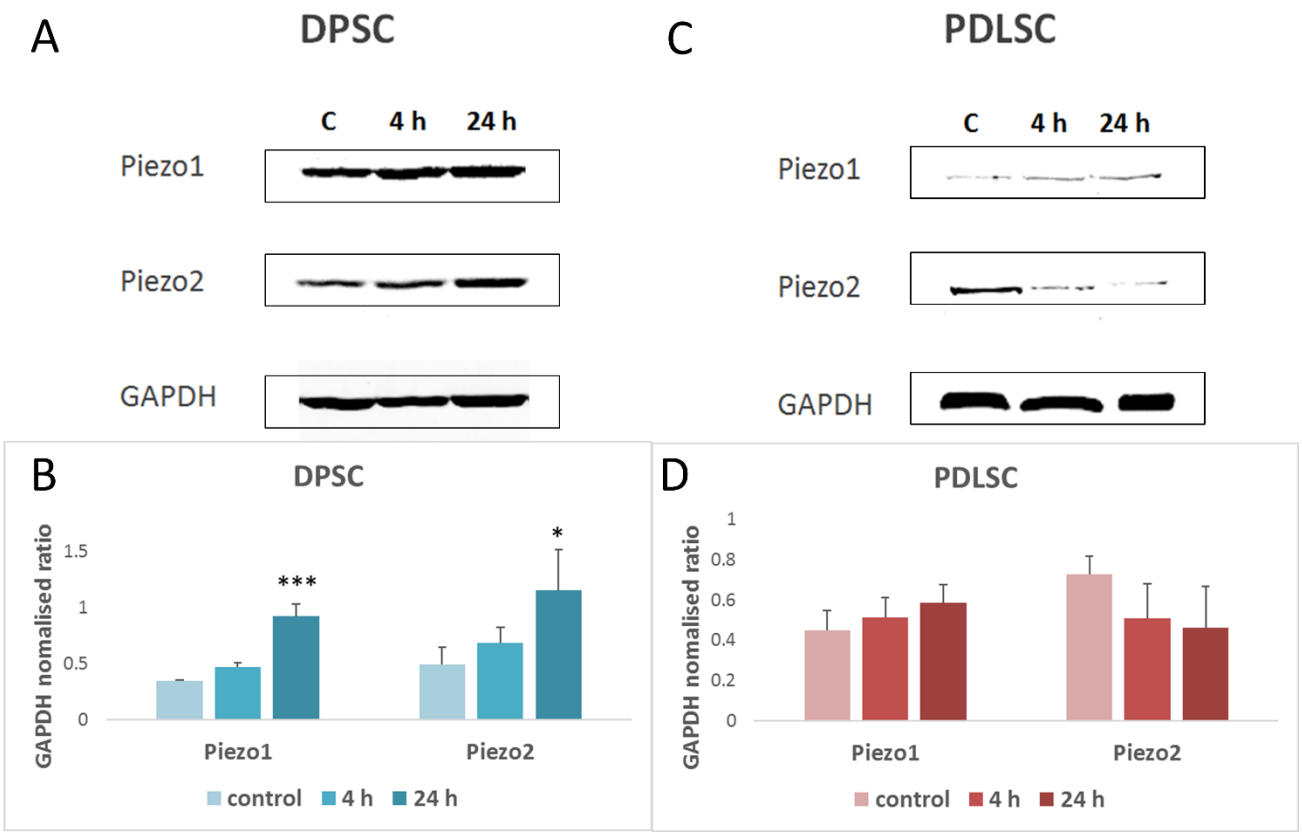


**Figure 17.** Expression of Piezo1 and Piezo2 in DPSC and PDLSC cultures following LIPUS treatment as determined by Western Blotting. A) and C): Immunoblotting image for DPSC and PDLSC protein expression, 4 h and 24 h after LIPUS exposure (LIPUS parameters see Section 4.3). Protein levels of Piezo1 and Piezo2 were normalized against GAPDH levels. **P*<0.05 and ****P*<0.001 compared with the untreated controls. Values represent the mean ± SD for three independent assays.

### *6.3 Piezo Inhibitor Ruthenium Red Cytotoxicity Analysis*

The MTT assay was performed to determine the cell type-specific cytotoxicity of RR. No significant difference in terms of cytotoxicity between the different concentrations tested were detected (Fig. 18). Thus, 20µM RR was used for the experiments, which also corresponded with concentrations used in the literature (Szallasi and Blumberg, 1999, Xu et al., 1999) and, was in accordance with the manufacturer's (Sigma-Aldrich, UK) recommendation. RR was added 5 min prior to US application to provide an optimal inhibition effect.

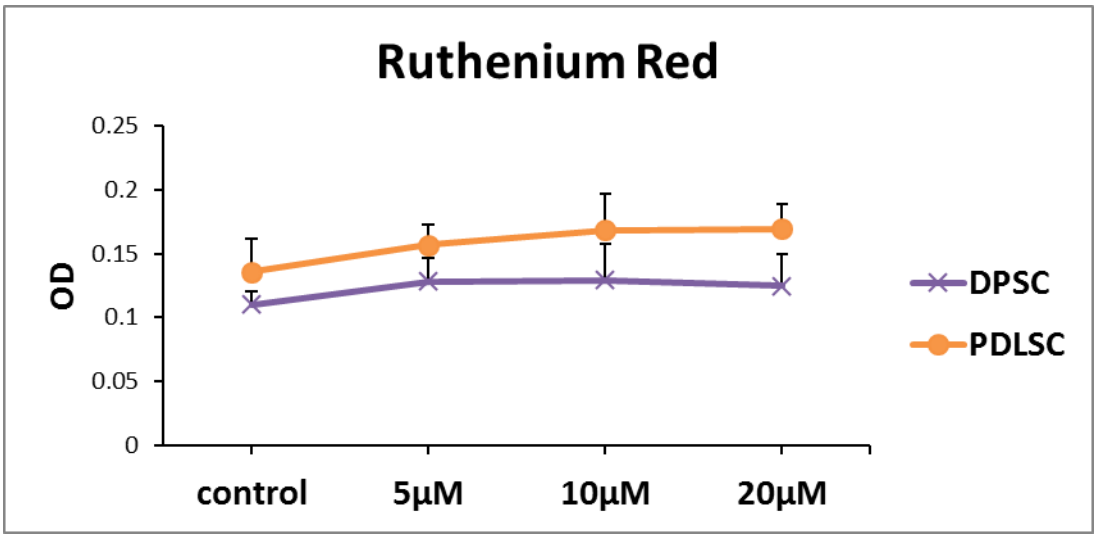


**Figure 18.** MTT assay to determine the cytotoxicity of Ruthenium Red. Three concentrations were tested: 5µM, 10µM and 20µM. Control group was cultured with 0µM inhibitor. MTT solution was added 24 h after exposure of cultures to RR. The absorbance (Optical Density; OD) was measured in an ELx800 plate reader (Biotek, UK) at 590nm. Values represent the mean ± SD for three independent assays.

### *6.4 Inhibition of Piezo1 and Piezo2 Suppress ERK1/2 MAPK*

The effects of RR on MAPK phosphorylation was initially evaluated by ELISA. Six groups were used which included: control, 5 min post-LIPUS, 1 h post-LIPUS, control with RR, 5 min post-LIPUS with RR, 1 h post-LIPUS with RR (Fig. 19). Consistent with previous data (Section 5.2), ERK1/2 MAPK was activated in DPSC after LIPUS treatment, but only JNK and p38 MAPK were activated in PDLSC 5 min or 1 h after LIPUS exposure.

In the RR pre-treated groups, ERK1/2 phosphorylation was significantly decreased by ~75% (Fig. 19 A, D) at one hour after LIPUS treatment, while ERK1/2 increased time-dependently in RR-free LIPUS treated groups, pre-treated DPSC and PDLSC both showed a decrease in ERK1/2 phosphorylation. However, addition of RR was not correlated with the change of JNK or p38 activation in both DPSC and PDLSC (Figure 19 B, C, E, F).

Conclusively, Piezo1 and Piezo2 inhibition blocks ERK1/2 activation which is not cell type-specific. These findings indicate that Piezo proteins are intimately involved in the ERK1/2 MAPK signalling.

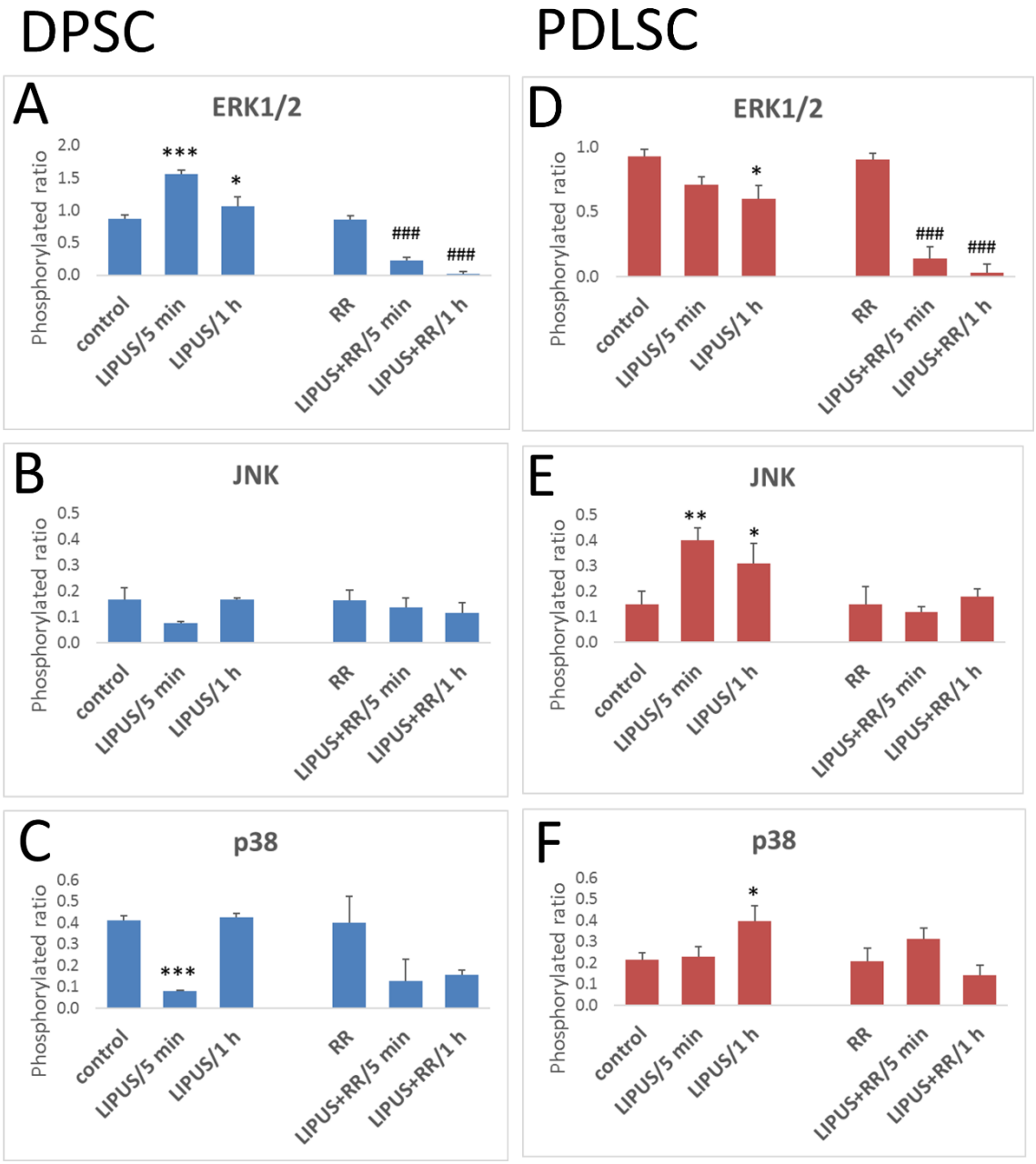


**Figure 19.** Effects of Ruthenium Red (RR) on ERK1/2 MAPK activation after LIPUS treated DPSCs and PDLSCs. Experimental groups were treated by RR and LIPUS. A) B) C): Change of ERK1/2, JNK and p38 MAPK activation with/without LIPUS and RR in DPSC. D) E) F): Change of ERK1/2, JNK and p38 MAPK activation with/without LIPUS and RR in PDLSC. *$p$<0.05, **$p$<0.01 and ***$p$<0.001 compared with the untreated controls. ###$p$<0.001 comparison among RR groups. Values represent the mean ± SD of three independent assays.

### *6.5 Piezo Inhibitor Suppresses Cell Proliferation After US Exposure*

In order to clarify if Piezo 1 and Piezo 2 are involved in LIPUS-induced proliferation, the pharmacological inhibitor (RR) of Piezo1 and Piezo2 was added 5 min prior to LIPUS treatment. Interestingly, adding RR prior to LIPUS treatment inhibited proliferation 24 h post-treatment, compared with RR-free LIPUS treated groups in DPSC cultures (Fig. 20). In addition, groups treated with RR only (no LIPUS exposure) showed no change in proliferation ratio for DPSCs 24 h post-treatment. However, the increase of proliferation of PDLSC by LIPUS was not reduced by RR and showed no statistical difference with the RR-free group (Fig. 20).

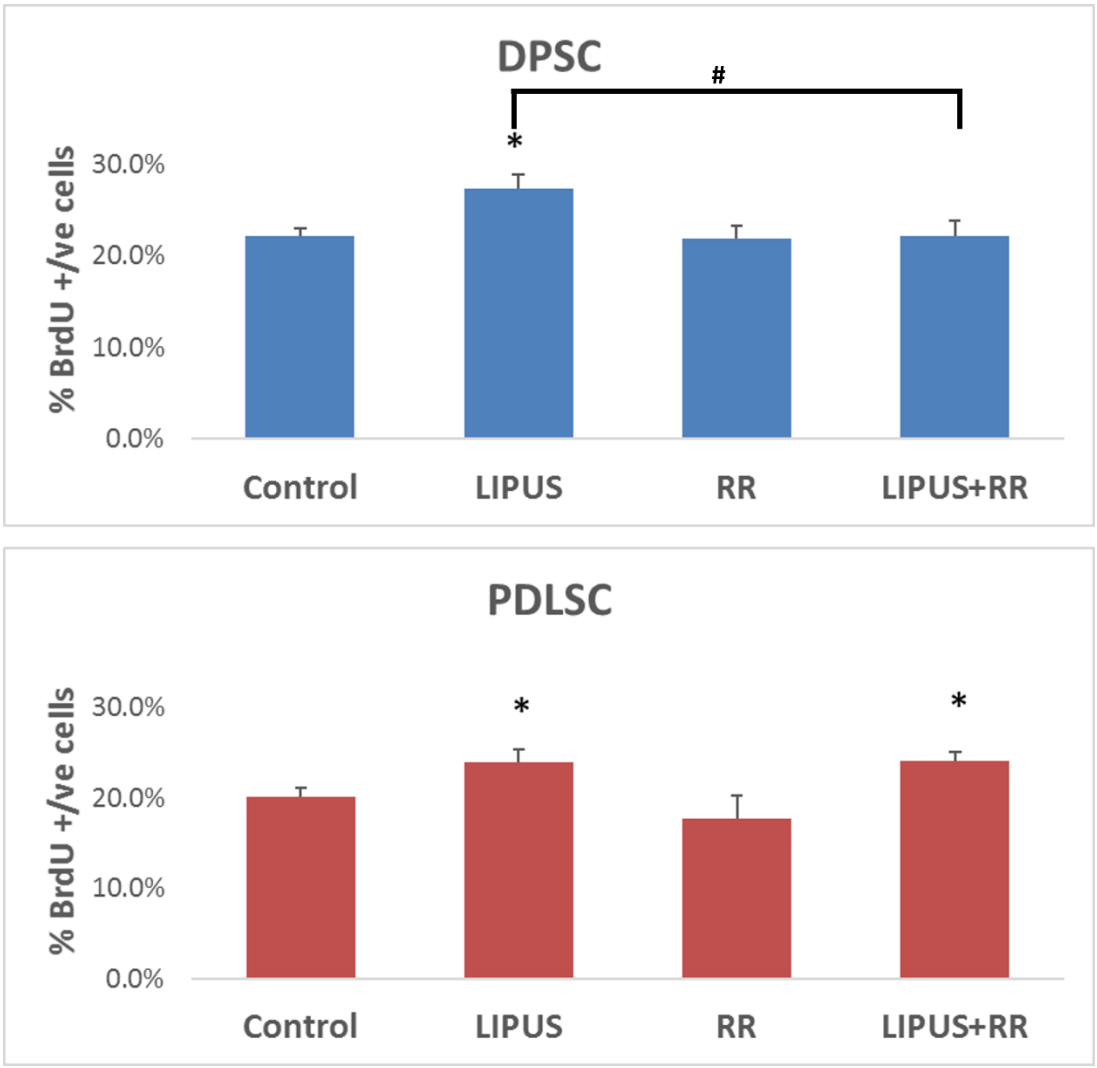


**Figure 20.** Effects of the piezo inhibitor RR on proliferation of DPSCs and PDLSCs as determined by BrdU labelling. RR decreased proliferation in LIPUS-treated DPSC but not in PDLSC cultures. *$p$<0.05 compared with the untreated controls. #$p$<0.05 comparison between experiment groups. Values represent the mean ± SD of three independent assays.

## *6.6 Conclusion*

LIPUS led to a significant increase in Piezo1 and Piezo2 protein expression in DPSCs but not in PDLSCs. Inhibition of Piezo proteins by RR abrogated activation of the ERK1/2 MAPK pathway and proliferation of DPSCs. These experiments indicated the involvement of Piezo1 and Piezo2 in LIPUS-activated ERK1/2 MAPK signalling in DPSC.

# Chapter 7

# Discussion

# Chapter 7 Discussion

Low intensity pulsed ultrasound is seen as a healing approach. The literature has used different methods of applying LIPUS to different therapeutic conditions and cells as previously discussed (Section 1.4 and 1.5). Dental tissue regeneration is of great interest and previous work has shown US-induced change of cell behaviours (Man et al., 2012a, Man et al., 2012b). The previous work characterised the therapeutic effects of LIPUS on dental stem cells and elucidated potential signalling mechanisms involved in LIPUS stimulation. The overall aim of this study was to evaluate the potential of LIPUS in stem cell-based dental tissue regeneration and then the objectives were as follows:

1) Isolation and characterization of dental stem cells;

2) Evaluation of the biological effect of LIPUS and selection of the most effective US parameters

3) Study of the underlying MAPK signalling processes activated by LIPUS.

For this work, rodent mesenchymal stem cell types were isolated: DPSC, BMSC and PDLSC. LIPUS parameter-dependently promoted the proliferation of DPSC, BMSC and PDLSC. ERK1/2 MAPKs have been proven to be involved in the signalling processes of DPSC, whereas JNK and p38 have been proven to be

involved in BMSC and PDLSC (See Supplement paper). Piezo1/2 located on cell membrane could possibly be mechanically activated by LIPUS and participate in ERK1/2 MAPK signalling.

The acoustic low-intensity pulsed energy of LIPUS has been shown to be beneficial for bone repair and wound healing (Romano et al., 2009, Khanna et al., 2009). There are properties of the ultrasound that are causing beneficial changes in the tissues. Ultrasound delivery is a non-invasive treatment which is relatively easy to apply, safe and inexpensive. This makes it very attractive as a means of stimulating the expansion of stem cells. LIPUS particularly exerts mechanical stimuli which effect intracellular mechanotransduction and signalling. LIPUS affect cells most likely through microstreaming and radiation force which generates oscillating strain on cell membrane (Padilla et al., 2014). What happens to the cell membranes after LIPUS-induced strain on the cells is an unknown field, however, we can speculate that the push and pull forces might cause membrane to be more penetrable and also change of mechanosensitive membrane molecules i.e. integrins, ion channels, focal adhesions (Schwartz and DeSimone, 2008). As a result, the related downstream signalling pathways and cellular processes are likely to be activated by LIPUS (Ren et al., 2013). Supportively, mechanical forces and LIPUS activate similar intracellular signalling such as the MAPK, Rho ROCK, and

Wnt pathways (Dyson and Brookes, 1983, Zhou et al., 2004, Mahoney et al., 2009).

Indeed, several commercial devices have been developed for therapeutic application, however, current clinical utilization of LIPUS remains limited. This shortcoming might be explained for a variety of reasons and include 1) controversies on the therapeutic efficacy of LIPUS; and 2) limited information with regard to the mechanism of action of LIPUS (Mitragotri, 2005, Tanaka et al., 2015). Thus, the current status of LIPUS treatment on bone fracture healing corroborates the importance of determining the most efficient LIPUS parameter and the mechanism underlying its therapeutic effects (Dyson and Brookes, 1983).

In the tissue engineering field, LIPUS is reported to promote stem cell proliferation, differentiation and matrix production to accelerate regenerative events (Ebisawa et al., 2004, Cui et al., 2006, Lee et al., 2006). It may therefore provide an ideal stimulus for dental tissue regeneration by stimulating endogenous stem cells to home and/or promote their expansion (Scheven et al., 2009b). This work focuses on identifying how LIPUS affects the proliferation of DPSCs and compared this with the responses of PDLSCs and BMSCs.

## *7.1 Isolation and Characterization of DPSC, BMSC and PDLSC*

Odontoblasts, periodontal ligament cells, cementoblasts, gingival fibroblasts, and osteoblasts have all been reported to be responsive to ultrasound exposure; and these cell types are important in craniofacial and dental tissue homeostasis and repair (Inubushi et al., 2008, Shiraishi et al., 2011, Man et al., 2012b). Postnatal stem cells isolated from a variety of tissues have been used for tissue regeneration *in vitro* and *in vivo* (Huang et al., 2009), and in this study, MSCs derived from dental pulp, periodontal ligament and bone marrow were adopted.

Adult MSCs separated from tissues are heterogeneous (Phinney, 2012). The heterogeneity between experiments however of the MSCs used could be minimised by utilising the following criteria: 1) adherence to culturewear surfaces in standard culture medium; 2) differentiation ability into osteoblasts, adipocytes, and/or chondroblasts under standard *in vitro* induction conditions, and 3) expression of certain cell surface antigens (e.g. CD29, CD90 and CD105) (Dominici et al., 2006).

Initially, the transcriptional analyses confirmed the expression of a range of MSCs markers. Subsequently, the osteogenic and adipogenic differentiation potential of the dental MSCs (DPSC, PDLSC) was demonstrated following osteogenic and adipogenic induction. DPSC and BMSC cultures demonstrated a greater ability for osteogenic and adipogenic differentiation compared with PDLSC as demonstrated

by ARS and ORO staining, respectively. As the semi-quantitative methods of ARS and ORO by extracting the dye manually are reported to lack precision (Zou and Shen, 2007), RT-PCR analyses of mineralization-related markers were performed on the isolated stem cells to substantiate these initial differentiation observations.

Interestingly, different patterns of mineralization were observed in various studies. Previously, DPSC displayed a sheet-like layer of mineral while ADSCs and BMSCs demonstrated more scattered mineralised nodule formation (Davies et al., 2015). However, analyses by others have underscored that the potential of DPSC for osteogenic differentiation was higher than that of BMSC (Davies et al., 2015). In this study, the pattern of mineralization in BMSC and DPSC demonstrated the converse (Fig. 7). Indeed, the mineralization nodules of DPSC appeared discrete while that of BMSC were merged together and densely displayed. This phenomenon might be explained by the fact that the pattern of mineralization is not dependent singularly on cell lineages, but also on experimental conditions, such as cell isolation / culture approaches, composition of induction medium, cell growth profiles, and cell viability.

Previous work from this group has confirmed the expression of CD29 and CD90 in rat DPSC and BMSC by flow cytometry, which also demonstrated the multi-differentiation potential of different MSC types (Davies et al., 2014, Augello et al.,

2010). A range of MSC surface markers, pluripotent markers as well as mineralization-related markers were analysed by RT-PCR, as good monoclonal antibodies required for flow cytometry are relatively difficult to obtain for rat-derived cells. Gene expression analysis demonstrated distinct expression of MSC, pluripotent and mineralization-related markers. Interestingly, passage 4 cells consistently showed lower expression of these markers compared with passage 2 cells, the expression of CD90 in particular, in all MSC culture types. Combined with evidence from the literature, passage 2 cells ware adopted in all experiments (Elkhenany et al., 2016).

### *7.2 LIPUS Promoted Proliferation of rat MSCs*

To determine the optimal efficacy of LIPUS delivery for different tissue-derived MSCs, the biological effects of ultrasound exposure duration and intensity conditions were compared. According to the data obtained, a single 5-min LIPUS treatment significantly promoted proliferation of DPSCs, PDLSCs and BMSCs. This result suggests that LIPUS can promote MSC expansion in stem cell-based therapy. Interestingly, the time of LIPUS exposure as determined from this investigation (5 or 20 min) was not a critical factor in LIPUS-induced DPSC and PDLSC proliferation. This is consistent with a well-established biomechanical theory that proposes that mechanosensitive cells can become sensitised following long-term mechanical loading (Schriefer et al., 2005). The results presented here indicate that a 5-min exposure of LIPUS is adequate for stimulating proliferation, and a longer treatment would not further enhance these biological effects. Clinically, 20-min LIPUS for daily treatment is widely applied for bone repair, however, the findings presented here suggest that shorter treatment duration may be adequate to achieve the same treatment efficacy (Khanna et al., 2009, Schriefer et al., 2005). Notably, the ultrasonic transduction environment in monolayer cells *in vitro* are largely different from cells reside in *in vivo* tissue. Thus, further *in vivo* research regarding the time-dependent effects of LIPUS need to be performed to warrant the 5-min treatment to be sufficient for therapeutic purposes.

There are reports indicating that DPSCs and PDLSCs are responsive to various mechanical stresses (Dhopatkar et al., 2005a). The dynamics of proliferation, differentiation and ECM secretion could be related to mechanical stimuli such as compression, stretch, and hydrostatic pressure (Han et al., 2008). Interestingly, in this study, proliferation of DPSC and BMSC were maximally promoted after 750mW/cm$^2$ treatment whilst PDLSC proliferate reached a maximum at 250mW/cm$^2$ LIPUS. Besides, the RT-PCR results showed varied expression level of pluripotent/differentiation markers among DPSC, BMSC, and PDLSC. It may be deduced that postnatal MSCs derived from different tissues may represent tissue/niche-specific biological characteristics, which may explain why MSCs respond in a distinct manner to different LIPUS intensities (Augello et al., 2010). It could be speculated that the reason why DPSCs are less responsive to mechanical intensity might be their residence in the hard-tissue-enclosed dental pulp which protects them from constant mechanical stimulation, unlike PDLSCs subjected to continual and dynamical mechanical forces such as biting and orthodontic forces. However, further biological evidences are required to fully understand the differences in various lineages of MSCs.

### *7.3 MAPKs Mediate Increase of Cell Proliferation Induced by LIPUS*

This study investigated intracellular signal transduction post-LIPUS via activation of MAPKs by analysing their phosphorylation levels using ELISA and Western blotting techniques.

The results obtained indicated that the proliferation of DPSC was dependent on ERK1/2 MAPK signalling, while BMSC and PDLSC proliferation was dependent on JNK and p38 MAPK signalling. MAPK inhibition suggested that the dental stem cell proliferative response to ultrasound was linked to specific MAPK pathways. Thus, ERK1/2 may participate in regulating LIPUS-induced DPSC proliferation, whereas in BMSCs, JNK activation may represent the main regulatory signalling pathway. Furthermore, data presented here indicated that, JNK and p38 signalling may be both involved in stimulation of PDLSC proliferation. These specific MAPKs were activated immediately post-LIPUS and remained activated for up to 24 h post-LIPUS treatment. The fact that the single LIPUS treatment still resulted in a subsequent increase in MAPK activation underlines the potential long-acting benefits of therapeutic ultrasound (Man et al., 2012b).

The role of MAPKs is to enable a cellular response to extracellular stimuli and rapidly facilitate further downstream intracellular signalling, which ultimately

leads to altered gene expression, molecular and cellular behaviour (Zhang and Liu, 2002). The up-regulation of the proliferation related genes, c-jun, c-fos and PCNA, post-LIPUS as observed here could be explained by the down-stream regulation following activation of MAPKs.

Notably, a pattern of MAPK pathway activation was observed in all the MSC types studied, which comprised a reduction of relevant phosphorylated MAPKs following the initial activation (phosphorylation). This phenomenon may be explained as the de-phosphorylation phase in the process of enzymatic alternating phosphorylation-dephosphorylation, which is an intracellular homeostatic mechanism to regulate cell function and mitosis (Bononi et al., 2011).

It should be noted that due to the limitations in the pharmacological inhibitors used, including off-target effects, cytotoxicity and transience of effect (Wauson et al., 2013), further work is needed to specify the role of each MAPK pathway. Application of RNA interference (RNAi) techniques to silence specific genes may be more informative and enable pathway-specific data to be generated.

### *7.4 Piezo1 and Piezo2 are Upstream Effectors of ERK1/2 MAPK*

Piezo proteins (Piezo1 and Piezo2) are membrane bound pore-forming ion channels which have recently been highlighted as mechanically activated (MA) and are expressed by several mammalian cell types (Coste et al., 2012). Piezo1 and Piezo2 proteins have been identified to be encoded by the FAM38A and FAM38B genes, respectively (Lee et al., 2014). Studies have reported that Piezo1 is expressed in human PDL cells, is associated with the NF-κB signalling pathway and involved in mechanical stress–induced osteoclastogenesis (Jin et al., 2015).

Derived from different mesenchymal origins during embryonic tooth development, DPSCs (from dental papilla) and PDLSCs (from dental follicle) are two of the most widely studied dental stem cells (Huang et al., 2010). In previous group work, DPSCs and PDLSCs showed diverse signalling mechanism in LIPUS-induced cell proliferation, possibly reflecting their different embryonic origins. To determine whether Piezo proteins might be important mechanotransduction components in MSCs, this research focused on DPSCs and PDLSCs which are biologically representative of dental stem cells characteristic. Initially, Western-blotting was performed to analyse the expression of piezo proteins in DPSCs and PDLSCs and to identify the possible association of the Piezo proteins with LIPUS induced responses. Notably Piezo proteins have reportedly shown the highest expression in

kidney and lung tissue, whilst their expression in rat dental tissue has not been shown (Volkers et al., 2015). In this study, the presence of Piezo1 and Piezo2 proteins in rat DPSC and PDLSC was demonstrated for the first time. Piezo1 and Piezo2 levels were significantly increased after LIPUS treatment in DPSC, however this phenomenon was not observed in PDLSCs. These observations underline the cell specific differences between these dental MSC types. These findings also indicate that Piezo1 and Piezo2 are responsive to LIPUS in DPSCs and may possibly be involved in their LIPUS-induced responses. It may be postulated that Piezo proteins might only be linked to specific MAPKs (such as ERK1/2 which involved in LIPUS stimulation of DPSC), but not other MAPKs due to the differential activation profiles of MAPKs in specific types of stem cells.

To elucidate the role of Piezo1 and Piezo2 following LIPUS exposure, an inhibitor of Piezos: Ruthenium Red (RR) was applied. RR is a polycationic pore blocker of transient receptor potential (TRP) channels, which blocks Piezo1- and Piezo2-induced MA currents (Coste et al., 2012, St Pierre et al., 2009). TRP channels are a group of ion channels located on the membrane of most cell types. RR blocks the pore of Piezo-induced MA channels from the extracellular surface, reportedly exerting its strongest inhibitory effect 5 to 20 min prior to LIPUS stimulation (Zagorodnyuk et al., 2005). Ion channels like Piezo1 and Piezo2 are also reported to be able to react immediately after external stimuli are delivered to cells. RR only

exerts transient blocking effect on ion channels, thus 5 min and 1 h time points were selected accordingly to show the immediate and direct effect of RR/Piezos inhibition on MAPK signalling (Xu et al., 1999). In the ELISA experiments performed here, a rapid decrease of ERK1/2 was observed, whilst the JNK and p38 assays showed no statistical difference in levels in both DPSC and PDLSC after RR treatment. These findings indicate the potential close correlation of Piezo proteins and ERK1/2 phosphorylation in dental stem cells.

Finally, cell proliferation analysis was undertaken using the BrdU incorporation assay to study the possible functional/causal role of Piezos in LIPUS induced proliferation. RR not only inhibited ERK1/2 activation, but also inhibited the stimulation of proliferation after LIPUS treatment of DPSC. Conversely, although RR inhibited ERK1/2 activation in PDLSCs, it exerted no effects on the increase in PDLSC proliferation post-LIPUS. These data suggested that other mechanisms are involved in LIPUS mechanotranduction in PDLSCs, potentially involving other mechano-responsive elements such as integrins and cytoskeleton signalling (Katsumi et al., 2004, Wu et al., 1999). Overall, these data underscore the intrinsic differences between these two dental MSC types which possibly may be traced back to their different embryonic origins, i.e. DPSC (dental papilla) and PDLSC (dental follicle) (Thesleff et al., 1995), and/or their tissue/niche-specific

microenvironment which closely regulate the stemness and function of stem cells (Gattazzo et al., 2014).

However, it should be noted that RR is non-specific inhibitor of most TRP channels. Thus, a more specific inhibition of Piezo1 and Piezo2 should be applied in future experiments to clarify the specific role of Piezo1 and Piezo2. At this stage, it can be concluded that LIPUS may promote cation transport via TRP/calcium channels which are directly related to ERK1/2 MAPK activation. Studies have proved that low intensity US led to a rise of calcium flow and that proliferative effects of LIPUS closely dependent on $Ca^{2+}$ receptors (Alvarenga et al., 2010). Ion channels like Piezo1/2 located on membrane are likely to be opened up by ultrasound thus cation transport are enhanced and acted as secondary messenger to trigger dynamic signalling processes.

PCNA, c-jun and c-fos are closely involved in the progression of cell cycle which determine proliferative responses of cells. c-Jun and c-Fos combine to form the activator protein-1 (AP-1) which is known as the early response transcription factor, which was upregulated by LIPUS in rat BMSCs (Sena et al., 2005). In our study, LIPUS increases expression of PCNA, c-jun and c-fos. It was reported that the rise in expression of early response genes c-Fos, c-Jun and c-Myc post-LIPUS treatment could be further abrogated by ERK inhibition (Louw et al., 2013). These

studies further enhanced our hypothesis that Piezo1/2 are possible membrane ion channels which are opened up by LIPUS and led to the rise of calcium flow which acted as secondary messenger to activate ERK1/2 MAPK to increase the progression of cell cycle by upregulated PCNA, c-fos and c-jun.

To summarise, Piezo1 and Piezo2 may be important membrane components involved in transduction of mechanical stimuli generated by LIPUS to the intracellular cytoplasm, activating the downstream cascades of ERK1/2 phosphorylation, followed by induction of mechanical response element genes, and ultimately leading to an increase in cell proliferation (Fig. 21).

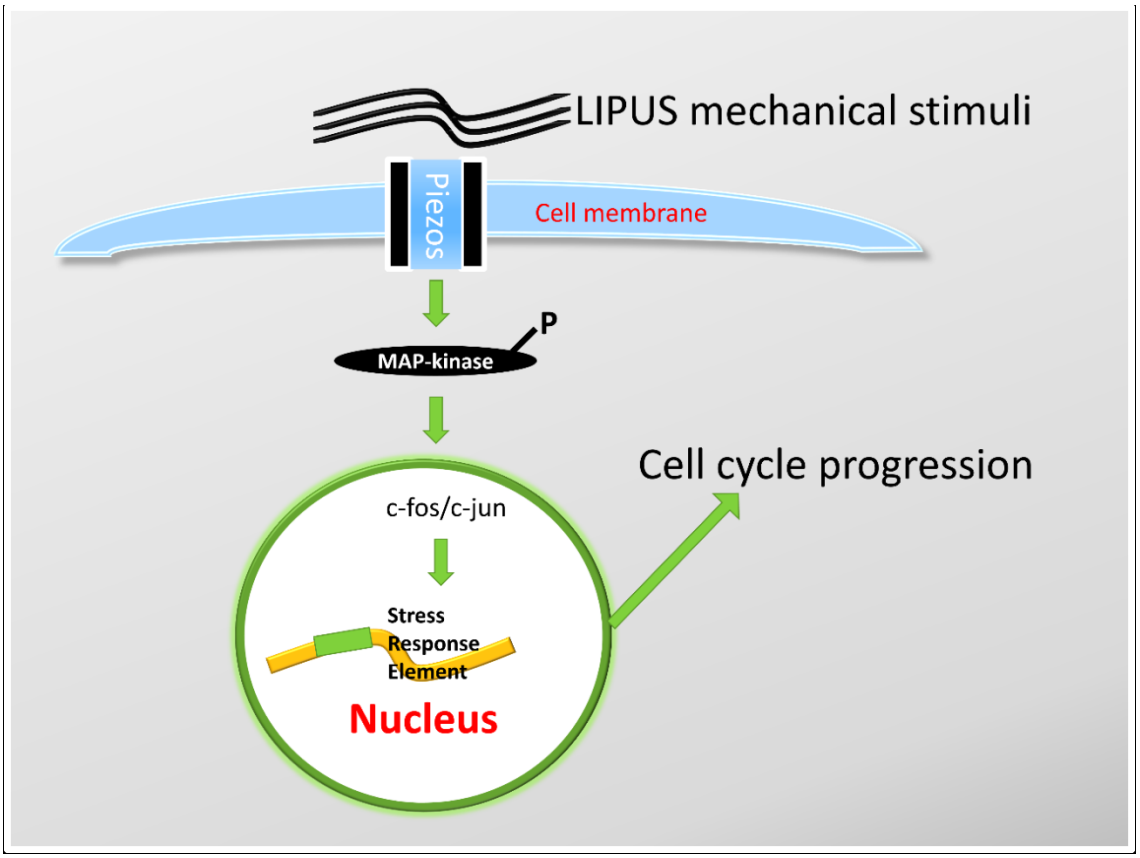


**Figure 21.** Diagrammatic representation of the possible signal transduction pathways stimulated by LIPUS in DPSCs. Mechanical stimuli generated by LIPUS treatment stimulate piezo channels located on the cell membrane and the associated ERK1/2 MAPK signalling. The signal cascade transduces to mechanical/stress response elements in the cell nucleus which affects cell cycle progression and cell proliferation.

## *7.5 Conclusion*

This study indicated that LIPUS is able to promote the proliferation of dental MSCs. Within the settings used, the exposure duration was found to be less important than intensity. LIPUS-stimulated proliferation is dependent on differential activation of MAPK signalling pathways in the different MSC types. Initial and novel evidences are provided to support an important and distinct role of Piezo1/2 in LIPUS stimulated proliferation and ERK1/2 MAPK signalling. The role of Piezo1/2 to activate ERK1/2 MAPK in particular may lead to other stem cell responses other than proliferation which could be studied in the further.

The findings also shed light on intrinsic differences between MSCs from different sources including dental tissues, which might have important implications for future stem cell-based dental tissue regeneration (Ghorayeb et al., 2013). The optimization of stem-cell-based tissue regeneration in the further should consider the cell lineage-dependent characteristics, which may contribute to select optimal stem cell lineage and stimuli to gain the maximum regenerative outcome, e.g parameters of mechanical stress, the use of growth factors, the selection of various biomaterials, and the set-up of particular micro-environment.

## *7.6 Clinical Significance/Applications and Future Research*

This study showed LIPUS-promoted proliferation of dental stem cells and the possible underlying signalling mechanism, which corroborated the clinical potential of LIPUS in treating dental diseases. However, much work remains to be done to strengthen our conclusions and also to achieve bench-clinical transitions

For further experiments,

1) siRNA could be used to determine the specific role of MAPKs in LIPUS-induced signal transduction.
2) siRNA could be used to determine the specific role of Piezo1/2 in LIPUS-induced signal transduction.
3) Other membrane molecules related in the mechanotranduction processes, i.e. focal adhesions, integrins, ion channels.
4) Other signalling pathways related in the mechanotranduction processes such as Rho ROCK and Wnt.
5) A wider range of ultrasound parameters can be investigated.
6) Other aspects of LIPUS-induced biological effects will also be interesting to investigate, such as migration and differentiation of DPSCs and PDLSCs.

7) More importantly, *in vivo* experiments could be designed to realize the development of clinical LIPUS devices for treatment of dental tissue injury and regeneration in the future.

## References


AHMADI, F., MCLOUGHLIN, I. V., CHAUHAN, S. & TER-HAAR, G. 2012. Bio-effects and safety of low-intensity, low-frequency ultrasonic exposure. *Prog Biophys Mol Biol,* 108**,** 119-38.

AL-BATAINEH, O., JENNE, J. & HUBER, P. 2012. Clinical and future applications of high intensity focused ultrasound in cancer. *Cancer Treat Rev,* 38**,** 346-53.

AL-DAGHREER, S., DOSCHAK, M., SLOAN, A. J., MAJOR, P. W., HEO, G., SCURTESCU, C., TSUI, Y. Y. & EL-BIALY, T. 2012. Long term effect of low intensity pulsed ultrasound on a human tooth slice organ culture. *Arch Oral Biol,* 57**,** 760-8.

ALVARENGA, E. C., RODRIGUES, R., CARICATI-NETO, A., SILVA-FILHO, F. C., PAREDES-GAMERO, E. J. & FERREIRA, A. T. 2010. Low-intensity pulsed ultrasound-dependent osteoblast proliferation occurs by via activation of the P2Y receptor: role of the P2Y1 receptor. *Bone,* 46**,** 355-62.

ARTHUR, A., RYCHKOV, G., SHI, S., KOBLAR, S. A. & GRONTHOS, S. 2008. Adult human dental pulp stem cells differentiate toward functionally active neurons under appropriate environmental cues. *Stem Cells,* 26**,** 1787-95.

AUGELLO, A., KURTH, T. B. & DE BARI, C. 2010. Mesenchymal stem cells: a perspective from in vitro cultures to in vivo migration and niches. *Eur Cell Mater,* 20**,** 121-33.

BAGRIANTSEV, S. N., GRACHEVA, E. O. & GALLAGHER, P. G. 2014. Piezo proteins: regulators of mechanosensation and other cellular processes. *J Biol Chem,* 289**,** 31673-81.

BAKER, K. G., ROBERTSON, V. J. & DUCK, F. A. 2001. A review of therapeutic ultrasound: biophysical effects. *Phys Ther,* 81**,** 1351-8.

BAKOPOULOU, A., LEYHAUSEN, G., VOLK, J., TSIFTSOGLOU, A., GAREFIS, P., KOIDIS, P. & GEURTSEN, W. 2011. Comparative analysis of in vitro osteo/odontogenic differentiation potential of human dental pulp stem cells (DPSCs) and stem cells from the apical papilla (SCAP). *Arch Oral Biol,* 56**,** 709-21.

BALMASEDA, M. T., JR., FATEHI, M. T., KOOZEKANANI, S. H. & LEE, A. L. 1986. Ultrasound therapy: a comparative study of different coupling media. *Arch Phys Med Rehabil,* 67**,** 147-50.

BANDOW, K., NISHIKAWA, Y., OHNISHI, T., KAKIMOTO, K., SOEJIMA, K., IWABUCHI, S., KUROE, K. & MATSUGUCHI, T. 2007. Low-intensity pulsed ultrasound (LIPUS) induces RANKL, MCP-1, and MIP-1beta

expression in osteoblasts through the angiotensin II type 1 receptor. *J Cell Physiol,* 211**,** 392-8.

BERSHADSKY, A. D., BALLESTREM, C., CARRAMUSA, L., ZILBERMAN, Y., GILQUIN, B., KHOCHBIN, S., ALEXANDROVA, A. Y., VERKHOVSKY, A. B., SHEMESH, T. & KOZLOV, M. M. 2006. Assembly and mechanosensory function of focal adhesions: experiments and models. *Eur J Cell Biol,* 85**,** 165-73.

BOHARI, S. P., GROVER, L. M. & HUKINS, D. W. 2012. Pulsed-low intensity ultrasound enhances extracellular matrix production by fibroblasts encapsulated in alginate. *J Tissue Eng,* 3**,** 2041731412454672.

BONONI, A., AGNOLETTO, C., DE MARCHI, E., MARCHI, S., PATERGNANI, S., BONORA, M., GIORGI, C., MISSIROLI, S., POLETTI, F., RIMESSI, A. & PINTON, P. 2011. Protein kinases and phosphatases in the control of cell fate. *Enzyme Res,* 2011**,** 329098.

BORSJE, M. A., REN, Y., DE HAAN-VISSER, H. W. & KUIJER, R. 2010. Comparison of low-intensity pulsed ultrasound and pulsed electromagnetic field treatments on OPG and RANKL expression in human osteoblast-like cells. *Angle Orthod,* 80**,** 498-503.

CAPLAN, A. I. 1991. Mesenchymal stem cells. *J Orthop Res,* 9**,** 641-50.

CHAN, Y. S., HSU, K. Y., KUO, C. H., LEE, S. D., CHEN, S. C., CHEN, W. J. & UENG, S. W. 2010. Using low-intensity pulsed ultrasound to improve muscle healing after laceration injury: an in vitro and in vivo study. *Ultrasound Med Biol,* 36**,** 743-51.

CHEN, F.-M., SUN, H.-H., LU, H. & YU, Q. 2012. Stem cell-delivery therapeutics for periodontal tissue regeneration. *Biomaterials,* 33**,** 6320-6344.

CHEN, F.-M., WU, L.-A., ZHANG, M., ZHANG, R. & SUN, H.-H. 2011. Homing of endogenous stem/progenitor cells for in situ tissue regeneration: Promises, strategies, and translational perspectives. *Biomaterials,* 32**,** 3189-3209.

CHEN, Z., GIBSON, T. B., ROBINSON, F., SILVESTRO, L., PEARSON, G., XU, B., WRIGHT, A., VANDERBILT, C. & COBB, M. H. 2001. MAP kinases. *Chem Rev,* 101**,** 2449-76.

COOPER, P. R., TAKAHASHI, Y., GRAHAM, L. W., SIMON, S., IMAZATO, S. & SMITH, A. J. 2010. Inflammation-regeneration interplay in the dentine-pulp complex. *J Dent,* 38**,** 687-97.

COSTE, B., XIAO, B. L., SANTOS, J. S., SYEDA, R., GRANDL, J., SPENCER, K. S., KIM, S. E., SCHMIDT, M., MATHUR, J., DUBIN, A. E., MONTAL, M. & PATAPOUTIAN, A. 2012. Piezo proteins are pore-forming subunits of mechanically activated channels. *Nature,* 483**,** 176-U72.

CUI, J. H., PARK, K., PARK, S. R. & MIN, B. H. 2006. Effects of low-intensity ultrasound on chondrogenic differentiation of mesenchymal stem cells embedded in polyglycolic acid: an in vivo study. *Tissue Eng,* 12**,** 75-82.

CUI, J. H., PARK, S. R., PARK, K., CHOI, B. H. & MIN, B. H. 2007. Preconditioning of mesenchymal stem cells with low-intensity ultrasound for cartilage formation in vivo. *Tissue Eng,* 13**,** 351-60.

DALLA-BONA, D. A., TANAKA, E., INUBUSHI, T., OKA, H., OHTA, A., OKADA, H., MIYAUCHI, M., TAKATA, T. & TANNE, K. 2008. Cementoblast response to low- and high-intensity ultrasound. *Arch Oral Biol,* 53**,** 318-23.

DAVIES, O. G., COOPER, P. R., SHELTON, R. M., SMITH, A. J. & SCHEVEN, B. A. 2014. A comparison of the in vitro mineralisation and dentinogenic potential of mesenchymal stem cells derived from adipose tissue, bone marrow and dental pulp. *J Bone Miner Metab*.

DAVIES, O. G., COOPER, P. R., SHELTON, R. M., SMITH, A. J. & SCHEVEN, B. A. 2015. A comparison of the in vitro mineralisation and dentinogenic potential of mesenchymal stem cells derived from adipose tissue, bone marrow and dental pulp. *J Bone Miner Metab,* 33**,** 371-82.

DHOPATKAR, A. A., SLOAN, A. J., ROCK, W. P., COOPER, P. R. & SMITH, A. J. 2005a. British Orthodontic Society, Chapman Prize Winner 2003. A novel in vitro culture model to investigate the reaction of the dentine-pulp complex to orthodontic force. *J Orthod,* 32**,** 122-32.

DHOPATKAR, A. A., SLOAN, A. J., ROCK, W. P., COOPER, P. R. & SMITH, A. J. 2005b. A novel in vitro culture model to investigate the reaction of the dentine-pulp complex to orthodontic force. *J. Orthod.,* 32**,** 122-32.

DOMINICI, M., LE BLANC, K., MUELLER, I., SLAPER-CORTENBACH, I., MARINI, F., KRAUSE, D., DEANS, R., KEATING, A., PROCKOP, D. & HORWITZ, E. 2006. Minimal criteria for defining multipotent mesenchymal stromal cells. The International Society for Cellular Therapy position statement. *Cytotherapy,* 8**,** 315-7.

DYSON, M. 1982. Non-thermal cellular effects of ultrasound. *Br J Cancer Suppl,* 5**,** 165-71.

DYSON, M. & BROOKES, M. 1983. Stimulation of bone repair by ultrasound. *Ultrasound Med Biol,* Suppl 2**,** 61-6.

EBISAWA, K., HATA, K., OKADA, K., KIMATA, K., UEDA, M., TORII, S. & WATANABE, H. 2004. Ultrasound enhances transforming growth factor beta-mediated chondrocyte differentiation of human mesenchymal stem cells. *Tissue Eng,* 10**,** 921-9.

EL-BIALY, T., ALHADLAQ, A. & LAM, B. 2012. Effect of therapeutic ultrasound on human periodontal ligament cells for dental and periodontal tissue engineering. *Open Dent J,* 6**,** 235-9.

EL-BIALY, T., LAM, B., ALDAGHREER, S. & SLOAN, A. J. 2011. The effect of low intensity pulsed ultrasound in a 3D ex vivo orthodontic model. *J Dent,* 39**,** 693-9.

ELKHENANY, H., AMELSE, L., CALDWELL, M., ABDELWAHED, R. & DHAR, M. 2016. Impact of the source and serial passaging of goat mesenchymal stem cells on osteogenic differentiation potential: implications for bone tissue engineering. *J Anim Sci Biotechnol,* 7**,** 16.

ESENALIEV, R. 2006. Ultrasound-based treatment methods for therapeutic treatment of skin and subcutaneous tissues. *US Patent App***,** 11/542,057.

FENG, Y., TIAN, Z. & WAN, M. 2010. Bioeffects of low-intensity ultrasound in vitro: apoptosis, protein profile alteration, and potential molecular mechanism. *J Ultrasound Med,* 29**,** 963-74.

FIX, S. M., BORDEN, M. A. & DAYTON, P. A. 2015. Therapeutic gas delivery via microbubbles and liposomes. *J Control Release,* 209**,** 139-49.

FOSTER, K. R. & WIEDERHOLD, M. L. 1978. Auditory responses in cats produced by pulsed ultrasound. *J Acoust Soc Am,* 63**,** 1199-205.

GALE, Z., COOPER, P. R. & SCHEVEN, B. A. 2011. Effects of glial cell line-derived neurotrophic factor on dental pulp cells. *J Dent Res,* 90**,** 1240-5.

GAO, Q., WALMSLEY, A. D., COOPER, P. R. & SCHEVEN, B. A. 2016. Ultrasound Stimulation of Different Dental Stem Cell Populations: Role of Mitogen-activated Protein Kinase Signaling. *J Endod,* 42**,** 425-431.

GATTAZZO, F., URCIUOLO, A. & BONALDO, P. 2014. Extracellular matrix: a dynamic microenvironment for stem cell niche. *Biochim Biophys Acta,* 1840**,** 2506-19.

GHORAYEB, S. R., BERTONCINI, C. A. & HINDERS, M. K. 2008. Ultrasonography in dentistry. *IEEE Trans Ultrason Ferroelectr Freq Control,* 55**,** 1256-66.

GHORAYEB, S. R., PATEL, U. S., WALMSLEY, A. D. & SCHEVEN, B. A. 2013. Biophysical characterization of low-frequency ultrasound interaction with dental pulp stem cells. *J Ther Ultrasound,* 1**,** 12.

GRAZIANO, A., D'AQUINO, R., LAINO, G. & PAPACCIO, G. 2008. Dental pulp stem cells: a promising tool for bone regeneration. *Stem Cell Rev.,* 4**,** 21-6.

GRONTHOS, S., BRAHIM, J., LI, W., FISHER, L. W., CHERMAN, N., BOYDE, A., DENBESTEN, P., ROBEY, P. G. & SHI, S. 2002. Stem cell properties of human dental pulp stem cells. *J. Dent. Res.,* 81**,** 531-5.

GRONTHOS, S., MANKANI, M., BRAHIM, J., ROBEY, P. G. & SHI, S. 2000. Postnatal human dental pulp stem cells (DPSCs) in vitro and in vivo. *Proc. Natl. Acad. Sci. U S A,* 97**,** 13625-30.

GUO, X. E., TAKAI, E., JIANG, X., XU, Q., WHITESIDES, G. M., YARDLEY, J. T., HUNG, C. T., CHOW, E. M., HANTSCHEL, T. & COSTA, K. D. 2006. Intracellular calcium waves in bone cell networks under single cell nanoindentation. *Mol Cell Biomech,* 3**,** 95-107.

HAN, M.-J., SEO, Y.-K., YOON, H.-H., SONG, K.-Y. & PARK, J.-K. 2008. Effect of mechanical tension on the human dental pulp cells. *Biotechnol. Bioprocess Eng.,* 13**,** 410-417.

HANDA, K., SAITO, M., TSUNODA, A., YAMAUCHI, M., HATTORI, S., SATO, S., TOYODA, M., TERANAKA, T. & NARAYANAN, A. S. 2002. Progenitor cells from dental follicle are able to form cementum matrix in vivo. *Connect Tissue Res,* 43**,** 406-8.

HARLE, J., SALIH, V., MAYIA, F., KNOWLES, J. C. & OLSEN, I. 2001. Effects of ultrasound on the growth and function of bone and periodontal ligament cells in vitro. *Ultrasound Med Biol,* 27**,** 579-86.

HSU, S. H. & HUANG, T. B. 2004. Bioeffect of ultrasound on endothelial cells in vitro. *Biomol Eng,* 21**,** 99-104.

HUANG, G. T., GRONTHOS, S. & SHI, S. 2009. Mesenchymal stem cells derived from dental tissues vs. those from other sources: their biology and role in regenerative medicine. *J Dent Res,* 88**,** 792-806.

HUANG, X., XU, X., BRINGAS, P., JR., HUNG, Y. P. & CHAI, Y. 2010. Smad4-Shh-Nfic signaling cascade-mediated epithelial-mesenchymal interaction is crucial in regulating tooth root development. *J Bone Miner Res,* 25**,** 1167-78.

IKAI, H., TAMURA, T., WATANABE, T., ITOU, M., SUGAYA, A., IWABUCHI, S., MIKUNI-TAKAGAKI, Y. & DEGUCHI, S. 2008. Low-intensity pulsed ultrasound accelerates periodontal wound healing after flap surgery. *J Periodontal Res,* 43**,** 212-6.

INUBUSHI, T., TANAKA, E., REGO, E. B., KITAGAWA, M., KAWAZOE, A., OHTA, A., OKADA, H., KOOLSTRA, J. H., MIYAUCHI, M., TAKATA, T. & TANNE, K. 2008. Effects of ultrasound on the proliferation and differentiation of cementoblast lineage cells. *J Periodontol,* 79**,** 1984-90.

ITO, K., YAMADA, Y., NAKAMURA, S. & UEDA, M. 2011. Osteogenic potential of effective bone engineering using dental pulp stem cells, bone marrow stem cells, and periosteal cells for osseointegration of dental implants. *Int J Oral Maxillofac Implants,* 26**,** 947-54.

JIANG, T., XU, T., GU, F., CHEN, A., XIAO, Z. & ZHANG, D. 2012. Osteogenic effect of low intensity pulsed ultrasound on rat adipose-derived stem cells in vitro. *J Huazhong Univ Sci Technolog Med Sci,* 32**,** 75-81.

JIN, Y., LI, J., WANG, Y., YE, R., FENG, X., JING, Z. & ZHAO, Z. 2015. Functional role of mechanosensitive ion channel Piezo1 in human periodontal ligament cells. *Angle Orthod,* 85**,** 87-94.

KANEDA, T., MIYAUCHI, M., TAKEKOSHI, T., KITAGAWA, S., KITAGAWA, M., SHIBA, H., KURIHARA, H. & TAKATA, T. 2006. Characteristics of periodontal ligament subpopulations obtained by sequential enzymatic digestion of rat molar periodontal ligament. *Bone,* 38**,** 420-6.

KATSUMI, A., ORR, A. W., TZIMA, E. & SCHWARTZ, M. A. 2004. Integrins in mechanotransduction. *J Biol Chem,* 279**,** 12001-4.

KAWANO, S., OTSU, K., KURUMA, A., SHOJI, S., YANAGIDA, E., MUTO, Y., YOSHIKAWA, F., HIRAYAMA, Y., MIKOSHIBA, K. & FURUICHI, T. 2006. ATP autocrine/paracrine signaling induces calcium oscillations and NFAT activation in human mesenchymal stem cells. *Cell Calcium,* 39**,** 313-24.

KHAN, Y. & LAURENCIN, C. T. 2008. Fracture repair with ultrasound: clinical and cell-based evaluation. *J Bone Joint Surg Am,* 90 Suppl 1**,** 138-44.

KHANNA, A., NELMES, R. T., GOUGOULIAS, N., MAFFULLI, N. & GRAY, J. 2009. The effects of LIPUS on soft-tissue healing: a review of literature. *Br Med Bull,* 89**,** 169-82.

KIM, J. Y., XIN, X., MOIOLI, E. K., CHUNG, J., LEE, C. H., CHEN, M., FU, S. Y., KOCH, P. D. & MAO, J. J. 2010. Regeneration of dental-pulp-like tissue by chemotaxis-induced cell homing. *Tissue Eng Part A,* 16**,** 3023-31.

KIM, S. H., KIM, K. H., SEO, B. M., KOO, K. T., KIM, T. I., SEOL, Y. J., KU, Y., RHYU, I. C., CHUNG, C. P. & LEE, Y. M. 2009. Alveolar bone regeneration by transplantation of periodontal ligament stem cells and bone marrow stem cells in a canine peri-implant defect model: a pilot study. *J Periodontol,* 80**,** 1815-23.

KIM, S. H., KIM, Y. S., LEE, S. Y., KIM, K. H., LEE, Y. M., KIM, W. K. & LEE, Y. K. 2011. Gene expression profile in mesenchymal stem cells derived from dental tissues and bone marrow. *J Periodontal Implant Sci,* 41**,** 192-200.

KOJIMA, K., KONOPLEVA, M., SAMUDIO, I. J., RUVOLO, V. & ANDREEFF, M. 2007. Mitogen-activated protein kinase kinase inhibition enhances nuclear proapoptotic function of p53 in acute myelogenous leukemia cells. *Cancer Res,* 67**,** 3210-9.

KOOK, S. H. & LEE, J. C. 2012. Tensile force inhibits the proliferation of human periodontal ligament fibroblasts through Ras-p38 MAPK up-regulation. *J Cell Physiol,* 227**,** 1098-106.

LAINO, G., GRAZIANO, A., D'AQUINO, R., PIROZZI, G., LANZA, V., VALIANTE, S., DE ROSA, A., NARO, F., VIVARELLI, E. & PAPACCIO, G. 2006. An approachable human adult stem cell source for hard-tissue engineering. *J. Cell Physiol.,* 206**,** 693-701.

LEE, H. J., CHOI, B. H., MIN, B. H., SON, Y. S. & PARK, S. R. 2006. Low-intensity ultrasound stimulation enhances chondrogenic differentiation in alginate culture of mesenchymal stem cells. *Artif Organs,* 30**,** 707-15.

LEE, S. K., LEE, C. Y., KOOK, Y. A. & KIM, E. C. 2010. Mechanical stress promotes odontoblastic differentiation via the heme oxygenase-1 pathway in human dental pulp cell line. *Life Sci.,* 86**,** 107-14.

LEE, S. K., MIN, K. S., YOUNGHO, K., JEONG, G. S., LEE, S. H., LEE, H. J., LEE, S. I., KIM, Y. S., LEE, Y. M., PARK, S. J., SEO, S. W. & KIM, E. C. 2008. Mechanical stress activates proinflammatory cytokines and antioxidant defense enzymes in human dental pulp cells. *J. Endod.,* 34**,** 1364-9.

LEE, W., LEDDY, H. A., CHEN, Y., LEE, S. H., ZELENSKI, N. A., MCNULTY, A. L., WU, J., BEICKER, K. N., COLES, J., ZAUSCHER, S., GRANDL, J., SACHS, F., GUILAK, F. & LIEDTKE, W. B. 2014. Synergy between Piezo1 and Piezo2 channels confers high-strain mechanosensitivity to articular cartilage. *Proceedings of the National Academy of Sciences of the United States of America,* 111**,** E5114-E5122.

LI, C. & XU, Q. 2007. Mechanical stress-initiated signal transduction in vascular smooth muscle cells in vitro and in vivo. *Cell Signal,* 19**,** 881-91.

LI, L., YANG, Z., ZHANG, H., CHEN, W., CHEN, M. & ZHU, Z. 2012. Low-intensity pulsed ultrasound regulates proliferation and differentiation of osteoblasts through osteocytes. *Biochem Biophys Res Commun,* 418**,** 296-300.

LIEDERT, A., KASPAR, D., BLAKYTNY, R., CLAES, L. & IGNATIUS, A. 2006. Signal transduction pathways involved in mechanotransduction in bone cells. *Biochem Biophys Res Commun,* 349**,** 1-5.

LIN, N. H., GRONTHOS, S. & BARTOLD, P. M. 2009. Stem cells and future periodontal regeneration. *Periodontol 2000,* 51**,** 239-51.

LIU, Z., XU, J., E, L. & WANG, D. 2012. Ultrasound enhances the healing of orthodontically induced root resorption in rats. *Angle Orthod,* 82**,** 48-55.

LOUW, T. M., BUDHIRAJA, G., VILJOEN, H. J. & SUBRAMANIAN, A. 2013. Mechanotransduction of ultrasound is frequency dependent below the cavitation threshold. *Ultrasound in Medicine & Biology,* 39**,** 1303-19.

LUAN, X., ITO, Y., DANGARIA, S. & DIEKWISCH, T. G. 2006. Dental follicle progenitor cell heterogeneity in the developing mouse periodontium. *Stem Cells Dev,* 15**,** 595-608.

LUMLEY, P. J., WALMSLEY, A. D. & LAIRD, W. R. 1988. Ultrasonic instruments in dentistry: 2. Endosonics. *Dent Update,* 15**,** 362, 364-6, 368-9.

MAHONEY, C. M., MORGAN, M. R., HARRISON, A., HUMPHRIES, M. J. & BASS, M. D. 2009. Therapeutic ultrasound bypasses canonical syndecan-4 signaling to activate rac1. *J Biol Chem,* 284**,** 8898-909.

MALIZOS, K. N., HANTES, M. E., PROTOPAPPAS, V. & PAPACHRISTOS, A. 2006. Low-intensity pulsed ultrasound for bone healing: an overview. *Injury,* 37 Suppl 1**,** S56-62.

MAN, J., SHELTON, R. M., COOPER, P. R., LANDINI, G. & SCHEVEN, B. A. 2012a. Low intensity ultrasound stimulates osteoblast migration at different frequencies. *J Bone Miner Metab,* 30**,** 602-7.

MAN, J., SHELTON, R. M., COOPER, P. R. & SCHEVEN, B. A. 2012b. Low-intensity low-frequency ultrasound promotes proliferation and differentiation of odontoblast-like cells. *J Endod,* 38**,** 608-13.

MARVEL, S., OKRASINSKI, S., BERNACKI, S. H., LOBOA, E. & DAYTON, P. A. 2010. The development and validation of a LIPUS system with preliminary observations of ultrasonic effects on human adult stem cells. *IEEE Trans Ultrason Ferroelectr Freq Control,* 57**,** 1977-84.

MASON, T. J. 2011. Therapeutic ultrasound an overview. *Ultrason Sonochem,* 18**,** 847-52.

MILLER, D. L., SMITH, N. B., BAILEY, M. R., CZARNOTA, G. J., HYNYNEN, K. & MAKIN, I. R. 2012. Overview of therapeutic ultrasound applications and safety considerations. *J Ultrasound Med,* 31**,** 623-34.

MITRAGOTRI, S. 2005. Healing sound: the use of ultrasound in drug delivery and other therapeutic applications. *Nat Rev Drug Discov,* 4**,** 255-60.

MITRANO, T. I., GROB, M. S., CARRION, F., NOVA-LAMPERTI, E., LUZ, P. A., FIERRO, F. S., QUINTERO, A., CHAPARRO, A. & SANZ, A. 2010. Culture and characterization of mesenchymal stem cells from human gingival tissue. *J Periodontol,* 81**,** 917-25.

MIURA, M., GRONTHOS, S., ZHAO, M., LU, B., FISHER, L. W., ROBEY, P. G. & SHI, S. 2003. SHED: stem cells from human exfoliated deciduous teeth. *Proc Natl Acad Sci U S A,* 100**,** 5807-12.

MOBASHERI, A., BARRETT-JOLLEY, R., SHAKIBAEI, M., CANESSA, C. M. & MARTIN-VASALLO, P. 2005. Enigmatic Roles of the Epithelial Sodium Channel (ENaC) in Articular Chondrocytes and Osteoblasts: Mechanotransduction, Sodium Transport or Extracellular Sodium Sensing?

*In:* KAMKIN, A. & KISELEVA, I. (eds.) *Mechanosensitivity in Cells and Tissues.* Moscow.
MOSTAFA, N. Z., ULUDAG, H., DEDERICH, D. N., DOSCHAK, M. R. & EL-BIALY, T. H. 2009. Anabolic effects of low-intensity pulsed ultrasound on human gingival fibroblasts. *Arch Oral Biol,* 54**,** 743-8.
O'BRIEN, W. D., JR. 2007. Ultrasound-biophysics mechanisms. *Prog Biophys Mol Biol,* 93**,** 212-55.
PADILLA, F., PUTS, R., VICO, L. & RAUM, K. 2014. Stimulation of bone repair with ultrasound: a review of the possible mechanic effects. *Ultrasonics,* 54**,** 1125-45.
PATEL, U. S., GHORAYEB, S. R., YAMASHITA, Y., ATANDA, F., WALMSLEY, A. D. & SCHEVEN, B. A. 2015. Ultrasound field characterization and bioeffects in multiwell culture plates. *J Ther Ultrasound,* 3**,** 8.
PENG, L., YE, L. & ZHOU, X. D. 2009. Mesenchymal stem cells and tooth engineering. *Int J Oral Sci,* 1**,** 6-12.
PFLIEGER, R., CHAVE, T., VIROT, M. & NIKITENKO, S. I. 2014. Activating molecules, ions, and solid particles with acoustic cavitation. *J Vis Exp*.
PHINNEY, D. G. 2012. Functional heterogeneity of mesenchymal stem cells: implications for cell therapy. *J Cell Biochem,* 113**,** 2806-12.
POUNDER, N. M. & HARRISON, A. J. 2008. Low intensity pulsed ultrasound for fracture healing: a review of the clinical evidence and the associated biological mechanism of action. *Ultrasonics,* 48**,** 330-8.
RANADE, S. S., WOO, S. H., DUBIN, A. E., MOSHOURAB, R. A., WETZEL, C., PETRUS, M., MATHUR, J., BEGAY, V., COSTE, B., MAINQUIST, J., WILSON, A. J., FRANCISCO, A. G., REDDY, K., QIU, Z. Z., WOOD, J. N., LEWIN, G. R. & PATAPOUTIAN, A. 2014. Piezo2 is the major transducer of mechanical forces for touch sensation in mice. *Nature,* 516**,** 121-U330.
REGO, E. B., TAKATA, T., TANNE, K. & TANAKA, E. 2012. Current status of low intensity pulsed ultrasound for dental purposes. *Open Dent J,* 6**,** 220-5.
REN, L., YANG, Z., SONG, J., WANG, Z., DENG, F. & LI, W. 2012. Involvement of p38 MAPK pathway in low intensity pulsed ultrasound induced osteogenic differentiation of human periodontal ligament cells. *Ultrasonics*.
REN, L., YANG, Z., SONG, J., WANG, Z., DENG, F. & LI, W. 2013. Involvement of p38 MAPK pathway in low intensity pulsed ultrasound induced osteogenic differentiation of human periodontal ligament cells. *Ultrasonics,* 53**,** 686-90.

ROMANO, C. L., ROMANO, D. & LOGOLUSO, N. 2009. Low-intensity pulsed ultrasound for the treatment of bone delayed union or nonunion: a review. *Ultrasound Med Biol,* 35**,** 529-36.

SCHEVEN, B. A., MAN, J., MILLARD, J. L., COOPER, P. R., LEA, S. C., WALMSLEY, A. D. & SMITH, A. J. 2009a. VEGF and odontoblast-like cells: stimulation by low frequency ultrasound. *Arch Oral Biol,* 54**,** 185-91.

SCHEVEN, B. A., MILLARD, J. L., COOPER, P. R., LEA, S. C., WALMSLEY, A. D. & SMITH, A. J. 2007. Short-term in vitro effects of low frequency ultrasound on odontoblast-like cells. *Ultrasound Med Biol,* 33**,** 1475-82.

SCHEVEN, B. A., SHELTON, R. M., COOPER, P. R., WALMSLEY, A. D. & SMITH, A. J. 2009b. Therapeutic ultrasound for dental tissue repair. *Med Hypotheses,* 73**,** 591-3.

SCHRENK-SIEMENS, K., WENDE, H., PRATO, V., SONG, K., ROSTOCK, C., LOEWER, A., UTIKAL, J., LEWIN, G. R., LECHNER, S. G. & SIEMENS, J. 2015. PIEZO2 is required for mechanotransduction in human stem cell-derived touch receptors. *Nature Neuroscience,* 18**,** 10-+.

SCHRIEFER, J. L., WARDEN, S. J., SAXON, L. K., ROBLING, A. G. & TURNER, C. H. 2005. Cellular accommodation and the response of bone to mechanical loading. *J Biomech,* 38**,** 1838-45.

SCHUMANN, D., KUJAT, R., NERLICH, M. & ANGELE, P. 2006. Mechanobiological conditioning of stem cells for cartilage tissue engineering. *Biomed Mater Eng,* 16**,** S37-52.

SCHWARTZ, M. A. & DESIMONE, D. W. 2008. Cell adhesion receptors in mechanotransduction. *Curr Opin Cell Biol,* 20**,** 551-6.

SENA, K., LEVEN, R. M., MAZHAR, K., SUMNER, D. R. & VIRDI, A. S. 2005. Early gene response to low-intensity pulsed ultrasound in rat osteoblastic cells. *Ultrasound Med Biol,* 31**,** 703-8.

SEO, B. M., MIURA, M., GRONTHOS, S., BARTOLD, P. M., BATOULI, S., BRAHIM, J., YOUNG, M., ROBEY, P. G., WANG, C. Y. & SHI, S. 2004. Investigation of multipotent postnatal stem cells from human periodontal ligament. *Lancet,* 364**,** 149-55.

SHAW, A. & HODNETT, M. 2008. Calibration and measurement issues for therapeutic ultrasound. *Ultrasonics,* 48**,** 234-52.

SHI, S., BARTOLD, P. M., MIURA, M., SEO, B. M., ROBEY, P. G. & GRONTHOS, S. 2005. The efficacy of mesenchymal stem cells to regenerate and repair dental structures. *Orthod. Craniofac. Res.,* 8**,** 191-9.

SHIRAISHI, R., MASAKI, C., TOSHINAGA, A., OKINAGA, T., NISHIHARA, T., YAMANAKA, N., NAKAMOTO, T. & HOSOKAWA, R. 2011. The effects of low-intensity pulsed ultrasound exposure on gingival cells. *J Periodontol,* 82**,** 1498-503.

SLOAN, A. J. & SMITH, A. J. 2007. Stem cells and the dental pulp: potential roles in dentine regeneration and repair. *Oral Dis,* 13**,** 151-7.
SONOYAMA, W., LIU, Y., YAMAZA, T., TUAN, R. S., WANG, S., SHI, S. & HUANG, G. T. 2008. Characterization of the apical papilla and its residing stem cells from human immature permanent teeth: a pilot study. *J Endod,* 34**,** 166-71.
ST PIERRE, M., REEH, P. W. & ZIMMERMANN, K. 2009. Differential effects of TRPV channel block on polymodal activation of rat cutaneous nociceptors in vitro. *Exp Brain Res,* 196**,** 31-44.
STRIDE, E. P. & COUSSIOS, C. C. 2010. Cavitation and contrast: the use of bubbles in ultrasound imaging and therapy. *Proc Inst Mech Eng H,* 224**,** 171-91.
SUGIYAMA, M., IOHARA, K., WAKITA, H., HATTORI, H., UEDA, M., MATSUSHITA, K. & NAKASHIMA, M. 2011. Dental pulp-derived CD31(-)/CD146(-) side population stem/progenitor cells enhance recovery of focal cerebral ischemia in rats. *Tissue Eng Part A,* 17**,** 1303-11.
SZALLASI, A. & BLUMBERG, P. M. 1999. Vanilloid (Capsaicin) receptors and mechanisms. *Pharmacol Rev,* 51**,** 159-212.
TANAKA, E., KURODA, S., HORIUCHI, S., TABATA, A. & EL-BIALY, T. 2015. Low-intensity pulsed ultrasound in dentofacial tissue engineering. *Ann Biomed Eng,* 43**,** 871-86.
TECHAWATTANAWISAL, W., NAKAHAMA, K., KOMAKI, M., ABE, M., TAKAGI, Y. & MORITA, I. 2007. Isolation of multipotent stem cells from adult rat periodontal ligament by neurosphere-forming culture system. *Biochemical and Biophysical Research Communications,* 357**,** 917-923.
TECLES, O., LAURENT, P., ZYGOURITSAS, S., BURGER, A. S., CAMPS, J., DEJOU, J. & ABOUT, I. 2005. Activation of human dental pulp progenitor/stem cells in response to odontoblast injury. *Arch Oral Biol,* 50**,** 103-8.
TER HAAR, G. 2007. Therapeutic applications of ultrasound. *Prog Biophys Mol Biol,* 93**,** 111-29.
THESLEFF, I., VAAHTOKARI, A., KETTUNEN, P. & ABERG, T. 1995. Epithelial-mesenchymal signaling during tooth development. *Connect Tissue Res,* 32**,** 9-15.
TITUSHKIN, I. A., SHIN, J. & CHO, M. 2010. A new perspective for stem-cell mechanobiology: biomechanical control of stem-cell behavior and fate. *Crit Rev Biomed Eng,* 38**,** 393-433.
TRAN, T. A., LE GUENNEC, J. Y., BOUGNOUX, P., TRANQUART, F. & BOUAKAZ, A. 2008. Characterization of cell membrane response to

ultrasound activated microbubbles. *IEEE Transactions on Ultrasonics Ferroelectrics & Frequency Control,* 55**,** 43-9.
VOLKERS, L., MECHIOUKHI, Y. & COSTE, B. 2015. Piezo channels: from structure to function. *Pflugers Archiv-European Journal of Physiology,* 467**,** 95-99.
WALMSLEY, A. D., LAIRD, W. R. & LUMLEY, P. J. 1992. Ultrasound in dentistry. Part 2--Periodontology and endodontics. *J Dent,* 20**,** 11-7.
WALMSLEY, A. D., LUMLEY, P. J. & LAIRD, W. R. 1988a. Ultrasonic instruments in dentistry: 3. The removal of restorations. *Dent Update,* 15**,** 401-4.
WALMSLEY, A. D., WALSH, T. F. & LAIRD, W. R. 1988b. Ultrasonic instruments in dentistry: 1. The ultrasonic scaler. *Dent Update,* 15**,** 321-3, 325-6.
WANG, L., SHEN, H., ZHENG, W., TANG, L., YANG, Z., GAO, Y., YANG, Q., WANG, C., DUAN, Y. & JIN, Y. 2011. Characterization of stem cells from alveolar periodontal ligament. *Tissue Eng Part A,* 17**,** 1015-26.
WANG, Y., JI, H. X., XING, S. H., PEI, D. S. & GUAN, Q. H. 2007. SP600125, a selective JNK inhibitor, protects ischemic renal injury via suppressing the extrinsic pathways of apoptosis. *Life Sci,* 80**,** 2067-75.
WAUSON, E. M., GUERRA, M. L., BARYLKO, B., ALBANESI, J. P. & COBB, M. H. 2013. Off-target effects of MEK inhibitors. *Biochemistry,* 52**,** 5164-6.
WOOD, R. W., LOOMIS, A.L. 1927. The physical and biological effects of high frequency sound waves of great intensity. *Phil. Mag.***,** 417–436.
WOZNIAK, M. A., MODZELEWSKA, K., KWONG, L. & KEELY, P. J. 2004. Focal adhesion regulation of cell behavior. *Biochim Biophys Acta,* 1692**,** 103-19.
WU, Z., WONG, K., GLOGAUER, M., ELLEN, R. P. & MCCULLOCH, C. A. 1999. Regulation of stretch-activated intracellular calcium transients by actin filaments. *Biochem Biophys Res Commun,* 261**,** 419-25.
XU, L., TRIPATHY, A., PASEK, D. A. & MEISSNER, G. 1999. Ruthenium red modifies the cardiac and skeletal muscle Ca(2+) release channels (ryanodine receptors) by multiple mechanisms. *J Biol Chem,* 274**,** 32680-91.
YOSHIDA, T., WASHIO, K., IWATA, T., OKANO, T. & ISHIKAWA, I. 2012. Current status and future development of cell transplantation therapy for periodontal tissue regeneration. *Int J Dent,* 2012**,** 307024.
YOUNG, H. T., CARR, N. J., GREEN, B., TILLEY, C., BHARGAVA, V. & PEARCE, N. 2013. Accuracy of visual assessments of proliferation indices in gastroenteropancreatic neuroendocrine tumours. *J Clin Pathol,* 66**,** 700-4.

YU, V., DAMEK-POPRAWA, M., NICOLL, S. B. & AKINTOYE, S. O. 2009. Dynamic hydrostatic pressure promotes differentiation of human dental pulp stem cells. *Biochem. Biophys. Res. Commun.,* 386**,** 661-5.

ZAGORODNYUK, V. P., LYNN, P., COSTA, M. & BROOKES, S. J. 2005. Mechanisms of mechanotransduction by specialized low-threshold mechanoreceptors in the guinea pig rectum. *Am J Physiol Gastrointest Liver Physiol,* 289**,** G397-406.

ZHANG, W. & LIU, H. T. 2002. MAPK signal pathways in the regulation of cell proliferation in mammalian cells. *Cell Res,* 12**,** 9-18.

ZHOU, S., SCHMELZ, A., SEUFFERLEIN, T., LI, Y., ZHAO, J. & BACHEM, M. G. 2004. Molecular mechanisms of low intensity pulsed ultrasound in human skin fibroblasts. *J Biol Chem,* 279**,** 54463-9.

ZINNER, D. D. 1955. Recent ultrasonic dental studies, including periodontia, without the use of an abrasive. *J Dent Res,* 34**,** 748-749.

ZOU, C. & SHEN, Z. 2007. One-step intracellular triglycerides extraction and quantitative measurement in vitro. *J Pharmacol Toxicol Methods,* 56**,** 63-6.

# APPENDIX

## PUBLICATION

*Q Gao，AD Walmsley，PR Cooper，BA Scheven. Ultrasound Stimulation of Different Dental Stem Cell Populations: Role of Mitogen-activated Protein Kinase Signaling.* J Endod, 2016. **42**(3): p. 425-431

*Q Gao，PR Cooper，AD Walmsley，BA Scheven. Role of PIEZOs in Low-intensity Ultrasound-stimulated Dental Stem Cells. J Dent Res. (Submitted)*

## ABSTRACTS/CONFERENCES

*Q. Gao, A.D. Walmsley, P.R. Cooper, B.A. Scheven. MAPK Signalling in Dental Stem Cells Following Ultrasound Stimulation. International Association for Dental Research, Boston, 2015*

*Q. Gao, A.D. Walmsley, P.R. Cooper, B.A. Scheven. Low Intensity Pulsed Ultrasound-induced MAPK Signalling in Dental Stem Cells. Research Poster Conference, University of Birmingham, 2015*